LOCALIZATION AND FUNCTION OF UNC-52/PERLECAN ISOFORMS IN THE NEMATODE *Caenorhabditis elegans.*

by

GREGORY PAUL MULLEN

B.Sc., The University of British Columbia, 1991

A THESIS SUBMITTED IN PARTIAL FULFILLMENT OF THE REQUIREMENTS OF THE DEGREE OF

DOCTOR OF PHILOSOPHY

in

THE FACULTY OF GRADUATE STUDIES

(Genetics Program)

We accept this thesis as conforming to the required standard

THE UNIVERSITY OF BRITISH COLUMBIA

October 1998

Department of Genetics Program

The University of British Columbia
Vancouver, Canada

Date Oct. 1998

Abstract.

The *unc-52* gene encodes the nematode homolog of mammalian perlecan, the major heparan sulfate proteoglycan of the extracellular matrix (Rogalski et al., 1993). This protein has five domains, with similarity to the LDL-receptor (domain II), laminin (domains III and V), and the neural cell adhesion molecule (domain IV). We identified three major classes of protein products that arise through alternative splicing: short (domains I - III), medium (domains I - IV), and long (domains I - V) isoforms. Alternative splicing also generates diversity within domains III and IV (Rogalski et al., 1993, 1995).

Immunolocalization studies indicate that UNC-52 is localized to basement membranes associated with contractile tissues in *C. elegans*. In addition, there are spatial and temporal differences in isoform localization. In embryos, short isoforms are associated with the pharynx and anal muscles, while domain IV-containing isoforms are associated with the body wall muscles. In adults, domain IV-containing isoforms become more widely distributed and are detected in basement membranes adjacent to most contractile tissues. Mutant studies indicate that domain IV-containing isoforms are essential for myofilament assembly in body wall muscles. In contrast, short isoforms are not required for myofilament lattice assembly in the pharyngeal muscles and their role in development remains unclear. Our results also suggest that alternative splicing within domain IV is associated with temporal changes in isoform expression.

Recently, the *mec-8* gene has been shown to encode a putative RNA-binding protein that regulates some of these splicing events (Lundquist et al., 1996). We characterized the interactions between *unc-52* and *mec-8*, and present a model for temporal and qualitative control of isoform expression through *mec-8* and a group of global regulators called heterochronic genes. Finally, we examined the distribution of perlecan in mutants lacking key muscle attachment proteins such as integrin, and our results suggest that perlecan acts upstream of membrane-associated components during muscle assembly.

Table of Contents

List of Tables

List of Figures

List of Abbreviations

bp	basepairs
Ca^{++}	calcium
dpy	dumpy
ECM	extracellular matrix
ina	integrin α
kb	kilobase
let	lethal
LDL	low-density lipoprotein
lin	abnormal cell lineage
mec	mechanosensory defective
ml	milliliter
mM	millimolar
mua	muscle-attachment defective
mup	muscle-positioning defective
NCAM	neural cell adhesion molecule
PAGE	polyacrylamide gel electrophoresis
pat	paralyzed, arrested elongation at two-fold
PCR	polymerase chain reaction
SDS	sodium dodecyl sulfate
sup	suppressor
µl	microliter
µg	microgram
unc	uncoordinated
Vul	vulvaless

Acknowledgment

I would like to express my sincerest thanks to my supervisor Dr. Donald Moerman, for his patience, support, and guidance. I have greatly enjoyed my time in the Moerman lab. I would also like to thank members of the Moerman lab, past and present, including Dr. Teresa Rogalski, Ken Norman, Poupak Rahmani Gorji, Danelle Devenport, Jason Bush and Dr. Mary Gilbert. Finally, I would like to thank my friends, colleagues, and mentors at the University of British Columbia, including Dr. Elaine Humphries, Dr. Donald Nelson, Dr. Jacob Hodgeson, Tom Milne, and my supervisory committee: Dr. Linda Matsuuchi, Dr. Terrence Snutch, Dr. Martin Adamson, and Dr. Peter Candido.

Dedication

This thesis is dedicated, with thanks and love, to my mother, Gillian Brangham, and to my wife, Eleanor Mathews.

Chapter 1. Introduction.

Basement membranes and the cytoskeleton.

Extracellular matrices are protein networks that surround most tissues (Martin and Timpl, 1987; Kleinman et al., 1989). Several types of extracellular matrices have been described, including connective tissues and basement membranes. Basement membranes are specialized regions of extracellular matrix that separate ectodermal and mesodermal cell types (Yurchenco and Schittny, 1990). Basement membranes have important roles in many fundamental developmental and regenerative processes, including cell adhesion and migration, signal transduction, and even gene regulation (reviewed in Martin and Timpl, 1987). Many of these processes are mediated by specific interactions between basement membrane components and transmembrane receptors such as integrin (reviewed in Hynes, 1992).

One consequence of these interactions is changes in the organization of the cytoskeleton. The cytoskeleton is an intracellular network of filaments that controls many aspects of cellular function, including cell morphology and motility. Certain cell types, such as muscle cells, have elaborate cytoskeletons for the purpose of locomotion. Similarly, other cell types such as neurons make use of local cytoskeletal changes to effect changes in cell shape or position (reviewed in Suter and Forscher, 1998). Underlying

these diverse uses of the cytoskeleton, however, are interactions between external ligands in the basement membrane and their cognate receptors.

Basement membranes contain a large number of different components, including laminin, type IV collagen, nidogen, and heparan sulfate proteoglycans (Timpl, 1993; Timpl and Brown, 1996). Furthermore, expression of alternate protein isoforms contributes to additional diversity in basement membranes (Heikkila and Soininen, 1996; Noonan et al., 1991; Timpl, 1993; Rogalski et al., 1993, 1995). In this study, we focus on perlecan, a basement membrane heparan sulfate proteoglycan, and its role in cytoskeletal organization. In the nematode *Caenorhabditis elegans*, alternative splicing gives rise to a number of distinct perlecan isoforms (Rogalski et al., 1993, 1995). Using genetic and immunological approaches, we hope to gain insight into the importance of structural diversity in basement membranes.

Structure and function of perlecan, the major basement membrane heparan sulfate proteoglycan.

Proteoglycans are a diverse family of molecules that consist of a protein core and one or more glycosaminoglycan side chains. Before widespread use of molecular biological methods, proteoglycans were classified according to the type of glycosaminoglycan side chain (for example, heparan sulfate and chondroitin sulfate proteoglycans). Increasingly, proteoglycans are now classified according to the primary sequence of the protein core (for example, perlecan and decorin).

Perlecan, a heparan sulfate proteoglycan, is an abundant component of most basement membranes. Perlecan is synthesized by a wide variety of cell types, including epithelial cells (Morris et al., 1994; Ohji et al., 1994; Van Det et al., 1995), fibroblasts (Heremans et al., 1989; Murdoch et al., 1992), and myocytes (Murdock et al., 1994), and has been detected in all mammalian basement membranes surveyed to date (reviewed in

Noonan and Hassell, 1992). Perlecan has also been identified in the nematode *Caenorhabditis elegans* (Rogalski et al., 1993).

Perlecan consists of a large (~400 kDa) core polypeptide and several glycosaminoglycan side chains (Laurie et al., 1987; Paulsson et al., 1987; Yurchenco et al., 1987). Typically, perlecan has three heparan sulfate side chains, but chondroitin sulfate side chains have also been detected (Hassell et al., 1992; Danielson et al., 1992). In electron microscopy studies, perlecan resembles a "string of beads" or "pearls", with the glycosaminoglycan side chains extending from one end (Laurie et al., 1987; Paulsson et al., 1987; Yurchenco et al., 1987). The name "perlecan" was suggested by this appearance (Laurie et al., 1987; Paulsson et al., 1987; Yurchenco et al., 1987).

The primary sequence of perlecan was first determined for the murine form of the protein (Noonan et al., 1991). Initially, cDNA clones were identified by screening an expression library with polyclonal anti-perlecan antibodies. These cDNAs hybridize to a ~13 kb mRNA on Northern blots and encode a 3707 amino acid polypeptide. This polypeptide has a signal sequence and five distinct domains (Figure 1). The first domain is unique to perlecan, while the remaining four domains are similar to those found in the LDL-receptor (domain II), laminin (domains III and V), and NCAM (domain IV). Later, human and nematode homologs were shown to have similar structure (Figure 1; Kallunki and Tryggvason, 1992; Rogalski et al., 1993; T. M. Rogalski, G. P. Mullen, and D. G. Moerman, unpublished results).

The first domain (domain I) contains a signal sequence followed by a region rich in acidic amino acids. This domain in mammalian perlecan contains several Ser-Gly-Asp (SGD) sequences that serve as sites of heparan sulfate attachment (Noonan et al., 1991). The presence of glycosaminoglycan side chains on nematode perlecan has not been investigated to date, and domain I of the nematode protein does not contain SGD sequences (Rogalski et al., 1993). Consequently, if there are heparan sulfate side chains on nematode perlecan, other sequences must mediate their attachment.

Figure 1. Structural comparison of perlecan from mice, humans, and the nematode *Caenorhabditis elegans*.

Protein domains are indicated with Roman numerals (I - V) and dashed lines indicate corresponding regions of each protein. The various protein modules are indicated with shaded boxes or circles and these symbols are defined at the bottom of the figure. Adapted from Iozzo et al., 1994.

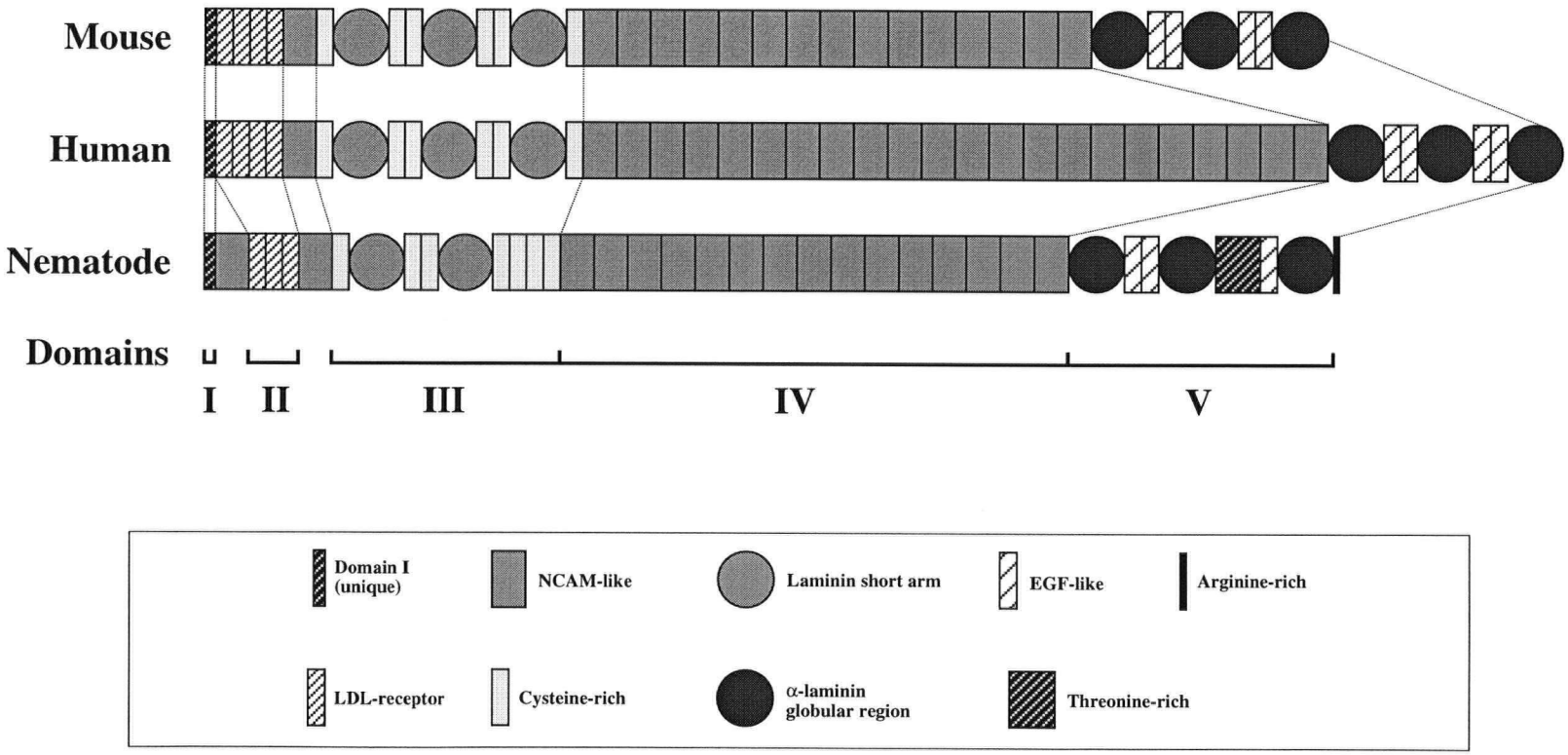
Mouse
Human
Nematode
Domains
I
II
III
IV
V
Domain I (unique)
NCAM-like
Laminin short arm
EGF-like
Arginine-rich
LDL-receptor
Cysteine-rich
α-laminin globular region
Threonine-rich

Domain II contains cysteine-rich repeats similar to those found in the low-density lipoprotein (LDL) receptor family of proteins. Mammalian perlecan has four LDL-receptor-like repeats in domain II (Noonan et al., 1991; Kallunki and Tryggvason, 1992), while nematode perlecan has only three repeats (Rogalski et al., 1993). In the LDL receptor, these repeats have been identified as ligand-binding sites (Russell et al., 1989). In nematode perlecan, domain II is flanked by two repeats similar to those found in the neural cell adhesion molecule (NCAM) (Rogalski et al., 1993). Mammalian perlecan lacks the NCAM repeat between domains I and II (Noonan et al., 1991; Murdoch et al., 1992; Kallunki and Tryggvason, 1992).

Domain III consists of cysteine-rich and globular regions similar to the amino-terminal domain of α-laminin. Mammalian perlecan has three globular regions in domain III (Noonan et al., 1991; Murdoch et al., 1992; Kallunki and Tryggvason, 1992), while nematode perlecan has only two (Rogalski et al., 1993). In addition, perlecan in mice and nematodes has an RGD (Arg-Gln-Asp) motif in domain III (Noonan et al., 1991; Rogalski et al., 1993). This motif in other extracellular proteins mediates interaction with integrin receptors. However, human perlecan lacks this motif (Murdoch et al., 1992; Kallunki and Tryggvason, 1992).

Domain IV consists of repeats most similar to the neural cell adhesion molecule (NCAM) family of immunoglobulin-like repeats. In mammalian perlecan, domain IV is thought to form a single globule through homophilic interactions of these NCAM repeats. The number of NCAM repeats in this domain varies between species; murine and nematode forms have fourteen repeats (Noonan et al., 1991; Rogalski et al., 1993), while human perlecan has twenty-two repeats (Murdoch et al., 1992; Kallunki and Tryggvason, 1992). In addition, alternative splicing gives rise to perlecan isoforms that differ in the number of NCAM repeats domain IV (Noonan and Hassell, 1992; Rogalski et al., 1993, 1995).

The final domain (Domain V) consists of three globular regions interspersed with short cysteine-rich repeats. The globular regions are similar to those found in the G-

domain of α-laminin and the carboxyl-terminal region of agrin. In addition, nematode perlecan contains a novel threonine-rich region between the second and third globular regions of domain V (T. M. Rogalski, G. P. Mullen, and D. G. Moerman, unpublished results). This threonine-rich region is not found in mammalian perlecan (T. M. Rogalski, personal communication).

These five domains are thought to form a series of globules separated by short segments (reviewed in Hassell et al., 1992). According to this model, domains I and II form a single globule, domain III forms three globules, and domains IV and V each form single globules. This predicted structure agrees reasonably well with the results of electron microscopy studies (Paulsson et al., 1987; Laurie et al., 1988).

The structure of perlecan permits a wide range of protein interactions. There is evidence for both homophilic and heterophilic interactions. The carboxyl-terminal domain of perlecan, for example, mediates homophilic interactions that lead to formation of dimers and trimers (Yurchenco et al., 1987). Such interactions may be important for higher-order structure in basement membranes (Yurchenco et al., 1987). Heterophilic interactions are mediated both by the glycosaminoglycan side chains and sites within the protein core. Perlecan binds to laminin, collagen IV, and fibronectin through its heparan sulfate chains (Battaglia et al., 1992). The glycosaminoglycan chains also mediate binding to growth factors such as basic fibroblast growth factor (bFGF; Aviezer et al., 1994). In addition, perlecan binds to nidogen (Battaglia et al., 1992) and integrin (Hayashi et al., 1992) through sites in the protein core. Fibronectin is also reported to bind sites in the protein core of perlecan (Heremans et al., 1990).

The multidomain structure of perlecan reflects the diverse functions proposed for this molecule. Perlecan has been implicated in a number of biological processes including glomerular filtration (Farquhar, 1982), mitogenesis, and angiogenesis (Aviezer et al., 1994), and cell adhesion through interactions with focal adhesion complexes (Hayashi et al., 1992; Rogalski et al., 1993; Chakravarti et al., 1995). Our studies using the nematode

C. elegans demonstrate that perlecan has an essential role in muscle development (Rogalski et al., 1993, 1995).

The nematode *Caenorhabditis elegans* is ideally-suited for the study of basement membrane biology. In particular, the study of muscle assembly has proven a powerful system for dissecting basement membrane composition and function. Using genetic, molecular, and biochemical approaches, over 80 genes affecting muscle structure and function have been identified in *C. elegans* (reviewed in Moerman and Fire, 1997; D. G. Moerman, personal communication). An extensive genetic map has been compiled for *C. elegans*, and most of the genome has been cloned into YAC and cosmid vectors (Coulson et al., 1986, 1989), allowing genes to be mapped either genetically or molecularly. Genes can then be cloned and manipulated using standard molecular methods and reintroduced into *C. elegans* by micro-injection (Mello et al., 1991). In addition, the Genome Sequencing Consortium will soon have completed sequencing the entire *C. elegans* genome (Waterston et al., 1997). This resource is already proving invaluable for the identification and analysis of genes encoding basement membrane and muscle components in *C. elegans*.

Anatomical description of basement membranes and muscles in *C. elegans*.

C. elegans has a simple anatomy (reviewed in White, 1988). The basic body plan is bilaterally symmetrical and pseudocoelomate. In most bilateral animals, the body wall is separated from internal organs by a fluid-filled cavity. In coelomates, this cavity is completely lined by mesoderm, while in pseudocoelomates, the cavity is only partially lined with mesoderm. The outer surface of the body wall is covered with an collagenous cuticle that is secreted by the underlying epidermis, called the hypodermis. The body cavity, in turn, is lined with a thin (20 nm) basement membrane that separates hypodermis from muscles and internal organs. A similar basement membrane surrounds the intestine and the reproductive organs. A distinct (45 nm) basement membrane surrounds the pharynx and

separates the pharyngeal nervous system from the somatic nervous system (Albertson and Thomson, 1976).

In *C. elegans*, a specialized basement membrane underlies the body wall muscles and anchors the myofilament lattice through integrin-mediated attachment (Figure 2; Francis and Waterston, 1985, 1991; reviewed in Moerman and Fire, 1997). In adult animals, there are 95 body-wall muscle cells arranged in four quadrants, two dorsal and two ventral, beneath the hypodermis. Each quadrant consists of a double row of spindle-shaped cells and runs the length of the animal. In each muscle cell, the thin and thick filaments of the myofilament lattice lie just beneath the plasma membrane facing the hypodermis. These filament networks are anchored by a series of attachment structures, the dense bodies and M-lines, to the underlying basement membrane (Figure 2; Francis and Waterston, 1985, 1991).

Nematode body wall muscle differs from vertebrate skeletal muscle in several respects (reviewed in Waterston, 1988). Vertebrate skeletal muscles contain many multinucleate cells termed muscle fibers. In contrast, nematode body wall muscles are mononucleate, much like vertebrate cardiac and smooth muscles. Secondly, in nematode muscles, filaments are oriented longitudinally, but adjacent structural units are staggered slightly with respect to one another (Waterston, 1988). Consequently, striations are oriented at a slight angle (~6°) relative to the longitudinal axis of the cell (Mackenzie and Epstein, 1980; Epstein et al., 1985), a pattern called oblique-striation (Rosenbluth, 1965; Hirumi et al., 1971; Waterston, 1988). In vertebrate skeletal muscles, adjacent structural units are aligned and oriented perpendicularly to the longitudinal axis of the muscle, a pattern called cross-striation. Thirdly, in vertebrate skeletal muscles, force of contraction is transmitted to the ends of the muscles and through the myotendinous junction to the skeleton. In *C. elegans*, force of contraction is transmitted perpendicularly to the length of the cell through dense bodies to the basement membrane and the hypodermis. Finally, thick and thin filaments in nematodes are substantially longer than in vertebrates. Thick

Figure 2. *C. elegans* anatomy and muscle organization.

(A) Schematic showing the position of body wall muscles in *C. elegans*. (B) Basal view of several adjacent body wall muscles. Dots represent dense bodies. (C) Hypothetical cross-section showing the muscle quadrants. Internal organs (pharynx, intestine, and gonad) have been omitted for simplicity. Basement membranes (black) surround the body wall muscles and line the pseudocoelomic cavity. (D) Tangential section of a body wall muscle cell. Dense bodies and M-lines are indicated. (E) Expanded view of the myofilament lattice, showing thick and thin filaments and their respective attachment structures, the M-lines and dense bodies. (F) Schematic of a dense body. Dense body components, including α-actinin, vinculin, and integrin, are indicated. Basement membrane, hypodermis, and cuticle are also shown. (G) Expanded view of a dense body showing molecular details.

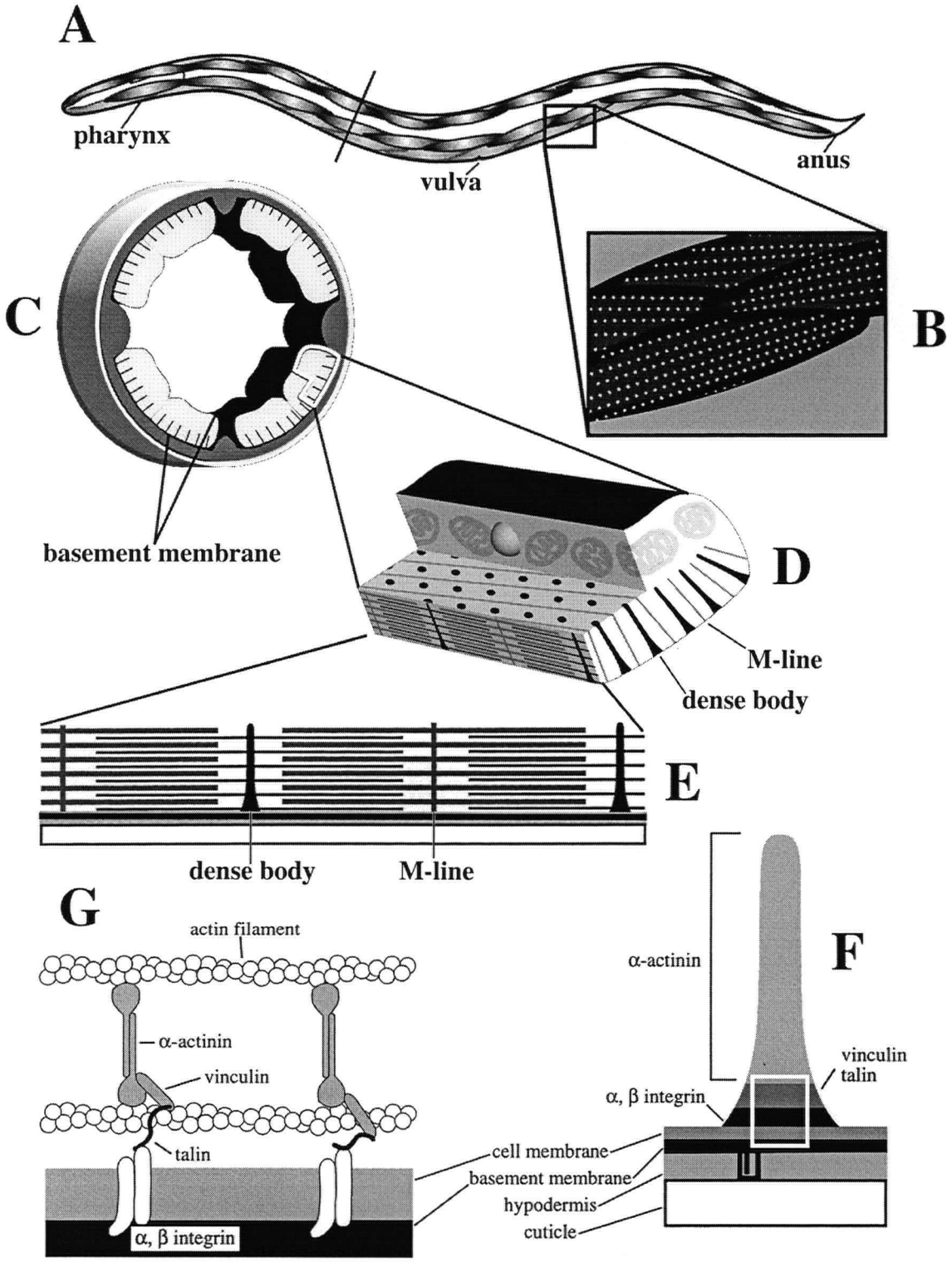
A
pharynx
vulva
anus
B
C
basement membrane
D
M-line
dense body
E
dense body
M-line
G
actin filament
α-actinin
vinculin
talin
α, β integrin
F
α-actinin
vinculin
talin
α, β integrin
cell membrane
basement membrane
hypodermis
cuticle

filaments in *C. elegans* are ~10 μm in length (Mackenzie and Epstein, 1980; Epstein et al., 1985), while vertebrate thick filaments are ~1.6 μm in length (reviewed in Harrington, 1979). Thin filaments in *C. elegans* are also substantially longer than vertebrate thin filaments. Despite these differences, however, muscles in nematodes and vertebrates share many structural features.

A prominent feature of all muscles is the array of thick and thin filaments that comprises the myofilament lattice. The principal component of thick filaments is myosin, although thick filaments in nematodes also contain paramyosin (Epstein et al., 1974; Waterston et al., 1974). Thick filaments are held in register by structures called M-lines in both nematodes and vertebrates. Thin filaments contain actin, tropomyosin, and troponins C, I, and T (Epstein et al., 1974; Waterston et al., 1974; Nakae and Obinata, 1993; Kagawa et al., 1995). The thin filaments are held in register by structures called Z-lines in vertebrate muscles and dense-bodies in nematodes.

Dense bodies are similar in composition to cell-matrix adhesion complexes found in mammalian systems (Figure 2; Burridge et al, 1988; Yamada and Geiger, 1997) and include vinculin (Barstead and Waterston, 1989), talin (Moulder et al., 1996), α-actinin (Francis and Waterston, 1985; Barstead et al., 1991), and β-integrin (Gettner et al., 1995). In addition, homologs of focal adhesion kinase (FAK; R. J. Barstead, personal communication), integrin-linked kinase (ILK; D. G. Moerman, personal communication), and other cell adhesion and signaling proteins have been identified in *C. elegans*, but the distribution of these proteins has not been determined. The composition of the M-line is less well-defined, but includes integrin (Francis and Waterston, 1985; Gettner et al., 1995) and the *unc-89* gene product (Benian et al., 1996). Integrins link both dense body and M-line components to the underlying basement membrane (Francis and Waterston, 1985; Gettner et al., 1995).

Integrins are cell surface receptors that play important roles in a number of cellular processes, including cell adhesion and signal transduction (reviewed in Yamada and

Miyamoto, 1995). In cell-adhesion complexes such as dense bodies and M-lines, integrins link the extracellular matrix to the intracellular cytoskeleton (reviewed in Moerman and Fire, 1997). Integrins are heterodimers consisting of α and β subunits; both subunits have extracellular, transmembrane, and cytoplasmic domains (reviewed in Hynes, 1992). The extracellular domain mediates attachment to the extracellular matrix, while the cytoplasmic domain interacts with cytoskeletal-associated proteins. Recent studies on lethal muscle-affecting mutants suggest that integrin nucleates formation of dense bodies and M-lines (Hresko et al., 1994; Williams and Waterston, 1994). Interactions between integrin and the basement membrane are clearly essential for dense body and M-line assembly (reviewed in Moerman and Fire, 1997).

UNC-52/perlecan is found in the basement membrane between the body wall muscle cells and the hypodermis, and is concentrated at muscle dense bodies and M-lines (Francis and Waterston, 1991; Rogalski et al., 1993). Genetic studies established that UNC-52/perlecan anchors dense bodies and M-lines, and is essential for assembly and maintenance of the myofilament lattice in body wall muscle cells (Rogalski et al., 1993; Hresko et al., 1994; Williams and Waterston, 1994).

Myofilament lattice assembly in *C. elegans*.

Muscle development in *C. elegans* can be divided into four phases: i) cell fate determination, ii) cell migration, iii) myofilament lattice assembly, and iv) muscle growth. During embryonic development, 81 of the 95 body wall muscle cells arise through cell division, migrate to form the dorsal and ventral quadrants, and assemble sarcomeres (Sulston et al., 1983). Consequently, embryogenesis is a critical period in the establishment of the basic muscle pattern.

Embryogenesis in *C. elegans* lasts ~800 min. at 22°c (reviewed in Wood, 1988). During the first ~100 min., the six founder cells (AB, MS, E, C, D, and P4) are generated

(Sulston et al., 1983). Four of these founder cells, AB, MS, C, and D, give rise to muscle cells, although only the D lineage produces muscle exclusively (Sulston et al., 1983). During the next ~250 min., gastrulation and most of the cell divisions are completed (Sulston et al., 1983). The final phase of embryogenesis, beginning ~350 min. after the first cell division, consists largely of morphogenesis and organogenesis (Sulston et al., 1983). During this phase, the embryo elongates from an ovoid to the characteristic worm shape, roughly a four-fold increase in length (Figure 3A).

Muscle structural proteins can first be detected in embryos ~290 minutes after the first cell division (Figure 3B; Epstein et al., 1992; Hresko et al., 1994). At this stage, gastrulation is complete and most of the embryonic myoblasts have finished dividing (Sulston et al., 1983). Myoblasts are now located laterally along the seam cells (lateral hypodermis) and form two rows of cells, one on each side of the embryo (Sulston et al., 1983). The myoblasts then migrate circumferentially to form the two dorsal and two ventral muscle quadrants. Some myoblasts divide again before completing their migration. By 350 min., myofilament proteins have concentrated beneath the sarcolemma in regions where muscle cells contact each other and the underlying hypodermis. This process is called muscle cell polarization (see Hresko et al., 1994; reviewed in Moerman and Fire, 1997). By 420 min., muscle cells have flattened against the hypodermis, and by 450 min., fully formed myofilaments are observed (Hresko et al., 1994).

During larval development, *C. elegans* increases substantially in size. This increase in size is largely a consequence of cell growth, although there is some increase in cell number. Within muscle quadrants, individual cells increase significantly in size, and the number of A-bands in each cell increases from two in embryonic muscles, to between eight and ten in adult muscles. In addition, fourteen body wall muscle cells are added during the first larval stage (Sulston and Horvitz, 1977). These cells are derived from the M lineage, which also gives rise to sex-specific muscles (Sulston and Horvitz, 1977). Consequently,

Figure 3. Morphogenesis and embryonic muscle assembly in *C. elegans*.

(A) Embryogenesis in wild-type embryos (adapted from Williams and Waterston, 1994). Expression of muscle-specific proteins is observed just prior to the comma stage. Movements generated by body-wall muscles begin when embryos reach the 1.5-fold stage. (B) Panels 1-4 summarize the process of myofilament assembly in *C. elegans*, depicting cross sections of embryos at various stages of development (adapted from Hresko et al., 1994; reviewed in Moerman and Fire, 1997). (1) An embryo 290 min. after the first cell division. Myofilament components (dots) are beginning to accumulate in the muscle cells (circles). Muscle cells are adjacent to the lateral hypodermis at this stage, but are beginning their dorsal and ventral migrations. (2) 350 min. embryo. Myofilament components (dots) are polarized to the plasma membrane in regions adjacent to other muscle cells and the hypodermis. Both basement membrane and hemidesmosomal components have become concentrated at these focal regions. (3) Dorsal muscle quadrant of 420 min. embryo. Muscle cells (now oval) have become flattened and myofilaments (dots), basement membrane (black), and hemidesmosome components (hatched region) are coextensive. (4) Dorsal muscle quadrant of 450 min. embryo showing complete organization of the myofilament lattice and its extracellular anchorage.

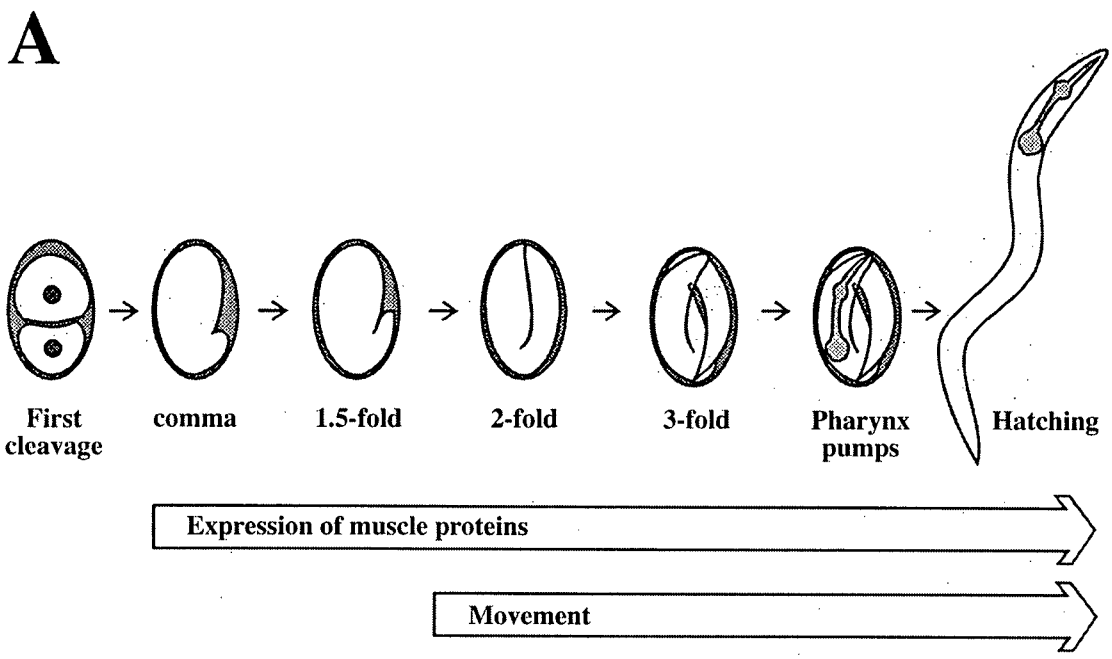
A
First cleavage
comma
1.5-fold
2-fold
3-fold
Pharynx pumps
Hatching
Expression of muscle proteins
Movement

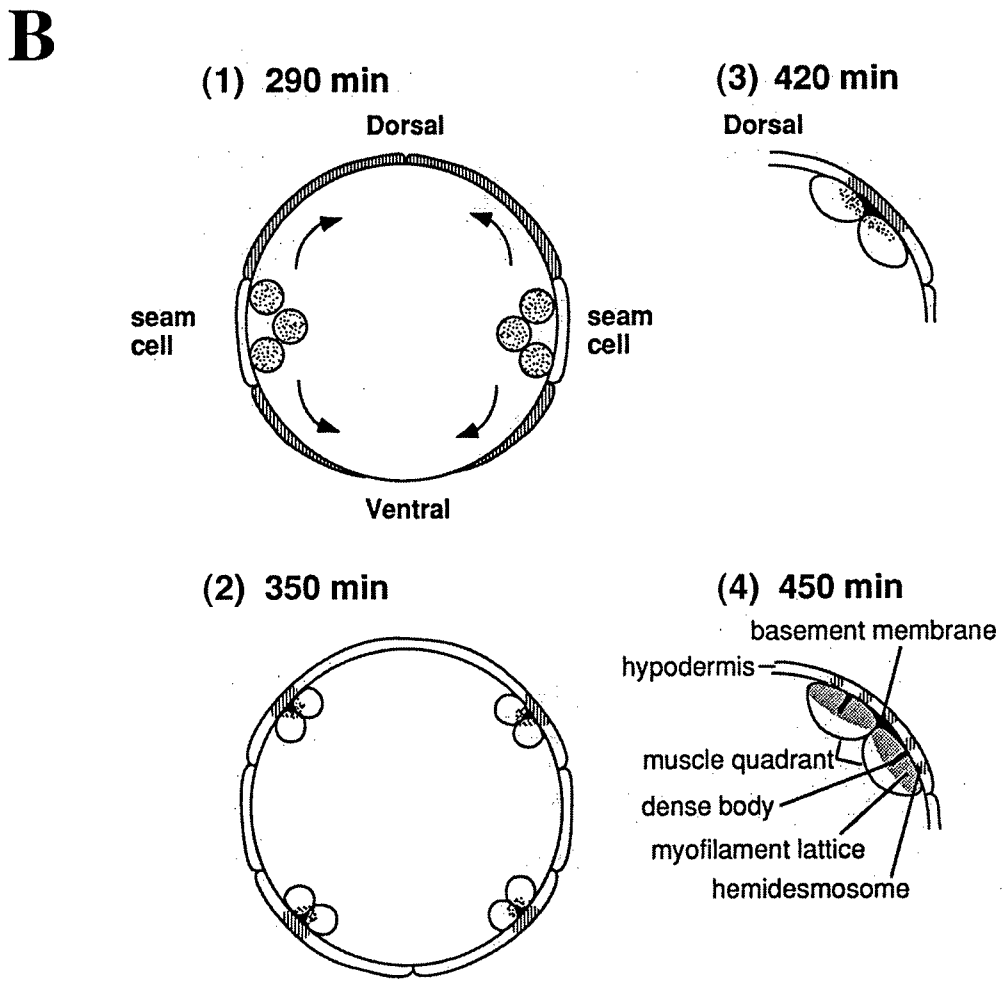
B
(1) 290 min
Dorsal
seam cell
seam cell
Ventral
(3) 420 min
Dorsal
(2) 350 min
(4) 450 min
basement membrane
hypodermis
muscle quadrant
dense body
myofilament lattice
hemidesmosome

this phase in muscle development is chiefly a period of growth, but there is some recruitment of new muscle cells, either to supplement the existing musculature, or to assemble the reproductive system.

Muscle-affecting mutations in *C. elegans*.

Mutations affecting muscle structure and function in *C. elegans* have been identified and assigned to over 80 genes (Appendix A; reviewed in Moerman and Fire, 1997; D. G. Moerman, personal communication). These mutations result in a range of phenotypes, from mildly uncoordinated movement to embryonic lethality. Mutations that affect movement of the animal are generally referred to as Unc (for uncoordinated; Brenner, 1974), while mutations resulting in embryonic lethality fall into three large groups: Pat (for paralyzed arrest at embryonic two-fold stage; Williams and Waterston, 1994), Mup (for muscle positioning; Hedgecock et al., 1987; Goh and Bogaert, 1991), and Mua (for muscle attachment abnormal; J. D. Plenefisch and E. M. Hedgecock, personal communication).

In addition to these phenotypic differences, muscle mutations have distinct cellular consequences. Morphological studies indicate that muscle-affecting mutants can be grouped according to these defects into three categories: i) thick filament-specific mutants, ii) thin filament-specific mutants, and iii) dense body and/or M-line-specific mutants (reviewed in Waterston, 1988; Moerman and Fire, 1997). Mutations in several genes, including *pat-3* (β-integrin) and *unc-52* (perlecan), disrupt assembly of both M-lines and dense bodies, and have systemic effects on the myofilament lattice, affecting both thick and thin filaments (Rogalski et al., 1993, 1995; Williams and Waterston, 1994; Gettner et al., 1995).

The *unc-52* gene encodes the nematode homolog of perlecan and is essential for myofilament lattice assembly and stability in *C. elegans*.

The *unc-52* gene encodes the nematode homolog of perlecan (Rogalski et al., 1993), the major heparan sulfate proteoglycan of mammalian basement membranes (Noonan et al., 1991; Murdoch et al., 1992; Kallunki and Tryggvason, 1992). The gene spans over 20 kb and consists of 37 exons that potentially encode a 3375 amino acid polypeptide (Rogalski et al., 1993; T. M. Rogalski, G. P. Mullen, and D. G. Moerman, unpublished results). The predicted polypeptide has five distinct domains, and the overall structure is quite similar to that of mammalian perlecan (Figure 4).

Both viable and lethal alleles of *unc-52* have been identified (Brenner, 1984; Gilchrist and Moerman, 1992; Rogalski et al, 1993; Williams and Waterston, 1994). Animals homozygous for viable alleles of *unc-52* do not exhibit obvious mutant phenotypes as embryos or young larvae, but become progressively paralyzed as they mature. This paralysis is caused by the gradual disruption of the myofilament lattice in body wall muscle cells posterior to the head (Mackenzie et al., 1978; Waterston et al., 1980). While these mutant animals are viable and fertile, they are partially egg-laying defective and have fewer progeny than wild-type animals (Gilchrist and Moerman, 1992). Seven of these mutations have been sequenced and all seven are clustered in three alternatively spliced exons, 16, 17 and 18, which encode NCAM repeats in domain IV (Rogalski et al., 1993, 1995).

Embryos homozygous for lethal alleles of *unc-52* have a Pat terminal phenotype (Rogalski et al., 1993). Body wall muscles in these mutants lack organized A- or I-bands, and morphological studies reveal that even the earliest stages of myofilament lattice assembly are defective (Rogalski et al, 1993; Hresko et al., 1994; Williams and Waterston, 1994). Included in the lethal class is the putative null allele, *st549*. This allele has a nonsense mutation in exon 7 which is expected to eliminate all *unc-52* gene products.

Figure 4. Structure of the *unc-52* gene and protein products.

The *unc-52* gene consists of 37 exons and spans over 19 kb. Exons (boxes), introns (lines), and the three general classes of protein isoforms are shown. Mutant alleles used in this study are also indicated. The longest open reading frame encodes a protein of approximately 3500 amino acids that is homologous to the mammalian heparan sulfate basement membrane proteoglycan, perlecan. Like mammalian perlecan, this polypeptide can be divided into five domains (I - V). The first domain is unique, while the remaining four domains show similarity to the LDL-receptor (domain II), α-laminin (domains III and V), and NCAM (domain IV). Additional UNC-52 isoforms are generated through alternative splicing of exons encoding alternative carboxyl termini, indicated on the gene as shaded regions. The various protein modules are indicated with shaded boxes or circles and these symbols are defined at the bottom.

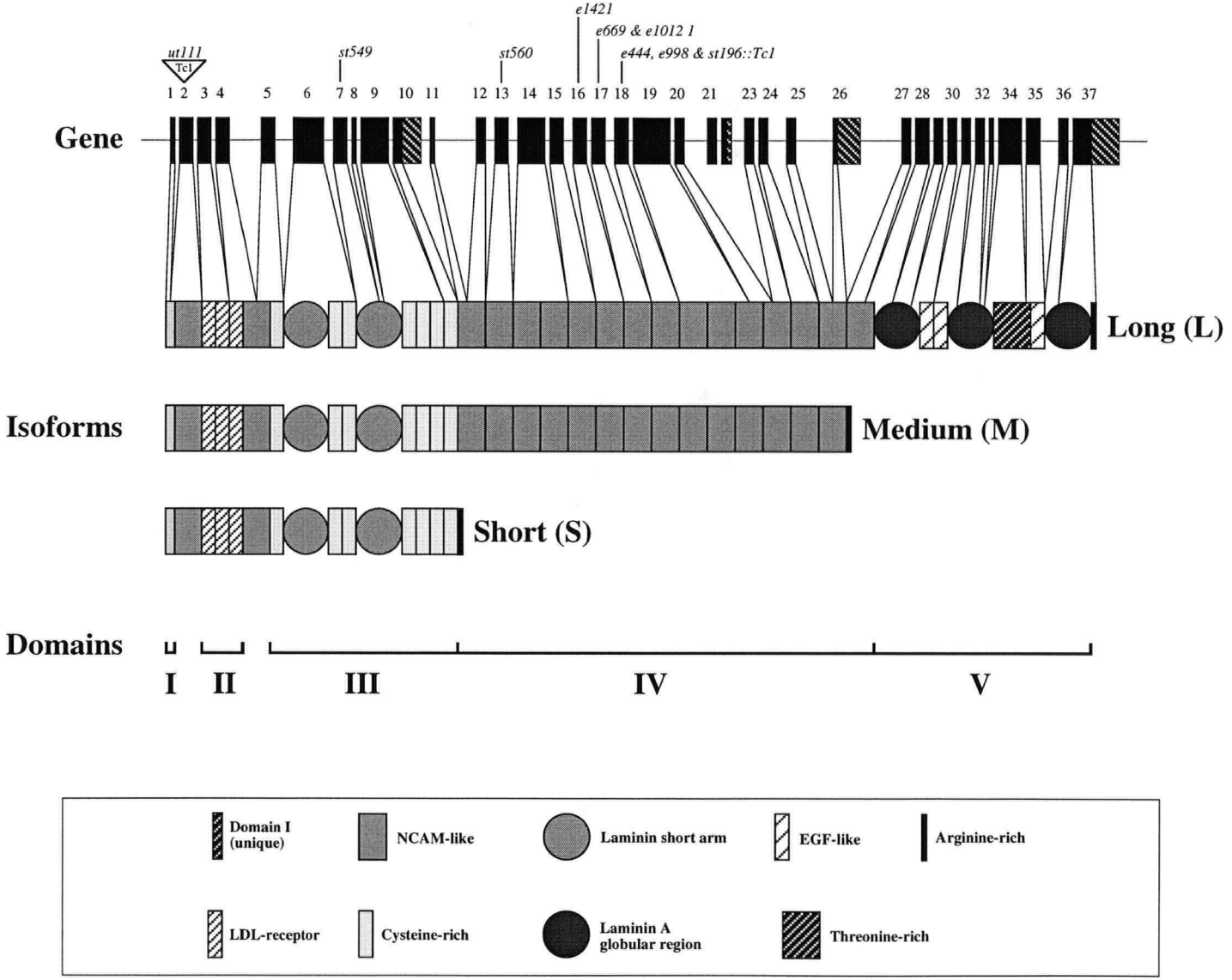
e1421
e669 & e1012 1
ut111
Tc1
st549
st560
e444, e998 & st196::Tc1
1 2 3 4 5 6 7 8 9 10 11 12 13 14 15 16 17 18 19 20 21 23 24 25 26 27 28 30 32 34 35 36 37
Gene
Long (L)
Isoforms
Medium (M)
Short (S)
Domains
I II III IV V
Domain I (unique)
NCAM-like
Laminin short arm
EGF-like
Arginine-rich
LDL-receptor
Cysteine-rich
Laminin A globular region
Threonine-rich

Homozygous *st549* embryos fail to stain with an antibody that recognizes all isoforms of UNC-52, supporting this view (Moerman et al., 1996). A second lethal allele, *ut111*, has a Tc1 insertion in exon 2; this mutation is also expected to affect all *unc-52* gene products. Five additional lethal alleles have been identified (Williams and Waterston, 1994; K. R. Norman, personal communication; P. Rahmani Gorji, personal communication) and are further characterized in this study.

Interpreting the effects of these mutations is complicated because alternative splicing of *unc-52* pre-mRNA gives rise to a number of distinct protein isoforms (Rogalski et al., 1993, 1995). These isoforms can be divided into three general groups based on their domain structure: short (domains I - III), medium (domains I - IV), and long (domains I - V) (Figure 4; Rogalski et al., 1993; T. M. Rogalski, G. P. Mullen, and D. G. Moerman, unpublished results). In addition, alternative splicing of exons 16, 17, and 18 gives rise to isoforms that vary in the number of NCAM repeats within domain IV (Rogalski et al., 1993, 1995). These exons each encode a single NCAM-repeat, and are arranged such that one or more exons can be spliced from the pre-mRNA without disrupting the reading frame. At least six different *unc-52* mRNA are generated by alternative splicing in this region (Rogalski et al., 1995). This region is also where all the viable mutant alleles are located (Rogalski et al., 1993, 1995). The net effect of these mutations is to eliminate some of the UNC-52 isoforms produced in larval and adult animals.

The *mec-8* gene interacts genetically with *unc-52* and regulates a subset of alternative splicing events in *unc-52* pre-mRNA.

Mutations in the *mec-8* gene affect sensory neuron function (Chalfie and Sulston, 1981; Perkins et al., 1986) and interact genetically with viable *unc-52* mutations (Lundquist and Herman, 1994). *mec-8* mutations were originally identified in screens for mechanosensory-defective (mec) mutants (Chalfie and Sulston, 1981). Later, *mec-8*

mutations were shown to strongly enhance the phenotype of viable *unc-52* mutations, resulting in synthetic lethality. *mec-8; unc-52 (viable)* double mutants are paralyzed and arrest at the two-fold stage of embryonic development, much like *unc-52(null)* mutants (Lundquist and Herman, 1994).

The longest open reading frame of the *mec-8* gene encodes a polypeptide with two RNA recognition motifs (RRMs) (Lundquist et al., 1996). Many proteins with RRMs are involved in RNA binding, and some of these proteins have roles in pre-mRNA processing (Burd and Dreyfuss, 1994). Products of the *sxl* (Sosnowski et al., 1989; Inoue et al., 1990) and *tra-2* (Ryner and Baker, 1991; Inoue et al., 1992) genes in *Drosophila*, for example, affect specific patterns of alternative splicing. Recently, *mec-8* has been shown to regulate accumulation of certain alternatively spliced *unc-52* transcripts (Lundquist et al., 1996).

Alternative splices between exons 15 and 19 of *unc-52* can be classified as either *mec-8*-dependent or *mec-8*-independent (Figure 5; Lundquist et al., 1996). For example, the 15 - 19 and 16 - 19 splices are *mec-8*-dependent; in the absence of *mec-8* function, these splicing events are not detected. Other alternative splices, including 15 - 18 and 17 - 19, occur in the absence of *mec-8* function and thus are *mec-8*-independent. In *mec-8* mutants, only *mec-8*-independent splice products can be detected, but these appear to be sufficient for viability and normal development. The genetic analysis of *unc-52* and its interaction with genes such as *mec-8* has provided insight into the mechanisms that regulate alternative splicing.

Localization and function of UNC-52/perlecan isoforms in *C. elegans*.

In this study, we examined the localization and function of UNC-52/perlecan isoforms in the nematode *C. elegans*. Because mutations in *unc-52* affect muscle assembly, we expected

Figure 5. The *mec-8* gene products regulate a subset of alternative splicing events in *unc-52* pre-mRNA.

Diagram of the exon 15 - 19 region of *unc-52*. The *mec-8* gene products regulate of subset of the alternative splicing events in this region, termed *mec-8*-dependent splices. The 15 - 19 and 16 - 19 splices are *mec-8*-dependent; the remaining splicing events are independent of *mec-8*.

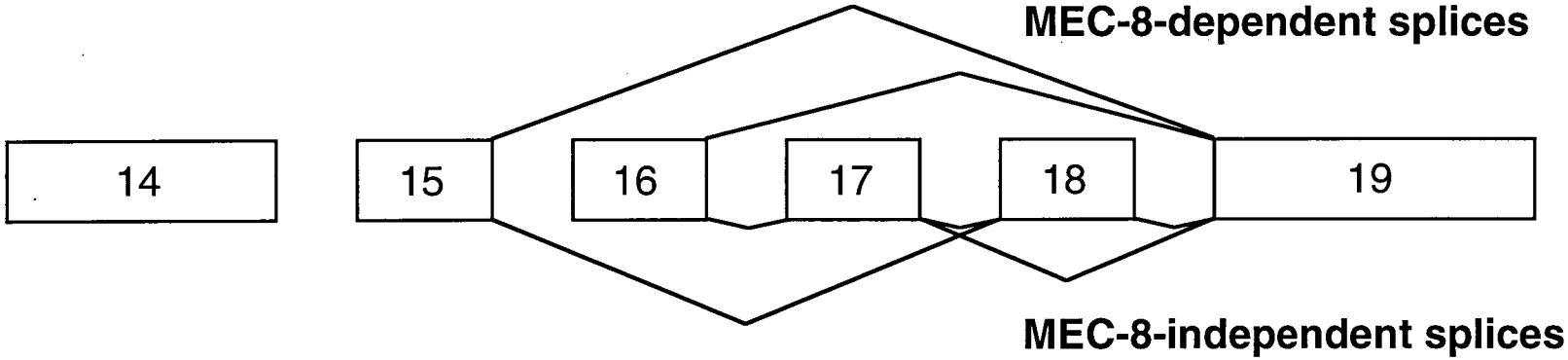
MEC-8-dependent splices
14
15
16
17
18
19
MEC-8-independent splices

that the gene products would be detected in basement membranes associated with muscles and other contractile tissues. In addition, because alternative splicing gives rise to a number of perlecan isoforms, we speculated that these isoforms might be differentially expressed. In many cases, alternative splicing is associated with the expression of tissue-specific isoforms, and we asked whether this was also true for UNC-52/perlecan. To test these predictions, antisera specific to domains III, IV, and V of UNC-52/perlecan were generated and used to study the localization of the three major groups of protein products, the short (domains I - III), medium (domains I - IV), and long (domains I - V) isoforms (Chapter 3). Using an isoform-general antiserum, we found that UNC-52 is localized to basement membranes associated with contractile tissues in *C. elegans*. Using a domain IV-specific antiserum, we found temporal and spatial differences in the localization of UNC-52 isoforms.

These differences in expression and localization suggested that UNC-52 isoforms have distinct roles in *C. elegans* development. To test this hypothesis, we used domain-specific antisera to characterize expression of UNC-52 isoforms in lethal and viable *unc-52* mutants. The molecular and phenotypic differences between these two classes of alleles led us to speculate that lethality is the result of eliminating all UNC-52 isoforms (Rogalski et al., 1993, 1995). In this study, we identified Pat alleles that specifically eliminate domain IV-containing isoforms, indicating that these isoforms are essential for myofilament lattice assembly in the body wall muscles. These observations imply that a specific subset of UNC-52 isoforms is required for body wall muscle development (Chapter 3).

To study the regulation of alternative splicing, we characterized the interactions between *unc-52* and *mec-8* (Chapter 4a). Our results suggest a model for the temporal and qualitative control of isoform expression through *mec-8* and a group of global regulators called heterochronic genes. Finally, we examined the distribution of UNC-52/perlecan in lethal muscle-affecting mutants, and our results suggest that perlecan acts upstream of membrane-associated proteins during myofilament lattice assembly (Chapter 4b).

Chapter 2. Methods and Materials.

Nematode strains and culture conditions.

Nematodes were grown on NGM plates streaked with *Escherichia coli* (OP50 strain), as described by Brenner (1974). Cultures were maintained at 20°, unless otherwise noted. Some strains were obtained from B. D. Williams (University of Illinois at Urbana-Champaign, Urbana, IL) and R. H. Waterston (Washington University, St. Louis, MO), E. A. Lundquist and R. K. Herman (University of Minnesota, St. Paul, MN), R. Schnabel (Max-Planck-Institut Fur Biochemie, Martinsreid, Federal Republic of Germany), and S. E. Mango (University of Utah, Salt Lake City, UT). Additional strains were provided by the Caenorhabditis Genetics Center (CGC). Strains used in this work include the wild-type strain N2; CB444, *unc-52(e444)*; CB669, *unc-52(e669)*; CB998, *unc-52(e998)*; CB1012, *unc-52 (e1012)*; CB1421, *unc-52(e1421)*; DM1184, *unc-52(ra38)*; DM2030, *dpy-10(e128) unc-52(e444)*; DM3102, *unc-52(ut111)/unc-52(e998)*; DM5401, *unc-52(ra401)/unc-52(ra401)/mnDp34*; DR441, *lin-14(n179ts)*; JK1505, *unc-32(e189) glp-1(e2072)/eT1*; MT1524, *lin-28(n719)*; MT3316, *lin-4(e912)/mnC1 dpy-10(e128) unc-52(e444)*; RW1329, *pat-12(st430)/unc-45(e286)*; RW1536, *unc-79(e1068) pat-2(st567)/dpy-17(e164)*; RW3518, *pat-11(st541)/dpy-5(e61)*; RW3538, *myo-3(st386)/sqt-3(e24)*; RW3550, *pat-4(st551)/unc-45(e286)*; RW3562, *unc-44(e362) deb-1(st555)/unc-*

82(e1223) unc-24(e138); RW3563, *pat-5(st556)/unc-82(st1323) unc-24(e138)*; RW3570, *unc-112(st562)/dpy-11(e224) unc-23(e25)*; RW3599, *unc-52(st572)/+*; RW3600, *pat-3(st564)/qC1 dpy-19(e1259) glp-1(q339)*; RW3609, *unc-112(st581)/unc-39(e257)*; RW6010, *unc-52(st549)/unc-52(st549)/mnDp34*; RW6011, *unc-52(st546)/unc-52(st546)/mnDp34*; RW6013, *unc-52(st560)/unc-52(st560)/mnDp34*; SP1248, *mec-8(u218); unc-52(e669su250)*; SP1837, *mec-8(mn463); unc-4(e120)/mnC1 dpy-10(e128) unc-52(e444)* and TU74, *mec-8(u74)*.

Genetics.

To construct *mec-8;unc-52(viable)* double mutants, wild-type (N2) males were crossed to *unc-52(viable)* hermaphrodites. Outcross male progeny (*unc-52/+*) were crossed to *mec-8(u74)* hermaphrodites and wild-type hermaphrodite progeny picked singly to new plates. In addition to the Mec and Dyf phenes (Lundquist and Herman, 1994), *mec-8(u74)* animals move sluggishly, so cross progeny could be reliably distinguished from self progeny on this basis. Genotypically, cross progeny should be either *mec-8/+;unc-52/+* or *mec-8/+;+/+*. Hermaphrodites were allowed to self and plates were scored for presence of Unc progeny, indicating the parental genotype was *mec-8/+;unc-52/+*. Unc progeny were picked singly to new plates and allowed to self; plates were scored for presence of arrested Pat embryos. Previous work established that *mec-8; unc-52(viable)* double mutants have a Pat phenotype (Lundquist and Herman, 1994; R. K. Herman, personal communication; D. G. Moerman, personal communication). Plates with Pat embryos were maintained until large numbers of arrested embryos had accumulated on the medium and used for embryo preparation.

To construct *lin-14;unc-52(viable)* double mutants, *unc-52/+* males were crossed to *lin-14(n179)* hermaphrodites at 15°. *n179* is a temperature-sensitive allele of *lin-14*; *n179* homozygotes exhibit the *lin-14(loss-of-function)* phenotype when grown at 25°, but are

essentially wild-type when grown at 15°. Wild-type hermaphrodites (*lin-14/+;unc-52/+*, *lin-14/+;+/+*, or self progeny) were picked singly to new plates and allowed to self at 15°. Plates were scored for presence of Unc progeny, indicating that the parental genotype was *lin-14/+;unc-52/+*. Unc hermaphrodites were picked singly to new plates, shifted to 25°, and allowed to self. *unc-52(viable)* mutants normally become paralyzed as either L4 larvae or young adults (Mackenzie et al., 1978; Gilchrist and Moerman, 1992). Since we predicted that *lin-14(loss-of-function)* mutations would cause the paralyzed phenotype of *unc-52(viable)* mutations to be manifested earlier in development, we scored plates for animals that became paralyzed before the L4 stage. Several plates were found to have paralyzed L2 and L3 larvae. These small, paralyzed animals were picked singly to new plates and allowed to self at 25°. Progeny were checked for *lin-14* phenes and scored for the stage at which paralysis occurred. Larval stages were determined by measuring body length (n=25) for putative *lin-14;unc-52(viable)* double mutants and for *unc-52(viable)* single mutants, and comparing these with established values for wild-type animals. The extent of distal-tip cell migration was used as an independent indicator of developmental age. *lin-14(n179ts);unc-52(viable)* double mutants were maintained at 15° because these animals have very few progeny at 20°.

To construct *lin-4;unc-52(viable)* double mutants, *unc-52/+* males were crossed to *lin-4(e912)/mnC1 dpy-10(e128) unc-52(e444)* hermaphrodites. Wild-type hermaphrodite progeny (*unc-52/lin-4*, *+/lin-4* or self progeny) were picked singly to new plates and allowed to self. Plates were scored for presence of Unc and Lin progeny, indicating the parental genotype was *unc-52/lin-4*. *lin-4* homozygotes can be recognized by their morphology (somewhat longer and thinner than wild-type) and by their Vul (vulvaless) phenotype. Unc animals were picked singly to new plates and allowed to self. *unc-52* and *lin-4* are ~20 map units apart on LGII, so ~20% of these Unc animals should carry *lin-4*. Plates were then scored for the Lin phenotype to identify *lin-4 unc-52* double mutants.

Subcloning for fusion protein expression.

Bacterial strains DH5α and XL1-Blue were used for subcloning and fusion protein expression. DM#178 and DM#180 clones were constructed by T. M. Rogalski as described in Rogalski et al. (1993). To construct the DM#181 clone, the DM#178 plasmid was digested with *Bam* HI to remove approximately 1200-bp of the insert and religated. To construct the DM#182 and DM#183 clones, 550- and 660-bp *Bam* HI fragments from the DM#178 clone were subcloned into pGEX-1 and pGEX-2T vectors, respectively. DM#184 clone was generated by subcloning a 260-bp *Bam* HI/*Eco* RI fragment from the DM#180 clone into the pGEX-2T vector. To generate the DM#190 clone, PCR was used to amplify a 600-bp fragment from *C. elegans* genomic DNA. The recognition sequence for *Bam* HI was incorporated into the forward primer to introduce this restriction site at the 5' end of the PCR product. Thus, the PCR product has an engineered *Bam* HI site at the 5' end and an internal *Bam* HI site near the 3' end. This PCR product was subcloned into the *Eco* RV site of pBluescript (Stratagene) using the "T-tailing" method described by Collins et al. (1990). Several recombinant clones were obtained and sequenced to confirm absence of PCR-induced errors. A 522-bp *Bam* HI fragment from one of these clones (DM#189) was gel-purified and subcloned into the pGEX-3X vector. To generate the DM#199 clone, PCR was used to amplify a 257-bp fragment from *C. elegans* genomic DNA. The recognition sequence for *Sau* 3A was incorporated into primers to introduce this restriction site at both ends of the PCR product. A 30:1 mixture of *Taq* (Gibco BRL) and *Vent* (New England Biolabs) DNA polymerases was used in amplification reactions to reduce incidence of PCR-induced errors and generate blunt-ended PCR products. These products were ligated into the *Eco* RV site of pBluescript and transformed into DH5α cells. Several recombinant clones were obtained and analyzed by restriction endonuclease digestion. Plasmid DNA from one of these clones, designated DM#198, was digested with *Xba* I and *Xho* I, which recognize sites flanking the insert. A 320-bp *Xba* I/*Xho* I

fragment containing the insert was gel-purified and digested with *Sau* 3A, yielding a 255-bp *Sau* 3A fragment. This fragment was gel-purified and ligated into the *Bam* HI site of the pGEX-3X vector.

Reverse transcription PCR.

C. elegans RNA was generously provided by E. Mathews. For reverse transcription, 1 µl (0.5 - 1 µg) of total RNA was combined with 1 ul reverse primer (25 pmol/µl), incubated at 70° for 10 min. and chilled on ice. 8 µl of a master mix containing 1 µl 10x PCR buffer (Gibco BRL), 1 µl 10 mM dNTPs (2.5 mM each dNTP), 1 µl 100 mM DTT, 0.5 µl 50 mM $MgCl_2$, 0.5 µl RNasin, 0.5 µl Superscript II RT (Gibco BRL) and 3.5 µl dH_2O per reaction, was added to each tube. Tubes were incubated at 42° for 60 min. and at 95° for 15 min. For PCR amplification, 1 µl of forward primer (25 pmol/µl) and 14 µl of a master mix containing 1.5 µl 10x PCR buffer, 1 µl 10 M dNTPs, 0.5 µl *Taq* DNA polymerase (Gibco BRL) and 11 µl dH_2O per reaction, were added to each tube. Reverse transcription products were amplified for 30 cycles consisting of 30 sec at 95°, 60 sec at 50 - 55°, and 90 sec at 72°.

Fusion protein expression, purification, and analysis.

To analyze expression of fusion proteins, cell lysates were prepared from cultures after induction with IPTG. 0.1 ml of overnight culture was added to 1 ml fresh medium and grown for 60 - 90 min. IPTG (Gibco BRL or Boehringer Mannheim) was added to 1 mM and the culture grown an additional 60-90 min. Cells were pelleted by centrifugation, resuspended in 50 µl 1x Laemmli sample buffer (50 mM Tris-CL (pH 6.8), 100 mM dithiothreitol, 10% glycerol, 2% SDS and 0.1% bromophenol blue), and boiled for 5 min.

4 - 5 µl of each sample was analyzed by SDS-PAGE and Coomassie staining or Western blotting.

GST fusion proteins were purified as described by Smith and Johnson (1988) with some modifications. For large scale preparations, 20 - 30 ml overnight cultures were grown at 37° with shaking in 2xYT containing 100 µg/ml ampicillin. 10 - 15 ml of overnight culture was added to 250 ml of fresh medium and grown for 2 - 3 hours at 37° with shaking. IPTG was added to a final concentration of 1 mM, and cultures were grown an additional 2 - 4 hours. Cells were pelleted by centrifugation at 10,000 RPM and resuspended in MT-PBS (150 mM NaCl, 16 mM Na_2HPO_4, 4 mM NaH_2PO_4) supplemented with PMSF and EDTA to a final volume of 9 ml. Cells were lysed by gentle sonication (6 x 30 sec. with chilling on ice between bursts). 1 ml of 10% Triton X-100 (in MT-PBS) was added and the suspension incubated for 5 min. at 4°. Insoluble debris was pelleted by centrifugation at 10,000 RPM and the supernatant transferred to a 15 ml conical centrifuge tube containing 2 - 3 ml pre-swollen glutathione-agarose beads (Sigma Chemical Company). The tube was rotated gently for 5 min. at room temperature. Beads were washed 5x in MT-PBS + 1% Triton X-100, followed by 2x in MT-PBS without detergent. Bound fusion protein was eluted 3x at room temperature with 1 volume of elution buffer (50 mM Tris-CL, 10 mM glutathione) and stored at -20°.

Generation of polyclonal antisera.

To generate polyclonal antisera, New Zealand White rabbits were injected subcutaneously with purified fusion protein emulsified in Freund's complete adjuvant (approximately 0.5 mg protein/rabbit). For each fusion protein, two rabbits were used, and serum from one of these was chosen for further study. In all cases, we found that antisera from these replicates gave similar results in Western blotting and immunofluorescence experiments. Rabbits were usually boosted at 4-week intervals with fusion protein emulsified in

Freund's incomplete adjuvant (approximately 0.25 mg protein/rabbit) and blood samples taken 10 to 12 days post injection. Immune response was monitored by Western blotting of purified fusion proteins and immunofluorescence staining.

Western blotting.

Proteins were resolved by SDS-PAGE and transferred to Hybond ECL nitrocellulose membrane (Amersham) for 15 - 30 min. at 12 - 15 V in a Trans-Blot SD Electrophoretic Transfer Cell (BioRad). Blots were blocked overnight at 4° in 5% milk powder-TBS-T (TBS-T: 20 mM Tris (pH 7.6), 137 mM NaCl, 0.1% Tween 20) and incubated with primary antibodies (see below) in 0.5% milk powder-TBS-T for 2 - 3 hours at room temperature. After washing in TBS-T, blots were incubated with horseradish peroxidase-labelled secondary antibodies (see below) in 0.5% milk powder-TBS-T for approximately 45 min. at room temperature. After washing in TBS-T and in TBS, blots were incubated for 1 min. in ECL detection reagents (Amersham) and exposed to film (Kodak X-OMAT).

For Western blotting, rabbit polyclonal sera were diluted as follows: GM1 (1:5000 - 1:20000), GM3 (1:10000 - 1:50000), and GM9 (1:5000 - 1:50000). Mouse monoclonal antibodies MH2 and MH3 (Francis and Waterston, 1991) were diluted 1:200 (for ascites fluid). Secondary antibodies, horseradish peroxidase-labelled goat anti-rabbit IgG or goat anti-mouse IgG (Amersham), were diluted 1:10000 and 1:5000, respectively.

Immunofluorescence staining.

Embryos were prepared and stained as described by Goh and Bogaert (1991) with some modifications. Worms were grown on 4 to 8 100 mm NGM plates until large numbers of mid- and late-stage embryos had accumulated. Worms and embryos were washed off plates and treated with an alkaline sodium hypochlorite solution to dissolve worms and

release any unlayed eggs. Embryos were washed several times in M9 buffer, fixed in 3% formaldehyde, and stored in 100% methanol at -20° until needed. For staining, embryos were rehydrated through a graded methanol series, washed several times in TBS, and resuspended in 2% milk powder-0.1% Tween 20-TBS. In some experiments, embryos were treated with acid-urea (6M urea, 100mM glycine, pH 3.5) for 15 min. at room temperature following rehydration, washed twice in dH_2O, and resuspended in 2% milk powder-0.1% Tween 20-TBS. This acid-urea treatment has been shown to unmask hidden epitopes in vertebrate basement membranes (Yoshioka et al., 1994). Primary antibodies (see below) were added and embryos incubated overnight at 4°. Embryos were washed extensively in TBS-T, resuspended in 2% milk powder-0.1% Tween 20-TBS, and incubated with fluorescently-labelled secondary antibodies for 2 hours at 20°. After extensive washing in TBS-T and in TBS, embryos were resuspended in mounting medium with an antifade agent (2.5% DABCO-90% glycerol-TBS).

Larvae and adults were stained as described by Finney and Ruvkun (1990), with some modifications. Worms were washed off 4 - 12 large NGM plates with M9 buffer and pelleted by gentle centrifugation. Worms were resuspended in 4% sucrose, 1 mM EDTA and gently rocked for 30 min. The worms were pelleted by gentle centrifugation and most of the sucrose solution was aspirated away, leaving worms in a small volume. An equal volume of 2x Ruvkun Fixation buffer with 50% methanol was added and contents of the tube were mixed gently. Formaldehyde (J.B. EM Services) was added to a final concentration of 2% and worms were frozen at -80° until needed. The tube was thawed under cold tap water and incubated on ice for 30 min. Worms were washed twice in Tris-Triton buffer (TBT - 100 mM Tris-Cl (pH 7.4), 1mM EDTA, 1% Triton X-100), resuspended in TBT + 1% 2-mercaptoethanol, and incubated for 2 hours at 37° with gentle rocking. This treatment reduces some of the disulfide bonds in the nematode cuticle. To complete the reduction reaction, worms were washed once in $1xBO_3$ (50 mM H_3BO_3 (pH 9.5), 2.5 mM NaOH)+ 0.01% Triton X-100, resuspended in $1xBO_3$ + 0.01% Triton X-

100 + 10 mM dithiothreitol, and incubated for 15 min. at room temperature. Worms were washed once in 1xBO_3 buffer + 0.01% Triton X-100. To oxidize -SH groups, worms were resuspended in 1xBO_3 buffer + 0.01% Triton X-100 + 0.3% hydrogen peroxide, and incubated for 15 min. at room temperature. Worms were washed once in 1xBO_3 buffer + 0.01% Triton X-100, followed by AbA (PBS + 0.01% Triton X-100 + 2% milk powder + 0.05% sodium azide) where they were stored until needed.

For immunofluorescence staining, worms were pelleted by gentle centrifugation and resuspended in fresh AbA. Primary antibodies were added and worms incubated overnight at 15°. After extensive washing in AbA, worms were pelleted by gentle centrifugation and resuspended in fresh AbA. Secondary antibodies were added and worms incubated overnight at 15°. After extensive washing in AbA and in PBS, worms were pelleted by gentle centrifugation, and resuspended in mounting medium.

In some experiments, larvae and adults were stained using a freeze-fracture procedure adapted from Albertson (1984). Worms were washed off 1 - 3 small NGM plates with M9 buffer and pelleted by gentle centrifugation. The worms were resuspended in 4% sucrose, 1 mM EDTA, and pelleted again by gentle centrifugation. Most of the sucrose solution was aspirated, leaving worms in approximately 250 µl of solution. 20 - 25 µl of suspended worms were pipetted onto a polylysine-coated slide and a 24x50 (thickness 2) coverslip placed on top. Slides were placed on a metal block (pre-cooled to -80°) and stored at -80° until needed. For staining, coverslips were flipped off with a razor blade and slides placed in a coplin jar filled with -20° methanol. Worms were fixed in -20° methanol for 4 min., -20° acetone for 4 min., and rehydrated through a graded acetone series. Slides were washed in TBS and the area surrounding the worms carefully dried with Whatman paper. Slides were placed in humidified chambers and 50 - 100 µl of diluted primary antibody (in 1% BSA-TBS-T) was carefully pipetted onto worms. Worms were incubated with primary antibodies overnight at 15° and washed extensively in TBS-T. The area surrounding the worms was carefully dried, the slides returned to the humidified

chambers, and 50 - 100 µl of diluted secondary antibodies (in 1% BSA-TBS-T) pipetted onto slides. Worms were incubated with secondary antibodies for 2 hours in the dark at room temperature and washed extensively in TBS-T. 10 - 15 µl of mounting medium was pipetted onto worms and a 24x50 (thickness 1 or 2) coverslip placed on top.

For immunofluorescence staining, rabbit polyclonal sera were diluted as follows: GM1 (1:400), GM3 (1:1500 - 1:6000), and NW68 (1:100; Graham et al., 1997). Mouse monoclonal antibodies DM5.6 (Miller et al., 1983), MH2/3 (Francis and Waterston, 1991), and MH25 (Francis and Waterston, 1985) were diluted 1:40 - 1:50, 1:100 - 1:200, and 1:50 - 1:100, respectively. Secondary antibodies, FITC-labeled donkey anti-rabbit IgG $F(ab')_2$ and TRSC-labeled donkey anti-mouse IgG $F(ab')_2$ (Jackson ImmunoResearch Laboratories), were diluted 1:200 for most experiments. We thank H. F. Epstein, D. M. Miller, M. C. Hresko, and J. M. Kramer for generously providing antibodies.

Phalloidin staining.

To visualize filamentous actin, embryos were stained with FITC-labeled phalloidin as described by Barstead and Waterston (1989). Briefly, embryos were prepared from mixed populations of worms and embryos, fixed in 100% ethanol for 10 min. at -20°, rehydrated through a graded ethanol series, and stained with 80 nM FITC-phalloidin (Sigma Chemical Company) in PBS for 2 hours at 20°. After washing in PBS, embryos were resuspended in mounting medium, as described previously.

Microscopy.

Immunofluorescence staining was viewed on either a Zeiss Axiophot or a Nikon Optiphot-2 microscope. The Optiphot-2 was equipped for both epifluorescence and confocal laser scanning microscopy (CLSM). Confocal images were captured on a BioRad MRC 600

system using the CoMOS 7.0a application. For single channel collection, either the BHS (blue excitation - 488 nm) or the YHS (yellow excitation - 568 nm) filter was used, depending on the fluorochrome. For dual channel collection, K1 and K2 filters were used. In practice, we captured each channel separately (using the K1 and K2 filters) instead of simultaneously because this reduced bleed-through between channels. For most samples, the confocal aperture was set between 2 and 3 because this provided the best compromise between brightness and confocality. The neutral density filter was usually set to 2 (attenuates laser to 3% of its maximal intensity), but settings of 1 (30%) or 3 (0.3%) were used for some specimens, depending on the brightness of the fluorescence. Scan speed was set to "normal" and a kalman filter (4 scans) was used to reduce background noise.

For embryos, we collected Z-series consisting of 400X400 pixel images taken at 0.2 μm intervals (Z-steps) for the full depth of the specimen (usually 20 to 30 μm). For larvae and adults, we collected Z-series consisting of 384X256 or 768X512 pixel images taken at 0.2 - 0.5 μm intervals for the depth of the tissue of interest (i.e. body wall muscles, pharynx, etc.). After collection, we generated maximum projections of each Z-series using the "enhance>project Z-series" function in CoMOS.

Z-series and projections were transferred to a Macintosh computer (Power Macintosh 7500/100) for analysis and assembly into figures for publication. Z-series were imported into NIH Image for viewing and manipulation, including making additional projections, rotating images, and generating vertical sections. For publication, projections were imported into Adobe Photoshop, cropped to desired size and resolution, arranged and labeled, and saved as Photoshop files. Figures were converted to TIFF format (with LZY compression) for printing on a Codonics NP-1600 Printer.

Chapter 3. Localization and Function of UNC-52 Isoforms.

Background.

Alternative splicing of *unc-52* pre-mRNA gives rise to a number of distinct protein isoforms (Rogalski et al., 1993, 1995). These isoforms can be divided into three general groups based on their domain structure (Figure 4; Rogalski et al., 1993; T. M. Rogalski, G. P. Mullen, and D. G. Moerman, unpublished results). Short (S) isoforms contain the first three domains (I - III), medium (M) isoforms contain the first four domains (I - IV), and long (L) isoforms contain all five domains (I - V) (Rogalski et al., 1993; T. M. Rogalski, G. P. Mullen, and D. G. Moerman, unpublished results). Alternative splicing of exons 6, 16, 17, 18, 21, and 22 generates additional diversity within domains III and IV (Rogalski et al., 1993, 1995).

We used antibodies to study the expression and localization of UNC-52 isoforms in wild-type and mutant animals. Two monoclonal antibodies (mAbs), MH2 and MH3, had been shown to recognize a component of basement membranes associated with contractile tissues in *C. elegans* (Francis and Waterston, 1991), but the identity of the corresponding gene was not known. We mapped the epitopes recognized by these mAbs to two NCAM repeats encoded by exon 19 of *unc-52*. These results demonstrated that UNC-52 is indeed a component of basement membranes in *C. elegans*.

However, MH2 and MH3 do not recognize all UNC-52 isoforms. S isoforms of UNC-52, which lack domain IV, are not recognized by MH2 or MH3, and were missed in studies using these mAbs. Potentially, the conformation of some UNC-52 isoforms might also preclude binding by these mAbs. Furthermore, because the NCAM repeats encoded by exon 19 may be present in all UNC-52 isoforms containing domain IV, it has not been possible to sub-divide this group of isoforms.

To extend our analysis of UNC-52 isoform localization, we raised polyclonal sera against distinct regions of the UNC-52 amino acid sequence. These antisera recognize defined groups of UNC-52 isoforms (Figure 6), and have been used to characterize the expression and localization of these isoforms in wild-type animals throughout development. These antisera have also been used to characterize the localization of UNC-52 isoforms in viable and lethal *unc-52* mutants. This allowed us to relate the distribution of UNC-52 isoforms to their specific roles in development.

Results.

Two monoclonal antibodies, MH2 and MH3, recognize epitopes in domain IV of UNC-52.

To confirm that MH2 and MH3 recognize proteins encoded by *unc-52*, we expressed regions of *unc-52* coding sequence as fusions with glutathione-S-transferase (GST) in *E. Coli*. *Eco* RI restriction fragments from *unc-52* cDNAs were subcloned into appropriate pGEX vectors. Initially, two constructs producing inducible fusion proteins were obtained (Figure 7): (i) DM#178, which contains a 1200-bp insert corresponding to exons 14, 15, 18, 19 and 20, and (ii) DM#180, which contains a 900-bp insert corresponding to exons 7, 8, 9 and 10. The corresponding fusion proteins were purified as described by Smith and Johnson (1989), and tested by Western blotting for MH2 and MH3 immunoreactivity.

Figure 6. Physical map of the *unc-52* gene and restriction fragments expressed as fusion proteins.

(A) Restriction fragments from *unc-52* cDNAs were subcloned into pGEX vectors and expressed as fusion proteins (DM#183, DM#184, and DM#199). These fusion proteins were then used to generate polyclonal antisera (GM1, GM3, and GM9) that recognize distinct regions of the UNC-52 protein sequence. The mAbs MH2 and MH3 are also indicated. (B) Flow chart indicating the specificity of these antibodies for the three major groups of UNC-52 isoforms.

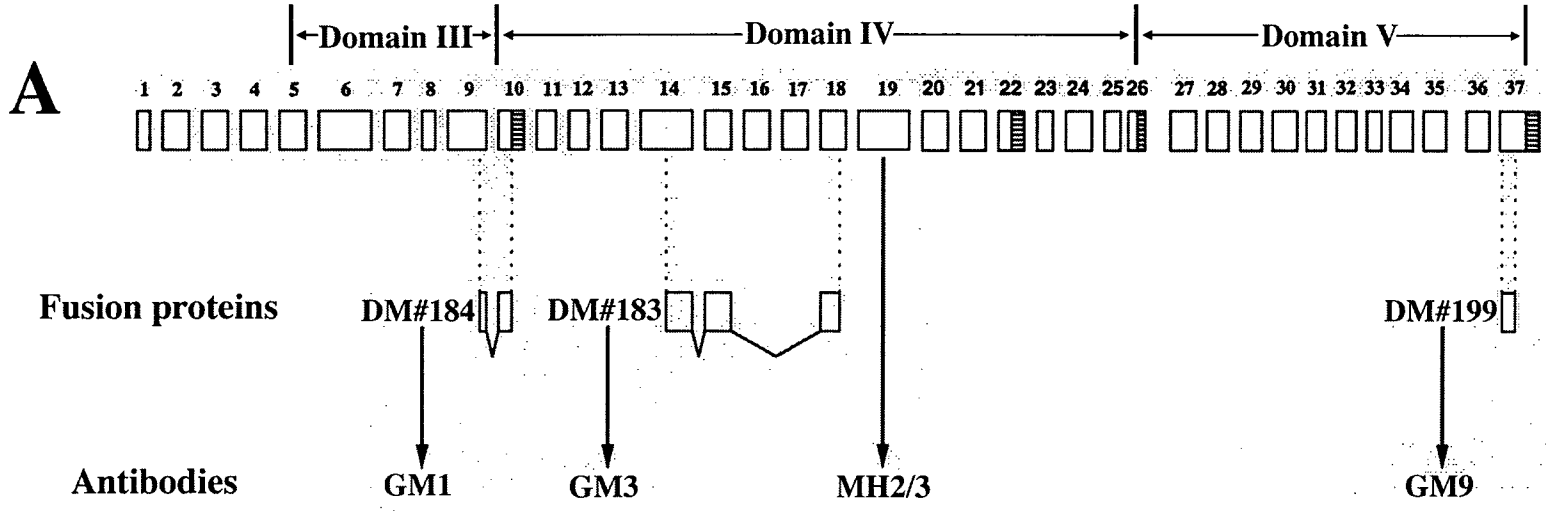

B

All isoforms - GM1
(short, medium & long isoforms)

↓

Domain IV-containing isoforms - GM3 & MH2/3
(medium & long isoforms)

↓

Domain V-containing isoforms - GM9
(long isoforms)

Figure 7. MH3 recognizes epitopes encoded by exon 19 of *unc-52*.

(A) Diagram of *unc-52* showing regions expressed as GST fusion proteins (DM#178 and DM#180). (B) Western blot of fusion proteins. Molecular weight markers (A lanes) and affinity-purified GST fusion proteins from DM#178 (B lanes), DM#180 (C lanes), and pGEX-3X (D lanes) were probed with anti-GST serum or the mAb MH3. Approximate positions of molecular weight markers are indicated. MH3 specifically recognizes the DM#178 fusion protein. (C) Summary of epitope mapping experiments. *Bam*HI restriction fragments from the positive clone DM#178 were subcloned into pGEX vectors and expressed as GST fusion proteins (DM#181, DM#182, and DM#183). Of these, only the DM#182 fusion protein is recognized by MH2 and MH3. An exon 19-specific fusion (DM#190) was then constructed; this fusion is recognized by MH2 and MH3, indicating that both mAbs recognize epitopes encoded by this exon. (D) Western blot of fusion proteins. Molecular weight markers (A lanes) and affinity-purified GST fusions from DM#178 (B lanes), DM#183 (C lanes), DM#182 (D lanes), DM#181 (E lanes), and DM#190 (F lanes) were probed with anti-GST serum or the MH3 mAb. Approximate positions of molecular weight markers are indicated.

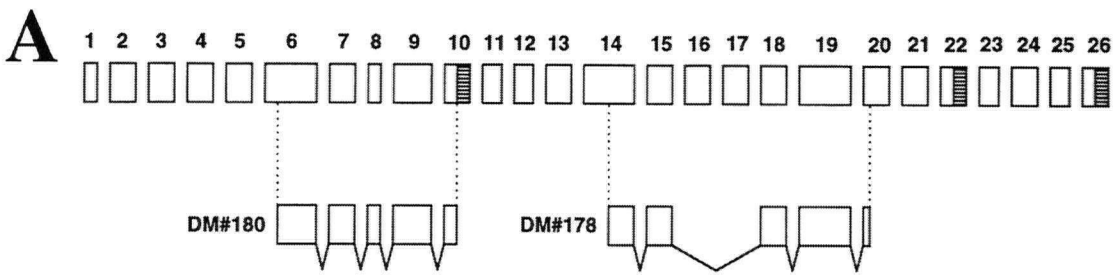
A
1 2 3 4 5 6 7 8 9 10 11 12 13 14 15 16 17 18 19 20 21 22 23 24 25 26
DM#180
DM#178

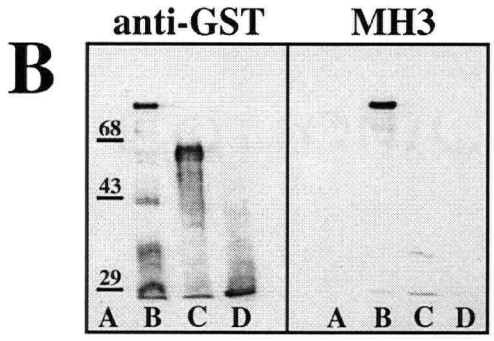
B
anti-GST
MH3
68
43
29
A B C D
A B C D

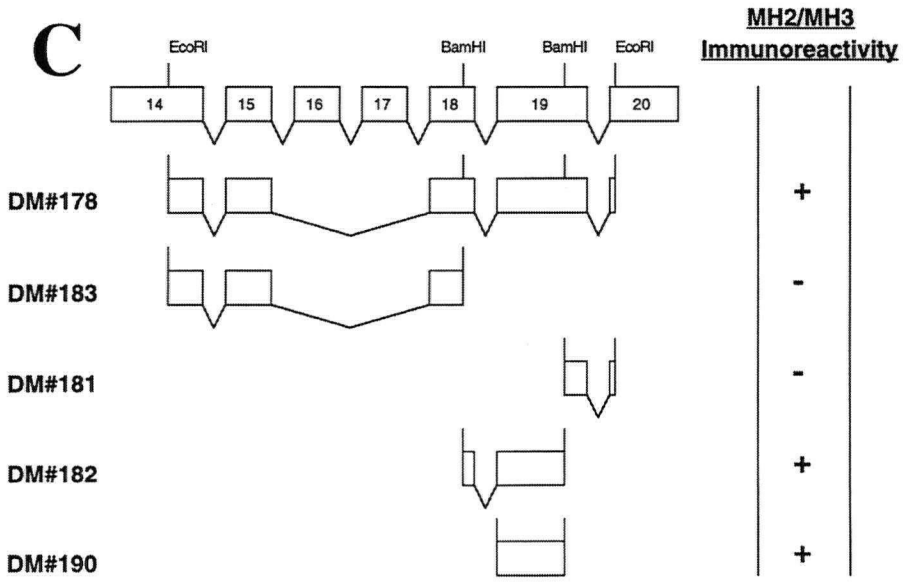
C
MH2/MH3
Immunoreactivity
EcoRI
BamHI
BamHI
EcoRI
14 15 16 17 18 19 20
DM#178
DM#183
DM#181
DM#182
DM#190
+
-
-
+
+

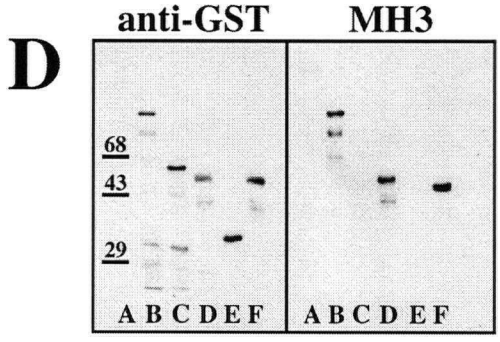
D
anti-GST
MH3
68
43
29
A B C D E F
A B C D E F

Results for MH3 are shown in Figure 7. We found that both mAbs specifically recognize the DM#178 fusion protein. This demonstrated that MH2 and MH3 recognize epitopes encoded by *unc-52* and that these epitopes are present in domain IV (Rogalski et al., 1993).

The epitopes recognized by MH2 and MH3 were mapped more precisely using a similar strategy. *Bam* HI restriction fragments from the positive clone (DM#178) were subcloned into pGEX vectors and expressed as fusion proteins. Three constructs were obtained (Figure 7): (i) DM#183, which contains a 660-bp insert corresponding to exons 14, 15, and 18, (ii) DM#182, which contains a 550-bp insert corresponding to exons 18 and 19, and (iii) DM#181, which contains a 250-bp insert corresponding to part of exons 19 and 20. We purified the corresponding fusion proteins and tested these for MH2 and MH3 reactivity by Western blotting. We found that the DM#182 fusion protein is specifically recognized by MH2 and MH3, indicating that both mAbs bind epitopes present in the region defined by this clone.

These mapping experiments suggested that the MH2 and MH3 epitopes were probably encoded by exon 19. To test this prediction, we amplified exon 19 sequences using PCR and constructed an exon 19-specific GST fusion (Figure 7). We purified and tested this fusion protein as described for the previous experiments. We found that this fusion, designated DM#190, is specifically recognized by MH2 and MH3, demonstrating that both antibodies bind epitopes encoded by exon 19 (Rogalski et al., 1995).

GM1, a polyclonal serum that recognizes all UNC-52 isoforms.

To extend our analysis of UNC-52 isoform localization, we generated a new polyclonal antiserum that recognizes all UNC-52 isoforms. This new antiserum, designated GM1, recognizes epitopes in domain III of UNC-52. These epitopes, encoded by a portion of

Figure 8. Western blotting with new polyclonal sera against UNC-52::GST fusion proteins.

(A) Molecular weight markers (A lanes) and affinity-purified GST fusion proteins from DM#184 (B lanes) and pGEX-3X (C lanes) were probed with anti-GST serum (left), GM1 (-GST) (middle), or pre-immune serum (right). GM1 specifically recognizes the DM#184 fusion protein. (B) Molecular weight markers (A lanes) and affinity-purified GST fusion proteins from DM#183 (B lanes) and pGEX-3X (C lanes) were probed with anti-GST serum (left), GM3 (-GST) (middle), or pre-immune serum (right). GM3 specifically recognizes the DM#183 fusion protein. (C) Molecular weight markers (A lanes) and affinity-purified GST fusion proteins from DM#199 (B lanes) and pGEX-3X (C lanes) were probed with anti-GST serum (left), GM9 (-GST) (middle), or pre-immune serum (right). GM9 specifically recognizes the DM#199 fusion protein. Approximate positions of molecular weight markers are indicated.

A

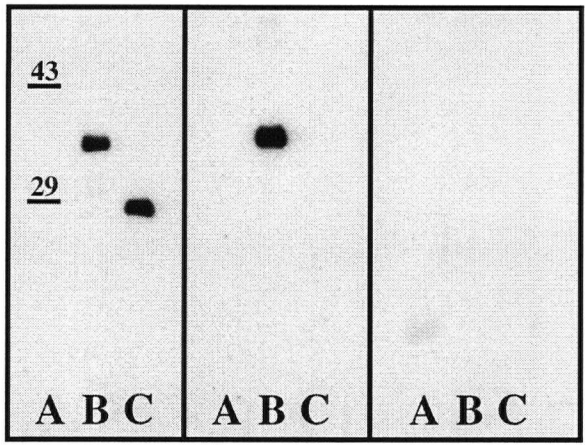

B

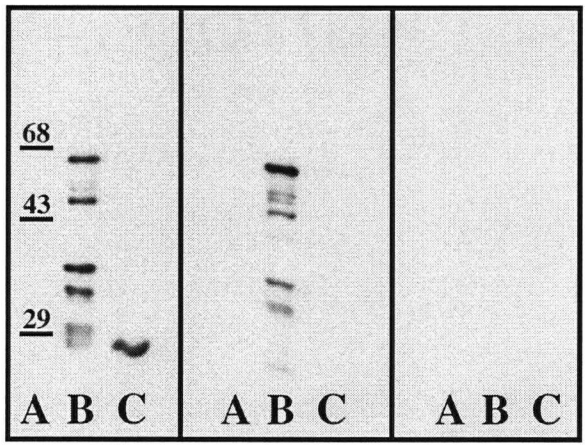

C

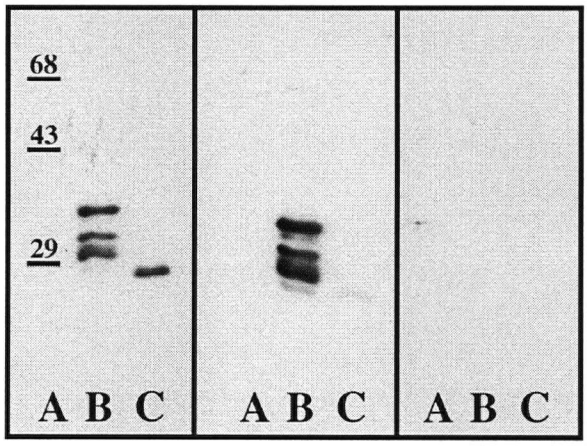

exons 9 and 10, are present in all *unc-52* gene products. GM1 was raised against an UNC-52::GST fusion protein (DM#184), and has been shown to recognize this fusion on Western blots (Figure 8). To verify that GM1 specifically recognizes UNC-52 in immunofluorescence experiments, we stained *unc-52(null)* embryos (Rogalski et al., 1993, 1995) with this antiserum and found no detectable staining. In addition, no staining was observed in wild-type animals stained either with secondary antibodies by themselves, or with pre-immune serum (data not shown).

We characterized the expression and localization of UNC-52 proteins in *C. elegans* using this new antiserum for immunofluorescence staining. In these experiments, we stained wild-type animals with GM1 and the mAb DM5.6, which recognizes the minor body wall muscle myosin, MHC A (Miller et al., 1983). DM5.6 was included to identify body wall and anal muscles, and allow visualization of the myofilament lattice. We used confocal laser scanning microscopy (CLSM) to capture high-resolution "3-dimensional" images of *C. elegans* embryos, larvae, and adults stained with these antibodies. Using this approach, we examined the distribution of UNC-52 throughout development to determine the developmental profile of expression and localization.

UNC-52 is expressed in the pharynx, body wall muscles, and anal muscles during embryonic development in *C. elegans*.

We found that UNC-52 is synthesized in the pharynx, body wall muscles, and anal muscles, and is detected in the adjacent basement membranes during embryonic development (Table 1). UNC-52 was detected in embryos as early as the comma stage (~350 minutes after the first cell division). By this stage, body wall muscle cells have completed their migrations and formed the dorsal and ventral muscle quadrants (Hresko et al., 1994; Moerman et al., 1996). In early comma stage embryos, GM1 stains regions of contact between adjacent body wall muscle cells (Figure 9). Intracellular staining of body

wall muscle cells can also be detected (Figure 9). In contrast, we have not detected staining in the hypodermis, suggesting that body wall muscle cells are the primary source of UNC-52. Our results, however, do not exclude the possibility of a minor contribution from hypodermis.

In early comma stage embryos, accumulation of MHC A within body wall muscles is detected with the mAb DM5.6. MHC A is reported to be expressed in earlier embryos (Hresko et al., 1994), but we did not observe significant staining until the comma stage. At this stage, MHC A has not yet assembled into A-bands, and is found throughout the cytoplasm of each body wall muscle cell. Localization of UNC-52 to regions of contact between muscle cells occurs prior to assembly of myosin into ordered A-bands.

In late comma stage embryos, MHC A is concentrated beneath the basal face of each muscle cell, particularly in regions where cells contact each other (also see Hresko et al., 1994; Moerman et al., 1996). Comparison of MHC A and UNC-52 in these embryos shows that MHC A is concentrated beneath regions where UNC-52 has accumulated. Concentration of muscle proteins such as myosin beneath the plasma membrane is called muscle cell polarization, and is disrupted in *unc-52(lethal)* mutants (Rogalski et al., 1993; Hresko et al., 1994; Williams and Waterston, 1994).

Between the comma and two-fold stages, staining spreads from these regions of cell-cell contact over the basal face of each muscle cell, where the basement membrane between the muscle and hypodermis is located. Concurrently, the distribution of myosin in muscle cells becomes increasingly filamentous. By the two-fold stage, GM1 stains the basal face of each body wall muscle cell and myosin is organized into distinct A-bands.

GM1 also stains the pharynx soon after the comma stage. In 1.5-fold embryos, GM1 stains the posterior end of the pharynx, which is composed of cells derived from the MS lineage (Sulston et al., 1983). The anterior pharynx, which is composed of cells derived from the AB lineage (Sulston et al., 1983), begins to stain somewhat later

Figure 9. Immunolocalization of UNC-52 and myosin at different stages of embryonic development.

Embryos were visualized by laser scanning confocal microscopy. Wild-type embryos were double-labeled with GM1 (UNC-52; panels A, C, E, and G) and DM5.6 (myosin heavy chain A; panels B, D, F, and H). Panels A and B show the dorsal view of a comma stage embryo (~350 min.); these images are projections of the dorsal Z-sections, while the remaining images are projections of the complete Z-series. Arrows indicate positions of two adjacent muscle cells; the arrowhead indicates intracellular staining with GM1. Panels C and D show the lateral view of late comma stage embryo (~350 - 400 min.). Arrows indicate the position of a muscle cell, while the arrowheads indicate the basal face of the cell. Note that myosin is not concentrated beneath the basal face of the muscle cell, but is present throughout the cell. Panels E and F show the lateral view of a 1.5-fold embryo (~420 min.). The arrow in both panels indicates the basal face of the muscle cells in a dorsal quadrant. Note that myosin is now concentrated beneath the basal face. Also note pharyngeal staining (arrowhead) in panel E. Panels G and H show a three-fold embryo (~800 min.). Note that UNC-52 is now associated with the pharynx (arrowhead in G) and body wall muscles, and myosin is organized into distinct A-bands (arrow in H). The anal muscles also stain, indicated with an arrow in G. Scale bar indicates 10 microns.

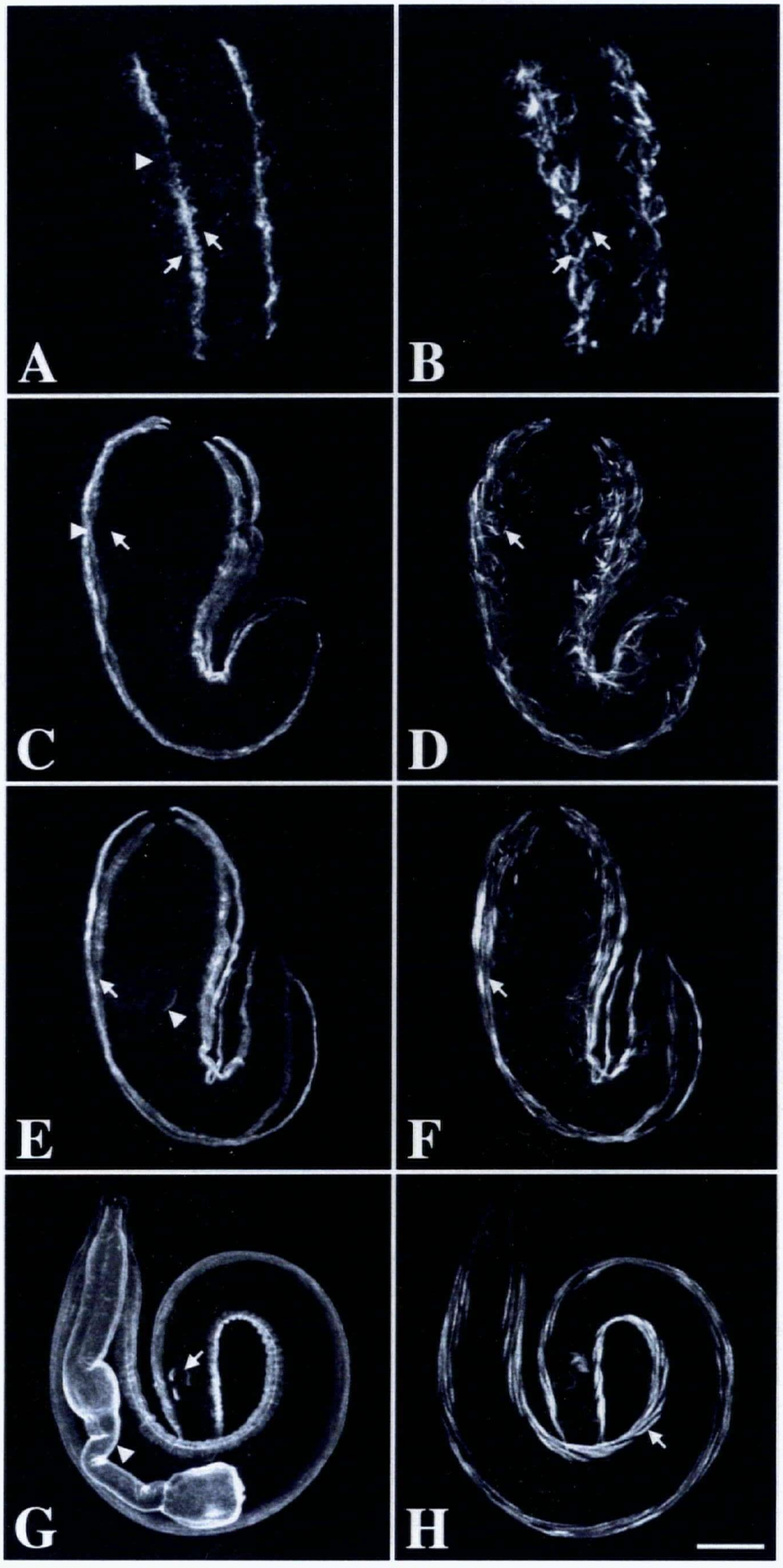
A
B
C
D
E
F
G
H

than the posterior. However, by the three-fold stage of development, GM1 staining completely surrounds the pharynx from the anterior margin to the pharyngeal-intestinal valve. Intracellular staining of both anterior and posterior pharyngeal cells has been observed, suggesting that pharyngeal cells from both lineages express *unc-52*. Analysis of *glp-1* and *pha-4* mutants (see below) has provided further evidence that *unc-52* is expressed in the pharynx and acts in a cell-autonomous manner.

There are few changes in the distribution of UNC-52 after the two-fold stage. In three-fold embryos, GM1 stains the anal sphincter and depressor muscles, in addition to the pharynx and body wall muscles (Figure 9). Surprisingly, the pair of muscle cells located at the posterior end of the intestine do not stain, although these cells are surrounded by basement membrane. Similarly, we have not observed staining of the basement membranes that line the pseudocoelom and surround the intestine. In summary, by the three-fold stage of embryogenesis, GM1 stains basement membranes associated with pharyngeal, body wall, and anal muscles (Table 1). This staining pattern was not affected by different fixation methods, nor by treatment with acid-urea, which has been shown to unmask hidden epitopes.

UNC-52 is expressed in the pharynx and acts cell autonomously.

The *glp-1* and *pha-4* genes specify the fate of cells destined to form part (*glp-1*) or all (*pha-4*) of the pharynx (Priess et al., 1987; Mango et al., 1994). Some *glp-1* alleles, such as *e2072*, are maternal effect lethals and affect specification of the ABa blastomere (Priess et al., 1987). Progeny of *glp-1(e2072)* homozygotes lack an anterior pharynx, which is derived from the ABa blastomere (Figure 10), and have extra neuronal and hypodermal cells instead. *pha-4* alleles, such as *q490*, are strictly zygotic lethals and affect generation of the pharyngeal primordeum. In *pha-4(q490)* embryos, the entire pharynx is missing, as well as certain rectal cells (Mango et al., 1994). We stained *glp-1(e2072)* and *pha-4(q490)*

Figure 10. Pharyngeal lineage and structure in *C. elegans*.

(A) The digestive tract in *C. elegans* can be divided into four sections: anterior pharynx, posterior pharynx, intestine, and rectum. The cell lineages from which these sections are derived are indicated (ABa, MS, E, and ABp). Adapted from Fukushige et al., 1996. (B) Organization of pharyngeal muscles (m1 - m8). Pharynx is oriented with the anterior at the top of the diagram. Shaded circles indicate positions of muscle cell nuclei. Adapted from Moerman and Fire, 1997.

A

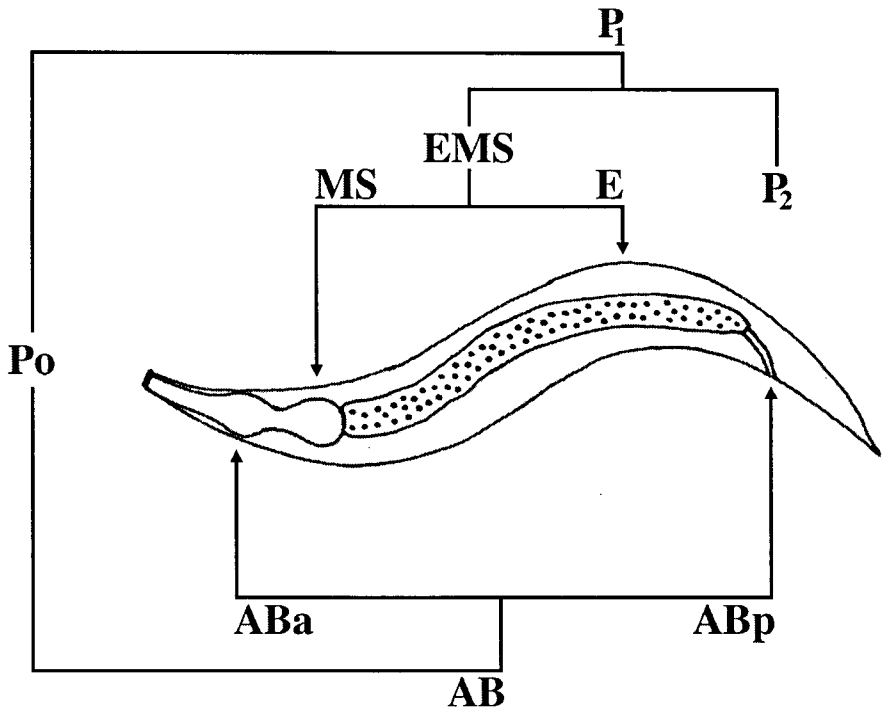
P1
EMS
MS
E
P2
Po
ABa
ABp
AB

B

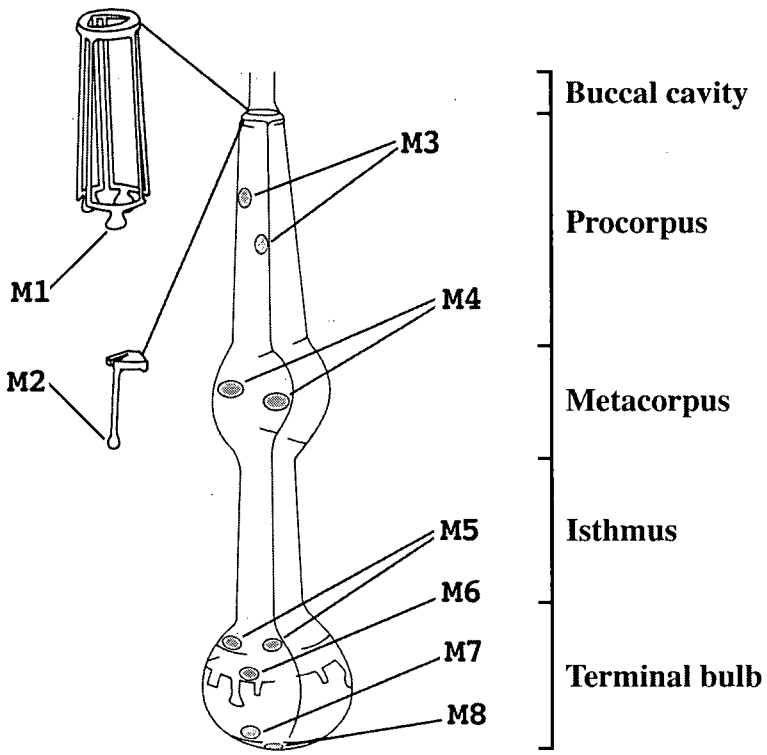
M1
M2
M3
M4
M5
M6
M7
M8
Buccal cavity
Procorpus
Metacorpus
Isthmus
Terminal bulb

Figure 11. Immunolocalization of UNC-52 in *pha-4* and *glp-1* mutant embryos.

Embryos were visualized by laser scanning confocal microscopy. *pha-4(q490)* (A and B) and *glp-1(e2072)* (C and D) mutant embryos were double labeled with GM1 (A and C) and the mAb MH3 (B and D). Arrows indicate the approximate position of the AB-derived anterior pharynx, while arrowheads indicate the position of the MS-derived posterior pharynx. Note the complete absence of pharyngeal staining in the *pha-4* mutant embryo. Also note that GM1 staining is associated with the MS-derived posterior pharynx in *glp-1* mutants, but is absent from the anterior where the AB-derived anterior pharynx would normally be found. Scale bar indicates 10 microns.

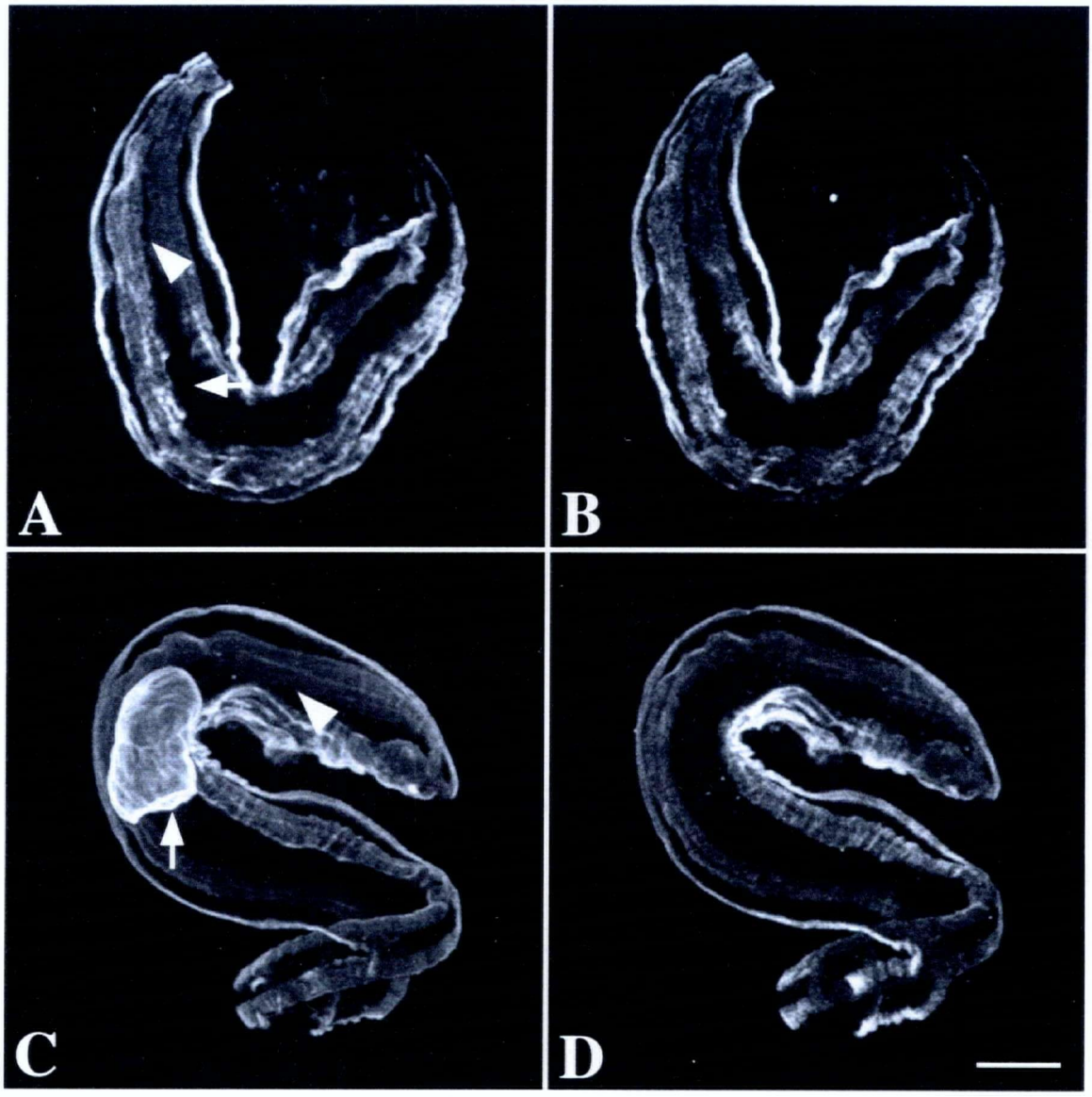
A
B
C
D

mutant embryos with GM1 to examine the localization of UNC-52 in animals missing part or all of the pharynx.

In *pha-4(q490)* mutant embryos, which completely lack a pharynx, GM1 stained the body wall muscle quadrants, but was completely absent from the head region where the pharynx would normally be found (Figure 11). This supports our conclusion, based on characterization of wild-type embryos, that *unc-52* is expressed in the pharynx. In *glp-1(e2072)* mutant embryos, which lack the ABa-derived anterior pharynx, GM1 staining was restricted to the posterior end of the pharynx and did not extend beyond this area into the head region (Figure 11). Thus, UNC-52 is associated with posterior pharyngeal cells, but is absent from the head where ABa-derived anterior pharyngeal cells would normally be found. This implies that UNC-52 acts cell autonomously with respect to the pharynx because it does not spread beyond the cells where it is expressed.

UNC-52 is localized to basement membranes of a variety of tissues in post-embryonic *C. elegans*.

We found that UNC-52 is localized to basement membranes of a variety of tissues in larval and adult animals, including the pharynx, body wall muscles, and anal muscles (Table 2). The pharyngeal and anal muscle staining patterns in these older animals do not differ greatly from those observed in three-fold embryos. However, we found that the pharyngeal staining pattern in larvae and adults varied somewhat with the method of preparation. In animals prepared as described by Finney and Ruvkun (1990), GM1 staining surrounds the pharynx from the anterior margin to the pharyngeal-intestinal valve, and muscle cells within the terminal bulb stain with a punctate pattern (Figure 12A). In contrast, this punctate staining pattern was not observed in animals prepared by the freeze-

Figure 12. Immunolocalization of UNC-52 in adult hermaphrodites. Wild-type hermaphrodites were labeled with GM1, using the method of Finney and Ruvkun (1990). Panel A shows the head region from a young adult. The arrow indicates the terminal bulb of the pharynx. Note the punctate pattern over this region. Panel B shows a section of the body wall muscles from a young adult. The large arrow indicates a dense body, while the small arrow indicates an M-line. Arrowhead indicates the margin of a body wall muscle cell (see Figure 2 for comparison). Panel C shows the uterine and vulva region from an older adult (dorsal view). Arrow indicates accumulation of UNC-52 at the base of a uterine muscle, while arrowhead indicates the vulva.

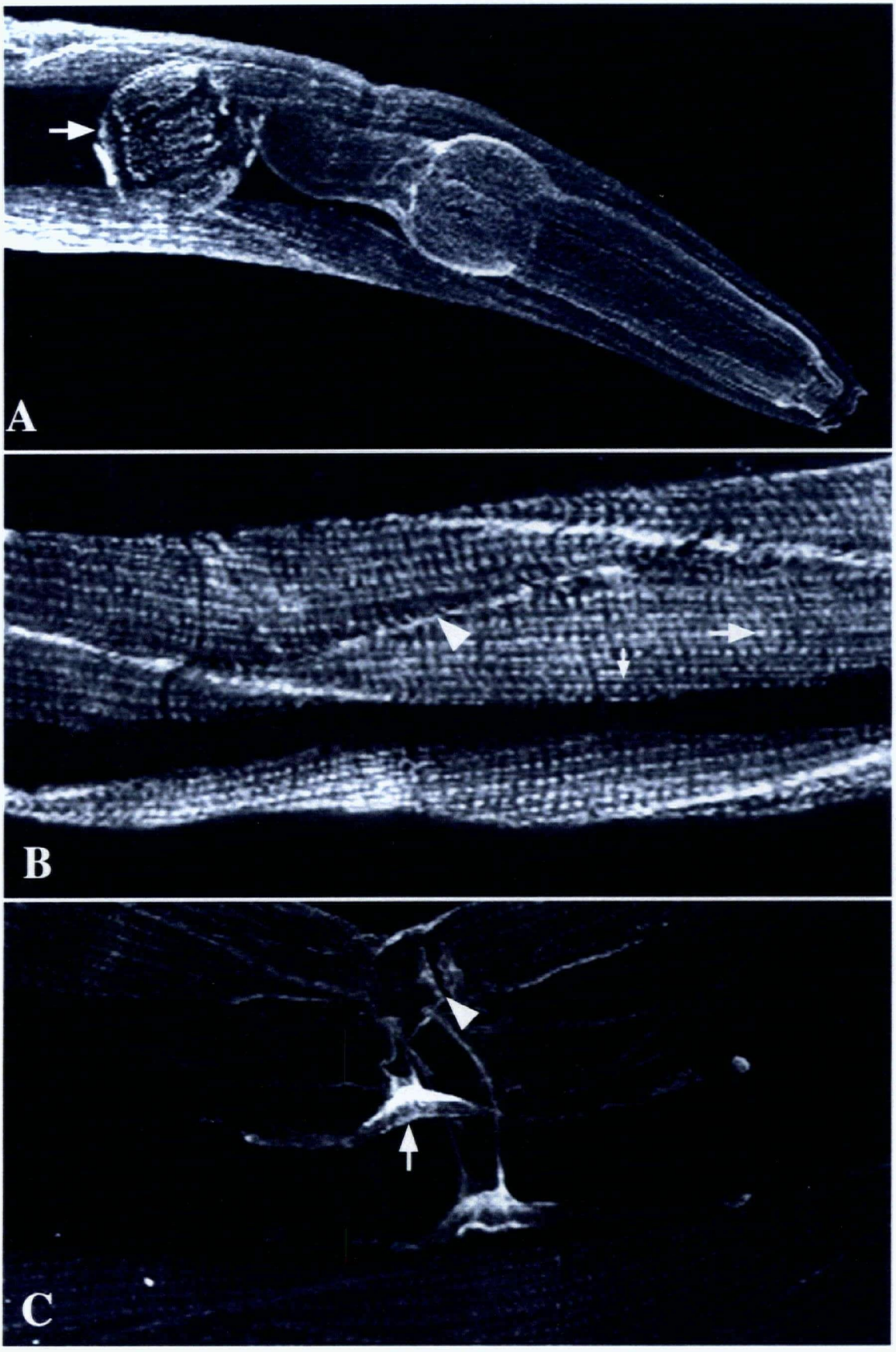
A
B
C

fracture method, although pharyngeal staining was otherwise quite similar (data not shown).

The body wall muscle staining pattern in larvae and adults differs slightly from that seen in embryos. At each of these stages, GM1 stains the basement membrane underlying the body wall muscles. However, in larvae and adults, staining is especially pronounced over dense bodies, M-lines, and muscle cell margins. Particularly in animals prepared by the Finney method, dense bodies and M-lines are clearly visible as rows of dots (dense bodies) interspersed with lines (M-lines) (Figure 12B). The margins of muscle cells also stain strongly, especially in regions of overlap between adjacent cells. This staining pattern is most easily observed in adult animals, when muscle cells and their attachment structures are relatively large. Because these structures are smaller in embryos, it is possible that we are unable to resolve them through the basement membrane staining.

In late larval and adult animals, GM1 stains several additional tissues, including sex-specific muscles (Table 2). In hermaphrodites, GM1 stains the 16 uterine and vulval cells that comprise the egg-laying muscles (Figure 12C). These muscles are surrounded by a basement membrane (White et al., 1986) and the GM1 staining pattern is consistent with the localization of UNC-52 to this basement membrane. In addition, myoepithelial cells of the gonad stain faintly with GM1. Because these cells have many of the characteristics of muscle cells, including myofilaments (Hirsh et al., 1976; Kimble and Hirsh, 1979), localization of UNC-52 over these cells is not surprising. In males, GM1 stains the male-specific muscles in the tail (D. G. Moerman, personal communication). In summary, UNC-52 can be detected in basement membranes associated with the pharyngeal, body wall, anal, and sex-specific muscles in late larvae and adult animals (Table 2).

Specific UNC-52 antibodies reveal temporal and spatial differences in the localization of UNC-52 isoforms.

In the previous sections, we examined the expression and localization of UNC-52 using a polyclonal serum that recognizes all UNC-52 isoforms. We detected UNC-52 in basement membranes associated with most contractile tissues in *C. elegans*, including the pharynx, body wall muscles, and anal muscles. Expression of specific UNC-52 isoforms, however, might be more restricted, either temporally or spatially. To determine whether there are temporal or spatial differences in the expression and localization of specific UNC-52 isoforms, we generated domain-specific polyclonal antisera.

UNC-52 isoforms can be divided into two groups based on the presence or absence of domain IV (Figure 4; Rogalski et al., 1993). S isoforms of UNC-52 lack domain IV, whereas both M and L isoforms contain this domain (Rogalski et al., 1993; T. M. Rogalski, G. P. Mullen, and D. G. Moerman, unpublished results). As described earlier, the MH2 and MH3 mAbs recognize domain IV-containing isoforms. In initial staining experiments, we noticed that these mAbs have a more restricted staining pattern than GM1. This observation could be explained by epitope inaccessibility, or by alternative splicing events in this region, although we have no evidence that exon 19 is alternatively spliced. Therefore, to ensure that we were detecting all domain IV-containing isoforms, we generated a polyclonal serum, designated GM3, against a conserved region of domain IV. This serum was raised against an UNC-52::GST fusion protein (DM#183; Rogalski et al., 1995) and has been shown to recognize this fusion on Western blots (Figure 8). GM3 cross-reacts weakly with other epitopes in UNC-52, but this was negligible under our experimental conditions (see methods and materials). The controls described for immunofluorescence experiments with GM1 were also used with this new serum and gave similar results.

To examine the localization of isoforms with domain IV in *C. elegans*, we stained wild-type animals at different stages of development with GM3 and DM5.6 (MHC A). Our results demonstrate that there are spatial and temporal differences in the localization of UNC-52 isoforms. Previous studies established that some UNC-52 isoforms are expressed in the body wall muscles during embryogenesis and are localized to the underlying basement membranes (Hresko et al., 1994; Moerman et al., 1996). In this study, we found that both GM1 and GM3 stain the body wall muscles and are essentially identical in this respect. Staining is first observed in comma stage embryos and is primarily found at regions of contact between adjacent muscle cells, although some intracellular staining of muscle cells is also observed (Figure 13). Between the comma and 1.5-fold stages, staining spreads from these regions of cell-cell contact over the basal face of each muscle cell (Figure 13).

However, beginning around the 1.5-fold stage, dramatic differences in staining are observed (Figure 13). Unlike GM1, which stains the pharynx, body wall muscles, and anal muscles, GM3 only stains the body wall muscles. This staining pattern was not affected by different fixation methods, nor by treatment with acid-urea. On this basis, we conclude that M and/or L isoforms are restricted to the body wall muscles during embryogenesis. GM1 staining of the pharynx and anal muscles must therefore be due to the presence of S isoforms in these tissues. Our studies on *unc-52* mutants (see below) suggest that S isoforms are not associated with body wall muscles in embryos, but are restricted to the pharynx and anal muscles.

Both GM1 and GM3 stain body wall muscles in embryos, larvae, and adults. In this respect, these antisera are essentially identical, so the GM3 body wall muscle staining pattern will not be described in detail. Briefly, in larvae and adults, GM3 stains dense bodies, M-lines, and muscle cell margins, in addition to the basement membrane underlying the muscle quadrants. In adults, GM3 also stains several additional tissues, including the pharynx and the anal muscles (Table 2). We conclude that there are

Figure 13. Immunolocalization of domain IV-containing UNC-52 isoforms and myosin at different stages of embryonic development.

Embryos were visualized by laser scanning confocal microscopy. Wild-type embryos were double-labeled with GM3 (UNC-52; panels A, C, E, and G) and DM5.6 (myosin heavy chain A; panels B, D, F, and H). Panels A and B show the dorsal view of a comma stage embryo (~350 min.); these images are projections of the dorsal Z-sections, while the remaining images are projections of the complete Z-series. Arrows indicate positions of two adjacent muscle cells; the arrowhead indicates intracellular staining with GM3. Panels C and D show the lateral view of late comma stage embryo (350 - 400 min.). Arrows indicate the position of a muscle cell, while the arrowhead indicates the basal face of the cell. Note that myosin is not concentrated beneath the basal face of the muscle cell, but is present throughout the cell. Panels E and F show the lateral view of a 1.5-fold embryo (~420 min.). The arrow in both panels indicates the basal face of the muscle cells in a dorsal quadrant. Note that myosin is now concentrated beneath the basal face. Panels G and H show a three-fold embryo (~800 min.). Note that myosin is organized into distinct A-bands (arrow in H). Also note that domain IV-containing UNC-52 isoforms are restricted to body wall muscles (compare with Figure 9). Scale bar indicates 10 microns.

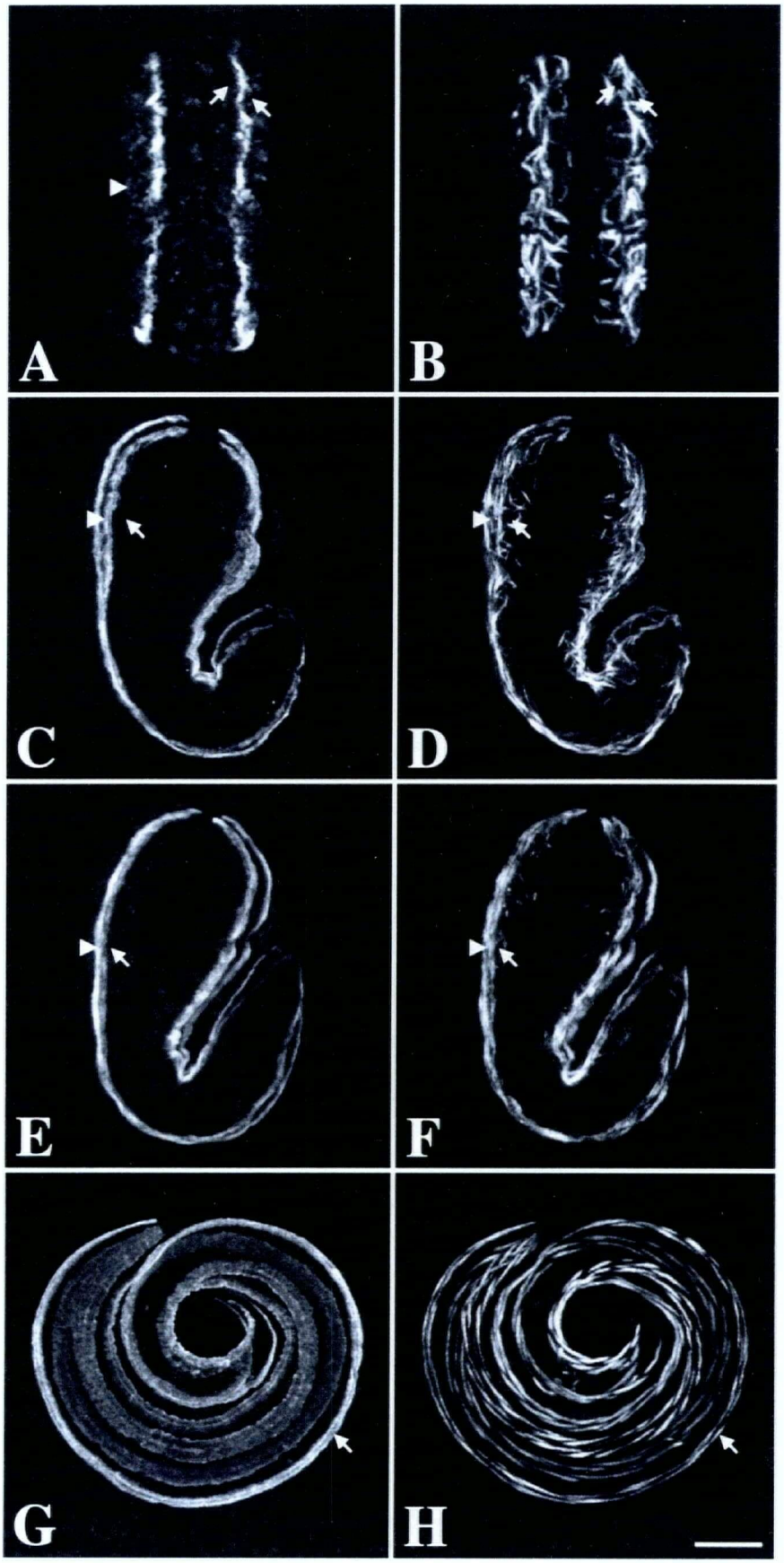
A
B
C
D
E
F
G
H

TABLE 1. Distribution of UNC-52/perlecan in wild-type embryos.

Antibody	Specificity	Pharynx	Body wall muscles	Anal muscles
MH3	Domain IV	-	+	-
GM1	Domain III	+	+	+
GM3	Domain IV	-	+	-
GM9	Domain V	-	+	-

TABLE 2. Distribution of UNC-52/perlecan in adult hermaphrodites.

Antibody	Specificity	Pharynx	Body wall muscles	Anal muscles	Egg-laying muscles	Gonad
MH3	Domain IV	+ (faintly)	+	+ (faintly)	+ (faintly)	+
GM1	Domain III	+	+	+	+	+
GM3	Domain IV	+ (faintly)	+	+ (faintly)	+ (faintly)	+
GM9	Domain V	-	-	-	-	-

developmental changes in isoform localization because neither of these tissues stain in embryos. GM3 also stains the uterine and vulval muscles and the myoepithelial cells of the gonad. In most respects, the GM3 staining pattern in adults is qualitatively the same as that observed with GM1. In summary, UNC-52 isoforms containing domain IV are more widely distributed in adults than in embryos. These isoforms can be detected in basement membranes associated with the pharyngeal, body wall, anal, and sex-specific muscles in adult animals. These results are consistent with those reported for the mAbs MH2 and MH3 (Tables 1 and 2; Francis and Waterston, 1991; Hresko et al., 1994), which also recognize domain IV-containing isoforms (Rogalski et al., 1993, 1995).

Localization of UNC-52 isoforms containing domain V.

The L isoforms of UNC-52 are characterized by the presence of the carboxyl-terminal domain V (Figure 4; T. M. Rogalski, G. P. Mullen, and D. G. Moerman, unpublished results). We generated a polyclonal serum that recognizes domain V of UNC-52. This serum, designated GM9, was raised against a bacterial fusion protein and has been shown to specifically recognize this fusion on Western blots (Figure 8). However, GM9 works poorly for immunofluorescence staining, and we were only able to detect staining in embryos, where it is restricted to the body wall muscles (data not shown). Thus, L isoforms are associated with the body wall muscles during early development (Table 2).

Analysis of UNC-52 polypeptides by Western blotting.

We attempted to analyze UNC-52 polypeptides by Western blotting. Unfortunately, antisera generated in this study worked poorly in Western blotting experiments against nematode proteins. This difficulty is most likely due to the size and insolubility of these high molecular weight proteoglycans. However, extraction with strong denaturants such

Figure 14. Analysis of UNC-52 polypeptides by Western blotting.

Molecular weight markers (lanes A1 and B1) and SDS-soluble nematode proteins (lanes A2 and B2) were probed with the GM3 serum (A) or pre-immune serum (B). Approximate positions of molecular weight markers are indicated. The GM3 serum reacts strongly with 300+ kd, 275 kd, 250 kd, 200 kd, and 180 kd polypeptides, in addition to several less prominent species. Positions of 300+ kd, 200 kd, and 180 kd polypeptides are indicated.

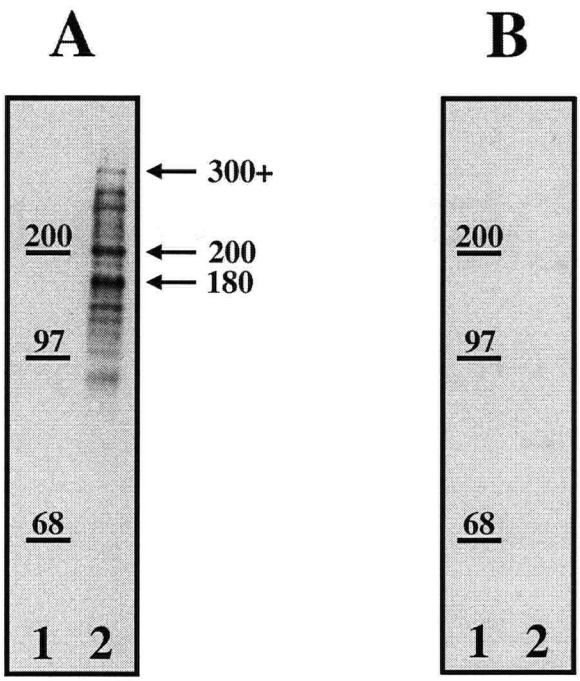
A
B
300+
200
180
200
97
68
1 2
200
97
68
1 2

as 8M urea or 6M guanidine did not resolve these difficulties. We were able to detect high molecular weight polypeptides in SDS extracts using the GM3 serum. This serum recognized proteins with approximate molecular weights of 300+ kd, 275 kd, 250 kd, 200 kd, and 180 kd (Figure 14). The two most prominent species were 200 and 180 kd, which may correspond to similar-sized polypeptides recognized by MH3 (Francis and Waterston, 1991). However, we did note considerable variation between experiments, which may be due to varying extents of degradation, and are uncertain which of these bands represent full-length polypeptides.

UNC-52 isoforms containing domain IV are essential for myofilament lattice assembly in the body wall muscles of *C. elegans*.

In previous studies, we identified a lethal allele of *unc-52*, *st549*, that represents the null state of the gene (Rogalski et al., 1995). Embryos homozygous for this allele exhibit a paralyzed, arrested at two-fold (Pat) phenotype and have severely disorganized body wall muscles (Rogalski et al., 1993; Williams and Waterston, 1994). Several additional Pat alleles were also identified, but their molecular basis was not determined (Williams and Waterston, 1994). Because *unc-52* gives rise to a number of protein isoforms, we speculated that the Pat phenotype could result from the specific absence of isoforms needed for embryonic body wall muscle assembly.

Using antibodies that recognize different regions of UNC-52, we examined the localization of UNC-52 isoforms in embryos homozygous for lethal alleles of *unc-52*. The polyclonal serum GM1 recognizes epitopes in domain III of UNC-52 that are present in all UNC-52 isoforms (Moerman et al., 1996). In wild-type embryos at the three-fold stage, GM1 stains basement membranes associated with the body wall muscles, pharynx, and anal muscles (Figure 9). The mAb MH3 recognizes an epitope encoded by exon 19 which is present in all UNC-52 isoforms with domain IV (Francis and Waterston, 1991; Rogalski

et al., 1993, 1995). In wild-type embryos at the three-fold stage, MH3 staining is limited to basement membranes underlying the body wall muscles.

In initial experiments, we stained mutant embryos prepared from balanced stocks with GM1 and the mAb DM5.6, which recognizes the minor body wall muscle myosin, MHC A (Miller et al., 1983). We found that a subset of lethal alleles have tissue-specific effects on GM1 staining. Three EMS-induced alleles, *st546*, *st560*, and *st578* lead to reduced staining of the body wall muscles relative to the pharynx or the anal muscles. For example, in homozygous *st560* embryos, staining of the body wall muscles with GM1 is greatly reduced or absent (Figure 15). Within body wall muscle cells, myosin is not organized into ordered A-bands, but instead forms large aggregates (Figure 15; Williams and Waterston, 1994). GM1 staining of the pharynx and the anal muscles in these mutants, however, appears to be unaffected (Figure 15). The other two EMS-induced alleles have similar effects on UNC-52, as does *ra112*, a deletion isolated in a screen for lethal Tc1 excision events (P. Rahmani Gorji, personal communication).

Our results suggest that these mutant embryos are specifically lacking UNC-52 isoforms associated with body wall muscles. We hypothesized that isoforms with domain IV, which are normally associated with body wall muscles, were absent in these mutants. To test this hypothesis, we stained mutant embryos prepared from balanced stocks with GM1 and the mAb MH3, which recognizes isoforms with domain IV (Rogalski et al., 1993, 1995). We observed no detectable staining of the body wall muscles in mutant embryos with MH3, indicating that isoforms with domain IV are greatly reduced or absent. In these same animals, GM1 staining of the pharynx and anal muscles was similar to wild-type. We conclude that these mutants are specifically deficient in isoforms containing domain IV. Embryos homozygous for these alleles have a severe Pat phenotype that is indistinguishable from that of *unc-52(st549)* embryos (Rogalski et al., 1993; Williams and Waterston, 1994). An implication of these observations is that the Pat phenotype results specifically from the absence of UNC-52 isoforms containing domain IV.

Figure 15. *unc-52(st560)* mutant embryos have tissue-specific staining defects and lack a subset of UNC-52 isoforms.

Embryos were visualized by laser scanning confocal microscopy. Embryos in panels A-F were double labeled with GM1 (green, FITC), which recognizes all UNC-52 isoforms, and DM5.6 (red, TRSC), which recognizes myosin heavy chain A (MHC A). Small arrows indicate the pharynx and large arrows indicate a body wall muscle quadrant. Panels A and D show both channels simultaneously, while panels B, C, E, and F show single channel images. Panels A-C show a wild-type embryo, while D-F show an arrested *unc-52(st560)* mutant embryo. Note the reduced staining of body wall muscles with GM1 and disorganization of MHC A in the mutant (panels E and F; compare with B and C). The pharynx and anal muscles (arrowhead in panel E) in the mutant, however, exhibit a wild-type staining pattern (compare panels B and E). Embryos in G-L were double labeled with GM1 (green, FITC), and MH3 (red, TRSC), which recognizes an epitope in domain IV of UNC-52. Panels G-I show a wild-type embryo, J-L an *unc-52(st560)* mutant embryo. G and J show both channels simultaneously. Note the absence of MH3 staining in the mutant embryo in panel L. Although the *unc-52(st560)* mutant embryos shown are arrested at the two-fold stage, they are comparable in age to three-fold wild-type embryos. Scale bar indicates 10 microns.

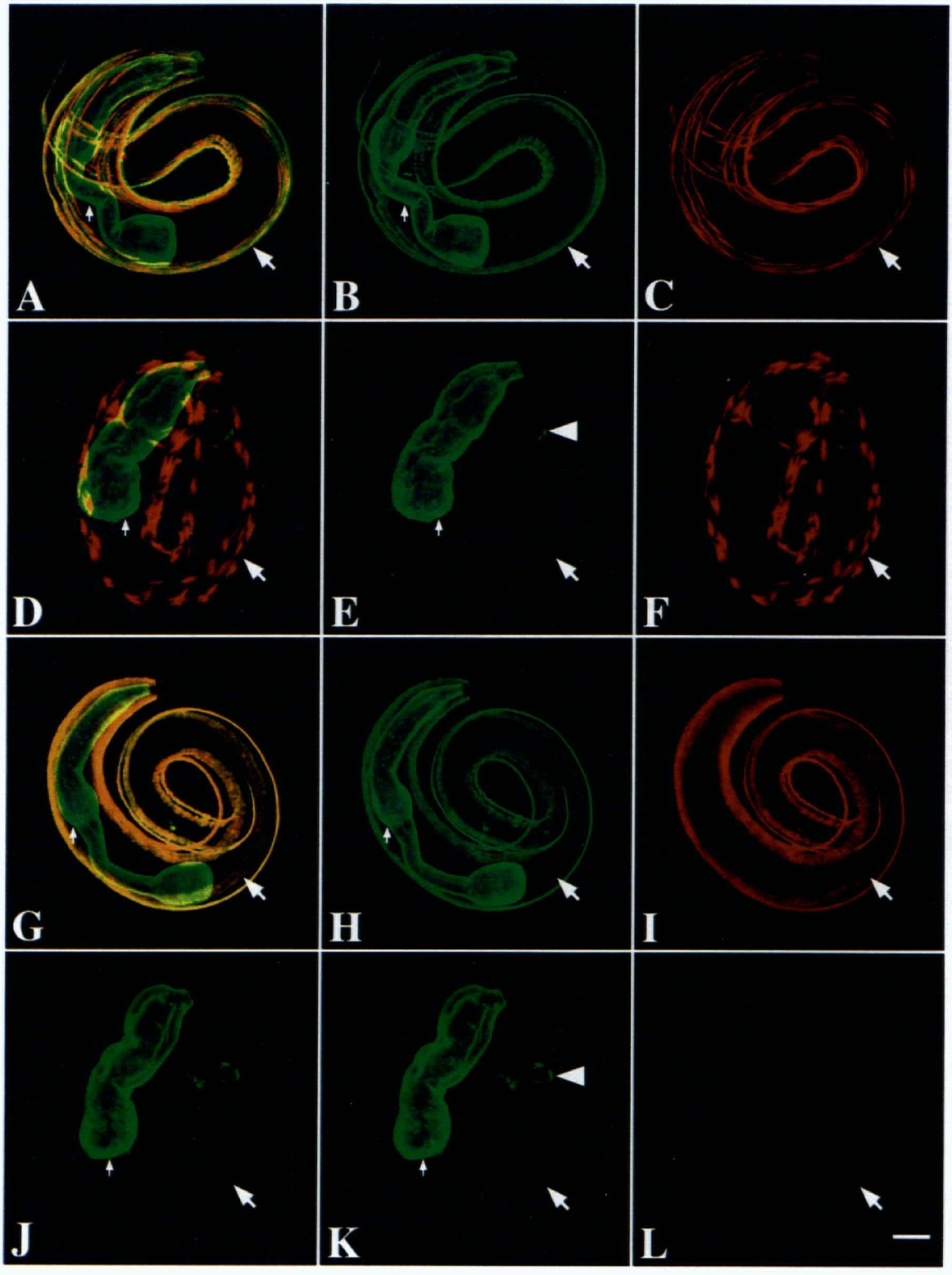
A
B
C
D
E
F
G
H
I
J
K
L

TABLE 3. anti-UNC-52 staining in *unc-52* mutant embryos.

Allele	Phenotype	GM1	GM3	MH3
st549, ra401	severe Pat	-	-	-
st560, st546,	severe Pat	+ (pharynx & anal muscles)	reduced	-
st578, ra112		- (body wall muscles)		
st572	severe Pat	reduced (all tissues)	reduced	-
ut111	mild Pat	reduced (all tissues)	reduced	reduced
e444	severe Unc	+	+	+
e1012	moderate Unc	+	+	+
e1421	mild Unc	+	+	+

To determine whether these alterations were localized to domain IV of UNC-52, we sequenced PCR-amplified DNA from homozygous mutant embryos (Bush, 1997). We identified the nucleotide alterations in two *unc-52* alleles, *st560* and *ra112*. The *st560* mutation is a C to T transition at nucleotide 8989 in exon 13, which changes a glutamine residue (CAA) to an ochre stop codon (TAA). The effect of this mutation would be to eliminate all *unc-52* gene products with domain IV. A second allele, *ra112*, has a 3283-bp out-of-frame deletion that extends from the 3' end of exon 13 to the 3' end of exon 19. This mutation is also expected to eliminate all UNC-52 isoforms with domain IV. Identification of these mutations demonstrates that isoforms with domain IV are essential for myofilament lattice assembly in body wall muscles. In addition, because body wall muscle staining with GM1 is greatly reduced or absent in these mutants, we suggest that UNC-52 isoforms with domain IV are the predominant body wall muscle isoforms during embryonic development.

UNC-52 isoforms with domain IV are necessary for proper localization of βpat-3 integrin in the body wall muscles of *C. elegans*.

Integrins are essential for myofilament lattice assembly in *C. elegans* (Hresko et al., 1994; Williams and Waterston, 1994). Loss-of-function mutations in *pat-3*, which encodes a β-integrin (βpat-3), disrupt assembly of dense bodies and M-lines (Hresko et al., 1994; Williams and Waterston, 1994; Gettner et al., 1995). Dense body components, including vinculin and talin, fail to assemble in *pat-3* mutants, demonstrating that integrin is required for localization of these proteins (Hresko et al., 1994; Moulder et al., 1996). Recent studies on Pat mutants suggest that integrin nucleates formation of dense bodies and M-lines (Hresko et al., 1994).

Hresko et al. (1994) found that βpat-3 is disorganized in *unc-52(null)* embryos. Because UNC-52 isoforms with domain IV are essential for myofilament lattice assembly,

we speculated that mutants specifically lacking these isoforms would also exhibit defects in integrin organization. To test this prediction, we examined the distribution of β-integrin in homozygous *unc-52(st560)* embryos, which are specifically deficient in UNC-52 isoforms with domain IV. We stained embryos prepared from a balanced strain with GM1 and the mAb MH25, which recognizes βpat-3 (Francis and Waterston, 1985; Williams and Waterston, 1994; Gettner et al., 1995).

We found that βpat-3 is highly disorganized in *unc-52(st560)* embryos. In two-fold embryos (~450 min.), for example, βpat-3 has a diffuse and patchy distribution, consistent with disruption of dense bodies and M-lines. We also looked at younger animals and found that βpat-3 is disrupted prior to the 1.5-fold stage, suggesting that there are very early defects in the distribution of β-integrin. These defects are identical to those reported for *unc-52(null)* embryos (Hresko et al., 1994) and are summarized in Table 4. We conclude that βpat-3 integrin is disorganized in mutant embryos lacking UNC-52 isoforms with domain IV.

UNC-52 is not essential for myofilament lattice assembly in the pharyngeal muscles of *C. elegans*.

In the previous section, we demonstrated that a subset of UNC-52 isoforms are essential for myofilament lattice assembly in body wall muscles. UNC-52 isoforms containing domain IV are restricted to body wall muscles during embryonic development. Mutant embryos lacking these isoforms have a Pat terminal phenotype and severely disorganized body wall muscles (Williams and Waterston, 1994). To determine the function of S isoforms, we undertook morphological studies on mutants lacking these isoforms. Because S isoforms of UNC-52 are restricted to the pharynx and anal muscles during embryonic development, we speculated that these isoforms might be required for

TABLE 4. βpat-3 staining in *unc-52* mutant embryos.

Mutation	Phenotype	β-integrin	Reference
st549	severe Pat	severely disorganized	Hresko et al., 1994.
st560	severe Pat	severely disorganized	-
st546	severe Pat	severely disorganized	-
ra112	severe Pat	severely disorganized	-

TABLE 5. Phalloidin staining in Pat mutants.

Gene	Allele	Phenotype	Body wall muscles	Pharyngeal muscles
unc-52	*st549, ra401, st560.*	severe Pat	severely disorganized	normal
unc-112	*st581*	severe Pat	severely disorganized	normal
deb-1	*st555*	severe Pat	severely disorganized	normal
pat-3	*st564*	severe Pat	severely disorganized	normal
pat-11	*st541*	severe Pat	severely disorganized	normal

myofilament assembly in these muscles. To test this prediction, we examined pharyngeal myofilament organization in *unc-52(lethal)* mutants. We used *unc-52(null)* alleles in our studies because we have not identified alleles that specifically eliminate S isoforms. In addition, we focused our analysis on pharyngeal muscles because they are larger and more easily studied than anal sphincter or depressor muscles.

The *st549* allele defines the null state of *unc-52* (Rogalski et al., 1995; Moerman et al., 1996). Homozygous *st549* embryos fail to stain with an antibody that recognizes all UNC-52 isoforms (Moerman et al., 1996), demonstrating that there is no detectable accumulation of UNC-52 in these animals. A second lethal allele, *ra401*, has similar effects on accumulation of UNC-52, suggesting that it is also null (K. R. Norman, personal communication). To examine the role of *unc-52* in pharyngeal myofilament assembly, we stained wild-type (N2) and *unc-52(st549)* embryos with fluorescently-labeled phalloidin, an actin-binding toxin from the mushroom *Amanita phalloides* (Wulf et al., 1979). We collected CLSM images of both mutant and wild type embryos, and compared I-band organization in these animals. We focused primarily on post-arrest mutant embryos because I-band defects, whether resulting from problems in assembly, or in stability, should be apparent in these older animals. N2 embryos at the three-fold stage were used for comparison because they are similar in age to arrested mutant embryos.

In wild-type three-fold embryos, phalloidin stains the well-ordered I-bands in the body wall, anal, and pharyngeal muscles. In addition, staining of filamentous actin in the intestine and hypodermis is observed. By this stage, actin is organized into distinct half I-bands in the pharyngeal muscles. For example, in lateral views of the M3 cells (procorpus), half I-bands can be seen extending inwards from the basal and luminal faces of each cell (Figure 16). The H-zone, which appears as a gap between half I-bands, can also be observed in appropriately oriented embryos. In computer-generated cross sections, thin filaments appear to radiate from a focal attachment site at the luminal face of each

pharyngeal muscle cell to more broadly distributed attachment sites on the basal face (Figure 16).

Surprisingly, pharyngeal thin filaments did not appear to be disorganized in *unc-52(st549)* mutant embryos. In a typical post-arrest embryo, the pharynx is compressed lengthwise and is often distorted in shape. The terminal bulb can be easily identified by its shape and position, but the metacorpus cannot be readily distinguished from the procorpus and isthmus. These morphological defects are observed in all Pat mutants and probably result from the failure of these mutants to elongate beyond two-fold. However, within the pharyngeal muscles, thin filaments are organized into well-ordered half I-bands extending from both luminal and basal faces (Figure 16). We examined the half I-bands in the 5 largest muscle layers (composed of the M3, M4, M5, M6, and M7 cells) and could not discern any disorganization in these cells. A second null allele, *ra401*, gave very similar results, suggesting that absence of *unc-52* function has no effect on assembly of thin filaments in the pharynx. The apparent organization of the pharyngeal muscle thin filaments in *unc-52(null)* mutants is consistent with our observation that there is some pharyngeal pumping in these animals (also see Williams and Waterston, 1994). We conclude that UNC-52 is not essential for myofilament lattice assembly in pharyngeal muscles.

These findings led us to examine pharyngeal myofilament organization in other lethal muscle-affecting mutants. Several cell adhesion proteins, including vinculin and β-integrin, are expressed in the pharynx (Francis and Waterston, 1985; Barstead and Waterston, 1992; Gettner et al., 1995). Potentially, these proteins could play a role in pharyngeal myofilament assembly. To test this hypothesis, we stained *deb-1* (vinculin; Barstead and Waterston, 1989, 1991) and *pat-3* (β-integrin; Gettner et al., 1995) mutant embryos with FITC-phalloidin. We also examined the organization of pharyngeal actin in *pat-2* (α-integrin; B. D. Williams, personal communication), *pat-11*, and *unc-112* mutant embryos. Phalloidin staining of *deb-1(st555)* and *unc-112(st581)* mutants is shown in

Figure 16. Phalloidin staining in wild-type and *unc-52(null)* embryos. Embryos were visualized by laser scanning confocal microscopy. Wild-type (A, B, and C) and *unc-52(st549)* (D, E, and F) embryos were labeled with FITC-phalloidin. Images in panels A and D are projected from the complete Z-series and show staining from all focal planes. Because these projections are somewhat difficult to interpret, computer-generated cross sections (B and E) and single focal plane images (C and F) are also shown. Arrows indicate the basal face of the body wall muscles, while the arrowhead indicates the basal surface of the pharynx. Note the well-organized thin filaments extending from the basal and apical faces of the pharynx in both wild-type and mutant embryos. Also note that actin in the body wall muscles is not associated with the basal cell membrane in the mutant. Scale bar indicates 10 microns.

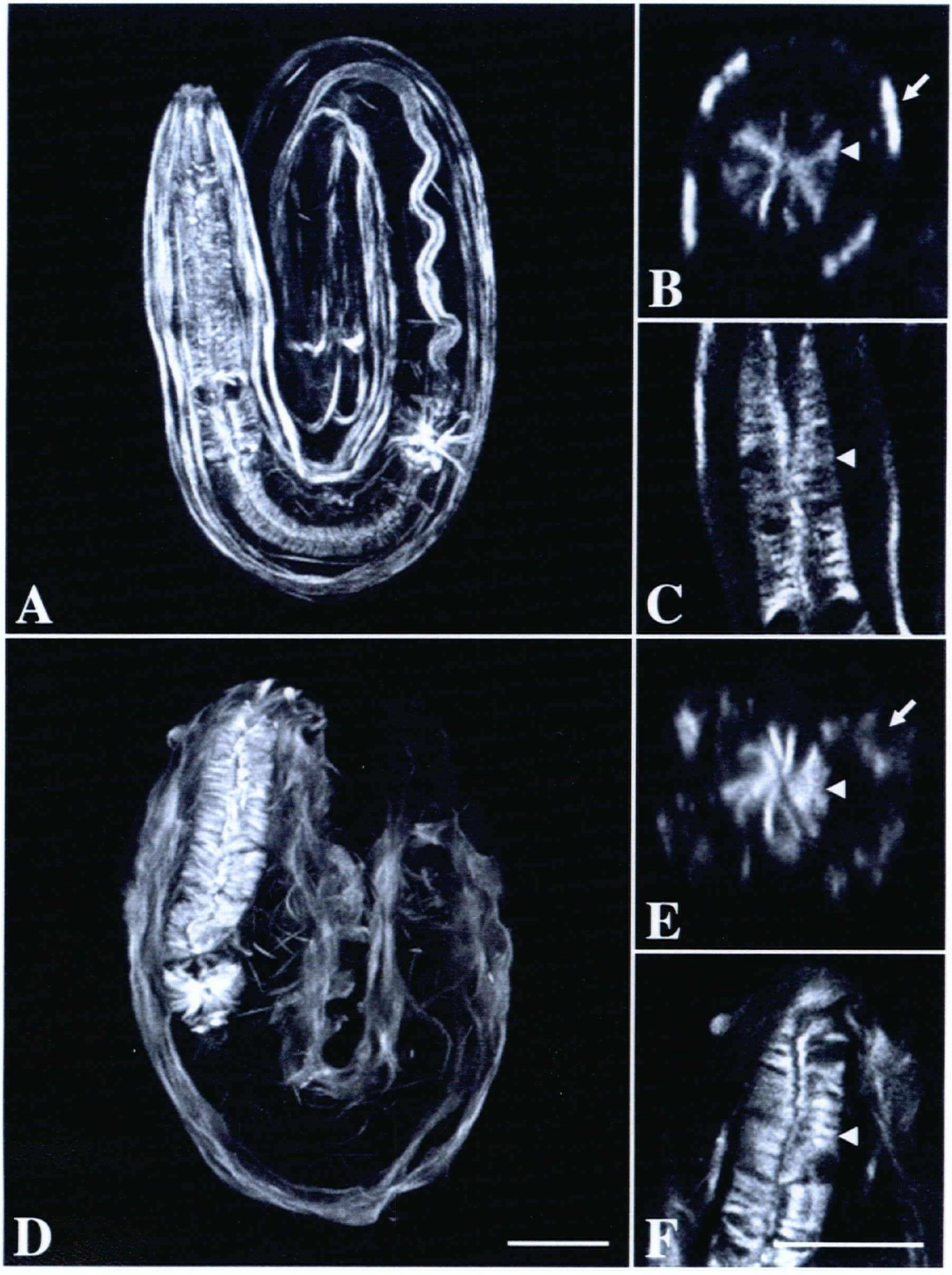
A
B
C
D
E
F

Figure 17. Phalloidin staining in *deb-1* and *unc-112* mutant embryos. Embryos were visualized by laser scanning confocal microscopy. *deb-1(st555)* (A, B, and C) and *unc-112(st581)* (D, E, and F) embryos were labeled with FITC-phalloidin. Images in panels A and D are projections of the complete Z-series and show staining from all focal planes. Because these projections are somewhat difficult to interpret, computer-generated cross sections (B and E) and single focal plane images (C and F) are also shown. Arrows indicate the basal face of the body wall muscles, while the arrowhead indicates the basal surface of the pharynx. Note the well-organized thin filaments extending from both the basal and apical faces of the pharynx in both *deb-1* and *unc-112* mutant embryos. Scale bar indicates 10 microns.

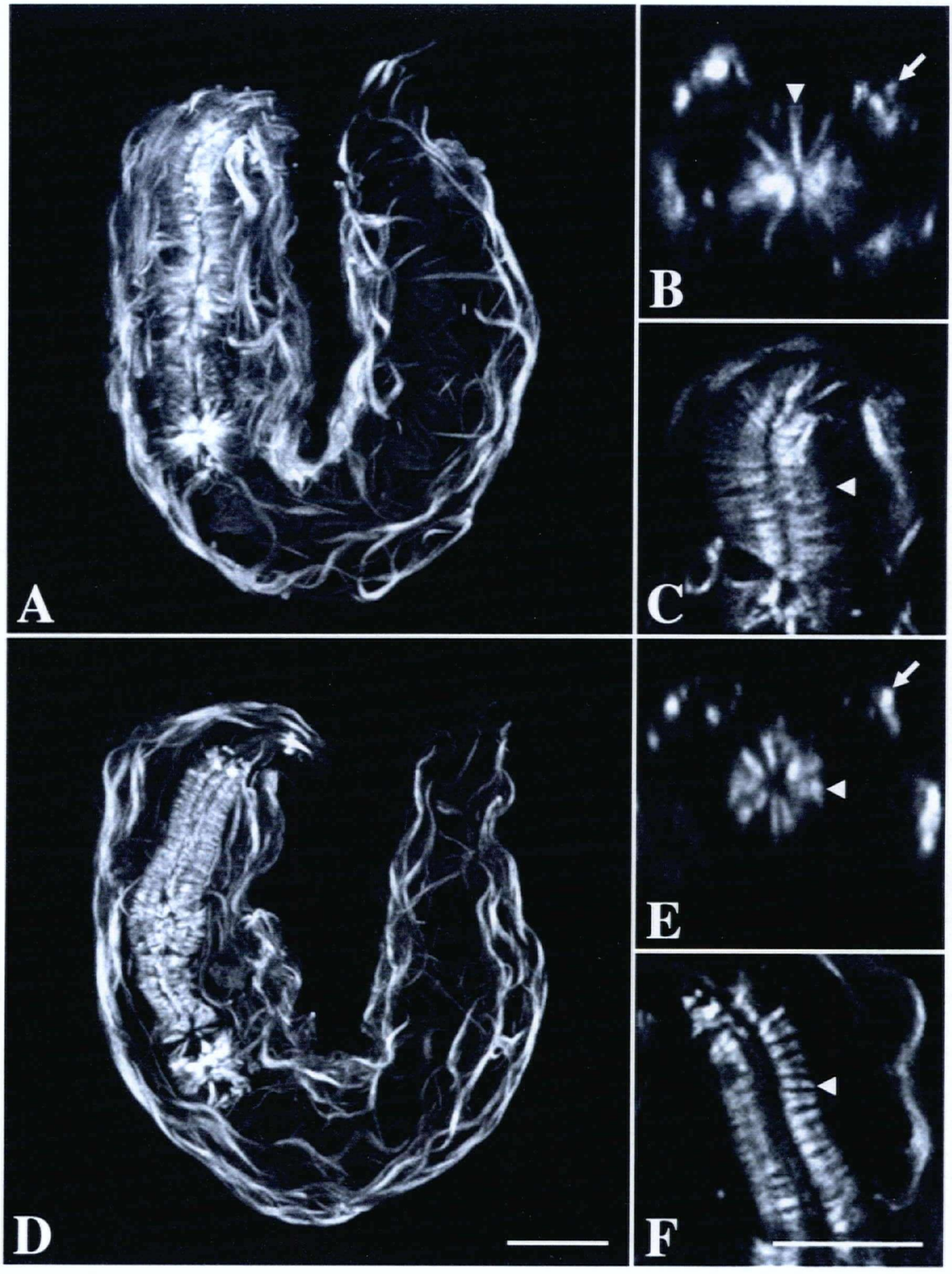
A
B
C
D
E
F

Figure 17. To our surprise, we found that these mutations have no effect on the organization of thin filaments in the pharynx. We examined the 5 largest pharyngeal muscle layers (composed of the M3, M4, M5, M6, and M7 cells) in these mutants and could not discern any disorganization. In all cases, thin filaments were organized into well-ordered half I-bands extending from both the luminal and basal faces of the muscle cells, and the H-zone could be readily observed. These results are summarized in Table 5. We conclude that none of these genes have an essential role in pharyngeal myofilament assembly.

UNC-52 is not essential for assembly of collagen type IV into basement membranes.

Type IV collagen is an abundant component of most basement membranes (Yurchenco and Schittny, 1990; Kuhn, 1994). Type IV collagen molecules are heterotrimers consisting of two nonidentical collagen (IV) chains. At least six collagen (IV) chains, designated α1 - α6, have been identified in mammals (Hudson et al., 1993; Kuhn, 1994). The most common form of type IV collagen in mammals consists of two α1 and one α2 chains (Yurchenco and Schittny, 1990; Kuhn, 1994). The *emb-9* and *let-2* genes encode collagen type IV chains in *C. elegans* (Guo and Kramer, 1989; Sibley et al., 1993, 1994). These collagen chains have strong similarity to the human α1 and α2 chains, respectively. The *emb-9* and *let-2* gene products are found in basement membranes associated with the pharynx, gonad, intestine, and body wall muscles in *C. elegans* (Graham et al., 1997).

Collagen type IV interacts with other basement membrane components, including laminin, perlecan, and nidogen (Laurie et al., 1986; Battaglia et al., 1992). These interactions are thought to be important for assembly of basement membranes (Yurchenco et al., 1987). We predicted that absence of UNC-52/perlecan would disrupt basement

Figure 18. Collagen type IV staining in wild-type and *unc-52(null)* mutant embryos.

Embryos were visualized by laser scanning confocal microscopy. Wild-type (A and B) and *unc-52(ra401)* (C and D) were labeled with NW68, which recognizes the α2 collagen (IV) chain encoded by *let-2* (Graham et al., 1997). Images in panels A and C are projected from the complete Z-series and show staining from all focal planes. Because these projections are difficult to interpret, computer-generated cross sections of the pharynx and head (panels B and C) are also shown. Arrow indicates the basal face of a muscle quadrant, while the arrowhead indicates the pharynx. Note that collagen is localized to basement membranes associated with these tissues in both wild-type and mutant embryos. Scale bar indicates 10 microns.

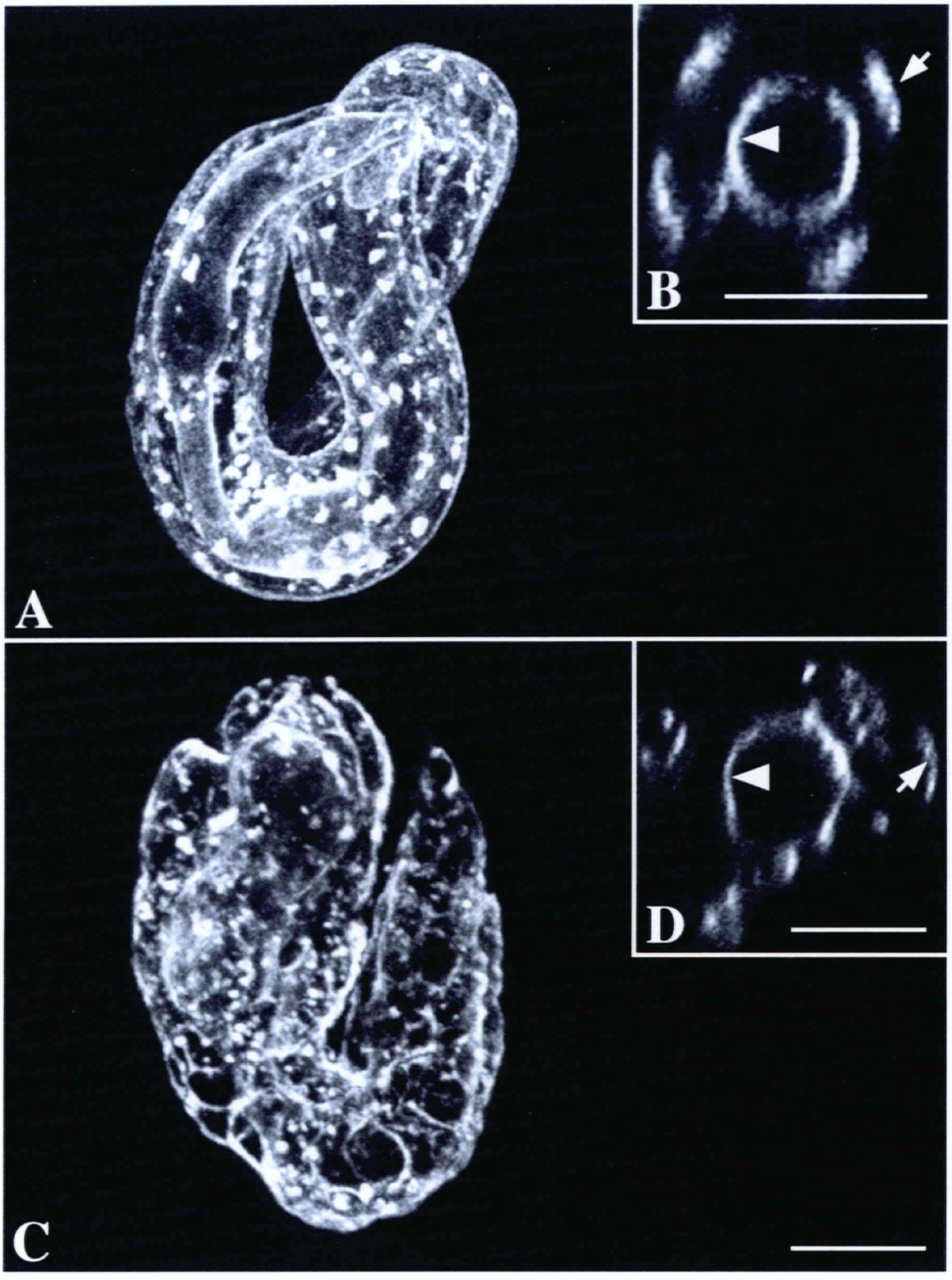
A
B
C
D

membrane assembly and alter the distribution of other basement membrane components, such as collagen type IV. To test this prediction, we examined the localization of collagen type IV in *unc-52(null)* mutants. We stained mutant embryos prepared from balanced stocks with the polyclonal serum NW68, which recognizes the α2 chain encoded by *let-2* (Graham et al., 1997). We found that *unc-52(null)* mutants exhibit a wild-type staining pattern with NW68; staining is localized to basement membranes associated with the pharynx, gonad, intestine, and body wall muscles, and there are no apparent disruption of the normal staining pattern in these animals (Figure 18). Our results suggest that UNC-52/perlecan is not required for proper localization of collagen type IV to basement membranes.

unc-52(viable) mutants exhibit stage- and tissue-specific defects in accumulation of UNC-52.

Alternative splicing of exons 16, 17 and 18 gives rise to isoforms that vary in the number of NCAM-like immunoglobulin repeats within domain IV (Rogalski et al., 1993, 1995). Mutations in these alternatively spliced exons are expected to eliminate full length M and L isoforms, but not alternatively spliced variants (Rogalski et al., 1993, 1995). Five point mutations in this region have been sequenced; four are nonsense mutations in either exon 17 (*e669* and *e1012*) or exon 18 (*e444* and *e998*), while the fifth (*e1421*) alters the splice donor site of exon 16 (Figure 1; Rogalski et al., 1995). Animals homozygous for these viable alleles develop normally as young larvae, but become progressively paralyzed as they mature. This paralysis is caused by gradual disruption of the myofilament lattice in body wall muscle cells posterior to the head (Mackenzie et al., 1978; Waterston et al., 1980). Because these mutants develop normally as embryos and young larvae, we expect that accumulation of UNC-52 would be relatively normal at these stages and that the body wall muscles would be reasonably well-organized. We stained homozygous *e444* embryos

Figure 19. Immunolocalization of UNC-52 and myosin in *unc-52(viable)* mutants.

unc-52(e669) embryos (panels A and B), and wild-type (panels C and D) and *unc-52(e669)* adults (E and F) were double labeled with GM1 (UNC-52) and DM5.6 (MHC A). Note the wild-type staining patterns in panel A and B (compare with panels G and H in Figure 9). The expression and localization of UNC-52 and myosin appear normal at this stage of development. In contrast, note the reduced GM1 staining in panel E and the disorganized myosin in panel F (compare with panels C and D). *unc-52(viable)* mutations disrupt accumulation of UNC-52 and organization of myosin in late larval and adult animals. Scale bar indicates 10 microns.

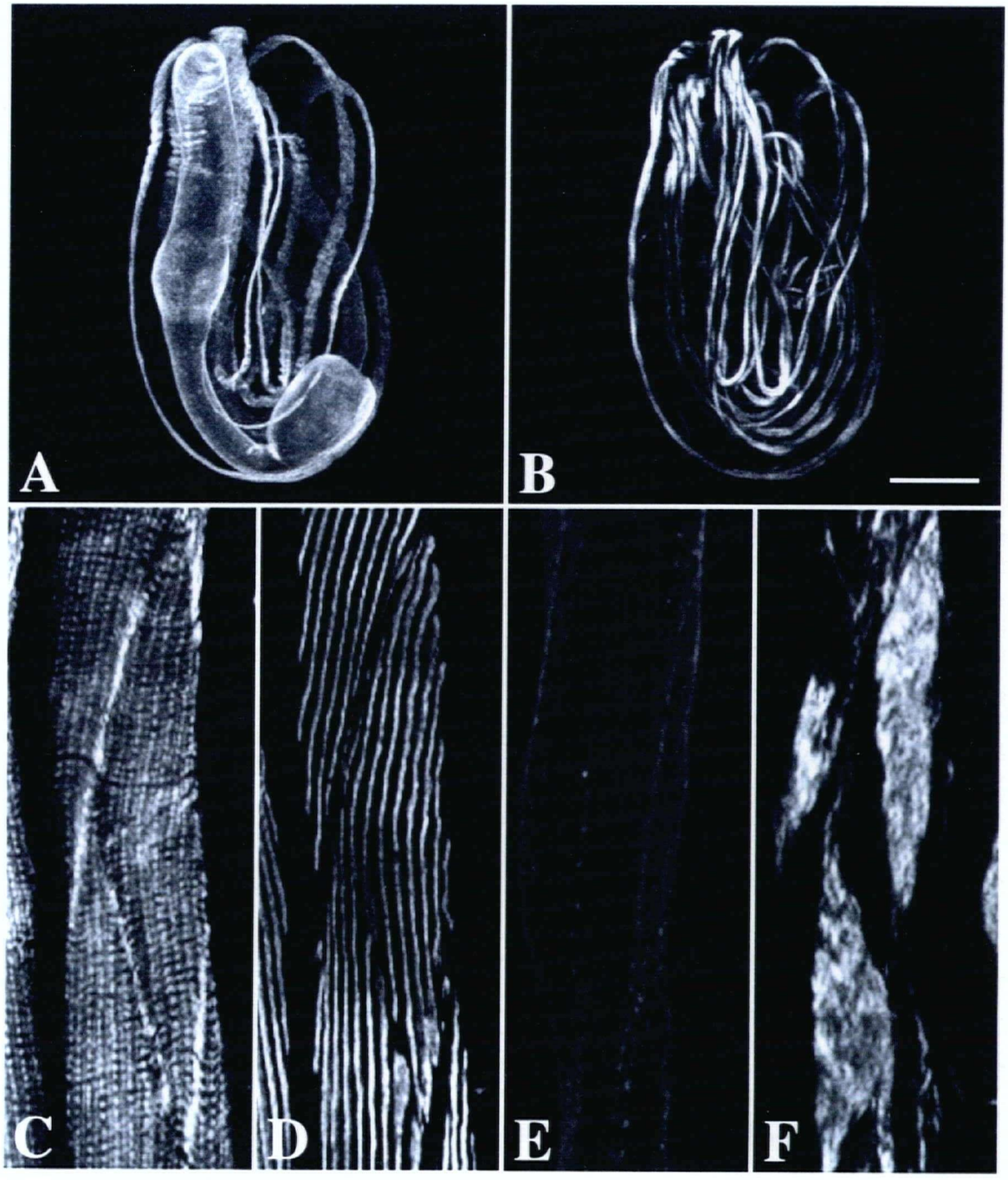
A
B
C
D
E
F

with GM1 (UNC-52) and DM5.6 (MHC A), and found that these embryos exhibit a wild-type staining pattern with both antibodies (Figure 19). Similar results were observed with *e669*, *e998*, *e1012*, and *e1421* mutant embryos. Clearly, nonsense mutations in exons 17 or 18 do not noticeably disrupt accumulation of UNC-52, or myofilament lattice assembly during embryonic development.

However, these alleles have dramatic effects on accumulation of UNC-52 in older animals (Figure 19; G. P. Mullen and T. M. Rogalski). We characterized several of these alleles by staining homozygous mutants with antibodies to UNC-52 and MHC A. Our results suggest that these alleles affect accumulation of UNC-52 isoforms associated with the body wall muscles and the myoepithelial cells of the gonad. Furthermore, these effects were observed only in older animals, suggesting that these alleles affect an "adult-specific" subset of isoforms. In *e669* homozygotes, for example, staining of the body wall muscles appears to be normal until the L4 stage. After this stage, the staining of the body wall muscles is greatly reduced relative to wild-type animals. Curiously, staining of body wall muscles in the head does not appear to be affected, even in older adults. Similarly, staining of the pharynx and the uterine muscles appears to be normal. We conclude that the *e669* mutation affects a "adult-specific" subset of UNC-52 isoforms associated with most of the body wall muscles and the myoepithelial cells of the gonad.

The other viable alleles of *unc-52* behave in a similar manner, although the severity of the staining defects depends on the allele. Strong alleles, including *e444* and *e669*, affected staining most dramatically, and these effects were observed as early as the L4 stage. Mild alleles, such as *e1421*, had less dramatic effects on staining and these effects were not observed until the young adult stage. We found that the onset of paralysis in both mild and strong *unc-52* mutants correlated with the loss of UNC-52 in the basement membrane underlying the body wall muscles.

Discussion.

The *unc-52* gene encodes the nematode homolog (Rogalski et al., 1993) of perlecan, (Noonan et al., 1991; Murdoch et al., 1992; Kallunki and Tryggvason, 1992), the major heparan sulfate proteoglycan of mammalian basement membranes. Like mammalian perlecan, this polypeptide can be divided into five domains, with similarity to the LDL-receptor (domain II), laminin (domains III and V), and the neural cell adhesion molecule (domain IV). We have identified three major classes of protein products that arise through alternative splicing: short (S) (domains I - III), medium (M) (domains I - IV), and long (L) (domains I - V) isoforms (Rogalski et al., 1993; T. M. Rogalski, G. P. Mullen, and D. G. Moerman, unpublished results). This study addresses the distribution of these isoforms and examines their role in muscle development and morphogenesis in *C. elegans*.

UNC-52 is detected in basement membranes associated with contractile tissues in *C. elegans*.

Using a polyclonal antiserum that recognizes all UNC-52 isoforms, we examined the localization of UNC-52 throughout development in *C. elegans*. We found that UNC-52 is localized to basement membranes associated with contractile tissues, including the pharynx, body wall muscles, and anal muscles. We did not detect UNC-52 in the basement membrane lining the pseudocoelom, except between the body wall muscles and hypodermis. Similarly, UNC-52 was not detected around the gonad during early development or around the intestine at any stage of development. Staining was not affected by different fixation methods, nor by treatment with acid-urea, which has been shown to unmask hidden epitopes in vertebrate basement membranes (Yoshioka et al., 1994). We conclude that UNC-52 is not a general basement membrane component in *C. elegans*, but is specifically associated with contractile tissues. In contrast, mammalian perlecan is

synthesized by a wide variety of cell types, including epithelial cells (Morris et al., 1994; Ohji et al., 1994; Van Det et al., 1995), fibroblasts (Heremans et al., 1989; Murdoch et al., 1992), and synovial cells (Dodge et al., 1995), and has been detected in all basement membranes surveyed to date (reviewed in Noonan and Hassell, 1992).

Recently, Graham et al. (1997) examined the distribution of the α1 (IV) and α2 (IV) collagen chains in *C. elegans*. The expression and localization of UNC-52 and collagen IV differ in several respects (also see Graham et al., 1997). Firstly, collagen IV is more widely distributed than UNC-52 and is associated with the gonad and intestine at most developmental stages (Graham et al., 1997). Secondly, collagen IV is expressed predominately in the body wall muscles, and is exported to basement membranes surrounding other tissues, including the pharynx and intestine (Graham et al., 1997). In contrast, UNC-52 is expressed in a wider range of cell types, including pharyngeal and anal muscle cells, but does not diffuse beyond the expressing cells. Laser ablation studies established that UNC-52 acts cell autonomously and does not spread beyond the site of expression (Moerman et al., 1996). We report here that UNC-52 isoforms exhibit spatial differences in localization. The inability of UNC-52 to diffuse or to be transported beyond the site of expression is probably important for establishing and maintaining these distinct spatial patterns of localization.

A subset of UNC-52 isoforms are associated with body wall muscles during embryogenesis and are required for myofilament lattice assembly.

Using a domain IV-specific polyclonal serum, we found that UNC-52 isoforms containing this domain (M and/or L isoforms) are associated with body wall muscles during embryogenesis. These isoforms were detected in embryos as early as the comma stage (~350 minutes after the first cell division). Other muscle structural components, including MHC A, integrin, and vinculin, are expressed earlier (~290 min.), but these proteins do not

become organized until later in embryogenesis (Hresko et al., 1994). By 350 min., myoblasts have completed their migrations and formed the dorsal and ventral muscle quadrants. We conclude that UNC-52 does not have a role in muscle cell migration because it is not detected in the basement membrane until after these migrations are complete. Morphological studies suggest that muscle cell migrations occur normally in *unc-52(lethal)* mutants, supporting this conclusion (Williams and Waterston, 1994). Instead, other basement membrane components such as laminin may be important for these migrations. However, accumulation of domain IV-containing UNC-52 isoforms at regions of contact between adjacent muscle cells precedes polarization of muscle structural components and assembly of dense bodies and M-lines.

Genetic studies demonstrated that *unc-52* is essential for myofilament assembly in *C. elegans* (Rogalski et al., 1993; Hresko et al., 1994; Williams and Waterston, 1994). Lethal alleles of *unc-52* have a recessive Pat phenotype which results from failure to initiate myofilament lattice assembly in the body wall muscles (Rogalski et al., 1993; Hresko et al., 1994; Williams and Waterston, 1994). Previous work established that one of these lethal alleles is null, suggesting that the Pat phenotype results from the complete absence of all UNC-52 isoforms (Rogalski et al., 1995). The results reported here suggest that this interpretation is not correct. Using antibodies to different regions of UNC-52, we characterized the expression and localization of UNC-52 isoforms in *unc-52(lethal)* mutants. We found that a subset of *unc-52(lethal)* mutants are specifically deficient in isoforms containing domain IV. These mutant embryos still express the S isoforms associated with the pharynx and anal muscles, but lack the M and L isoforms associated with the body wall muscles. In agreement with our immunofluorescence results, two of these mutations were located within the domain IV-encoding region of *unc-52* (Bush, 1997; P. Rahmani Gorji, personal communication). These observations imply that it is the absence of M and/or L isoforms that leads to paralysis and embryonic lethality. At this

time, we do not know whether this reflects a specific requirement for either domain IV or V, or whether both domains are necessary.

Muscle sarcomere assembly in the nematode is remarkably similar to assembly of focal adhesions in mammalian cell culture (reviewed in Burridge et al, 1988; Moerman and Fire, 1997). In both processes, integrin-ECM interactions are required to initiate assembly and stabilize existing adhesion complexes (reviewed in Yamada and Geiger, 1997; Moerman and Fire, 1997). The localization of UNC-52 over the body wall muscles and the effects of *unc-52(lethal)* mutations on myofilament assembly suggest that UNC-52 anchors the dense bodies and M-lines, perhaps through interactions with integrin. Whether UNC-52 plays an instructive role or simply an attachment role in assembly of integrin complexes at the muscle cell membrane is not clear. However, without a stable focal attachment structure at the muscle cell membrane, sarcomere units within muscle cells cannot be properly organized (Williams and Waterston, 1994; reviewed in Moerman and Fire, 1997).

Mammalian perlecan is widely expressed and has been detected in basement membranes of skeletal and cardiac myocytes (Murdock et al., 1994). A number of studies have demonstrated cell adhesive properties for various domains within perlecan (Hayashi et al., 1992; Battaglia et al., 1993; Chakravarti et al., 1995), and integrin has been identified as a cell surface mediator in this attachment (Hayashi et al., 1992; Battaglia et al., 1993). However, several of these studies implicated domain III of perlecan in cell adhesion (Hayashi et al., 1992; Chakravarti et al., 1995). Our results demonstrate that S isoforms are not associated with body wall muscles, and imply that domains IV and/or V are specifically required for body wall muscle assembly in *C. elegans*. Interestingly, a recent study found that recombinant domain III from mammalian perlecan has no significant cell-adhesive activity and is not sufficient to bind integrin (Schulze et al., 1996).

βpat-3 integrin is highly disorganized in *unc-52(st560)* mutant embryos, which supports the idea that UNC-52 isoforms containing domain IV are required to anchor

integrin. Within domains IV and V, there are several regions that might mediate interaction with integrin. One of the NCAM repeats in domain IV, IgR12, has an RGD sequence (Arg-Gln-Asp), that could mediate direct interaction with integrin. To date, no direct evidence for interaction between domain IV and integrin has been demonstrated, and presence of an RGD tripeptide is not necessarily indicative of integrin-binding activity *in vivo*. Alternatively, domain V could interact with integrin. This domain is similar to the globular G-domain of α-laminin and the carboxyl region of agrin (Noonan et al., 1991; Kallunki and Tryggvason, 1992; Murdock et al., 1992; Patthy and Nikolics, 1994; Iozzo et al., 1994). The G-domain of α-laminin is important for cell adhesion, including myoblast adhesion, neurite outgrowth, and has been shown to bind β-integrin (Skubitz et al., 1991; Yurchenko et al., 1993; Sonnenberg et al., 1990; Timpl and Brown, 1994). Consequently, domain V could interact directly with cell surface components such as integrin and this may be the important difference between L and S isoforms. We are attempting to obtain mutations in the domain V-encoding region of *unc-52* to determine the significance of this domain.

A subset of UNC-52 isoforms are associated with the pharynx and the anal muscles during embryogenesis, but are not essential for myofilament assembly in these tissues.

In this study, we found that S isoforms of UNC-52 are associated with the pharynx and the anal sphincter and depressor muscles during embryogenesis. Using a polyclonal serum that recognizes all UNC-52 isoforms, we first observed pharyngeal staining in embryos around the 1.5-fold stage (~450 min.). At this stage, staining was associated with the posterior end of the pharynx, which is composed of cells from the MS lineage (Sulston et al., 1983). Staining of the anterior pharynx, which is composed of cells from the AB lineage (Sulston et al., 1983), was observed somewhat later. Intracellular staining of both

anterior and posterior pharyngeal cells was observed, indicating that pharyngeal cells from both lineages synthesize UNC-52. By the three-fold stage, staining completely surrounded the pharynx from the anterior margin to the pharyngeal-intestinal valve. In addition, staining of the anal sphincter and depressor muscles was noted at this stage.

The role of S isoforms of UNC-52 in pharyngeal or anal muscle development is not clear. We predicted that S isoforms would be important for myofilament lattice assembly in the pharynx and anal muscles because M and/or L isoforms of UNC-52 are required for myofilament lattice assembly in the body wall muscles. Therefore, we examined *unc-52(null)* mutant embryos for pharyngeal myofilament defects. However, we found no evidence of pharyngeal disruption in these mutants. Phalloidin staining established that absence of UNC-52 has no discernible effect on assembly of thin filaments in the pharynx. Similarly, preliminary studies suggest that the pharyngeal muscle-specific myosin, MHC C, assembles into well-ordered A-bands in these mutants (G. P. Mullen, unpublished results). We conclude that S isoforms of UNC-52 are not essential for pharyngeal myofilament assembly.

There are several possible roles for S isoforms in pharyngeal development and function. Mammalian perlecan has been shown to act as a co-receptor for growth factors such as basic fibroblast growth factor (bFGF), and thereby regulate cell growth and proliferation (Aviezer et al., 1994). Recently, the *let-756* gene has been shown to encode a *C. elegans* homolog of bFGF that is highly expressed in pharyngeal and body wall muscles (R. Roubin, G. P. Vatcher, M. Voinier, D. L. Baillie, and D. Thierry-Mieg, personal communication). S isoforms of UNC-52 could function in binding and sequestering bFGF and/or other growth factors that are important for pharyngeal development.

Secondly, S isoforms might be important for assembly of the pharyngeal basement membrane. As noted earlier, the ability of perlecan to interact with a variety of basement membrane components, including type IV collagen, laminin, and nidogen, is thought to be important for assembly of basement membranes (reviewed in Ruoslahti, 1988). However,

we found that type IV collagen localization is not disrupted in *unc-52(null)* mutants, implying that UNC-52 does not play an essential role in this respect.

Thirdly, S isoforms could play a role in pharyngeal morphogenesis. Recent work on the *ina-1* gene in *C. elegans* has established that integrin-mediated adhesion to the basement membrane is essential for pharyngeal morphogenesis (Baum and Garriga, 1997). The *ina-1* gene encodes an α-integrin (αina-1) that is required for a number of developmental processes, including neuronal migration, axon fasciculation, and pharyngeal morphogenesis (Baum and Garriga, 1997). However, like UNC-52, αina-1 is not essential for pharyngeal myofilament assembly (Baum and Garriga, 1997; G. P. Mullen, unpublished results). αina-1 is highly expressed in the pharynx and is concentrated beneath the pharyngeal basement membrane (Baum and Garriga, 1997). Preliminary experiments suggest that S isoforms of UNC-52 co-localize with αina-1 at the basal surface of the pharynx (G. P. Mullen, unpublished results). Since this study implicates M and/or L isoforms of UNC-52 in integrin-mediated adhesion, S isoforms could also be involved in anchoring integrin. Domain III of UNC-52 contains an RGD (Arg-Gln-Asp) sequence that could mediate interaction with integrin receptors (Rogalski et al., 1993). As noted earlier, domain III of mammalian perlecan has been implicated in integrin-binding (Hayashi et al., 1992; Chakravarti et al., 1995), although this is controversial (Schulze et al., 1996).

An intriguing possibility is that UNC-52 isoforms are capable of directly interacting with different integrin heterodimers and that the structural differences between these isoforms confer distinct integrin-binding activities. As noted earlier, distinct integrin heterodimers are expressed in the pharyngeal and body wall muscles and these integrin complexes co-localize with different UNC-52 isoforms. In the body wall muscles, M and/or L isoforms of UNC-52 co-localize with βpat-3 integrin. In the pharynx, S isoforms of UNC-52 co-localize with αina-1 integrin (G. P. Mullen, unpublished results). Additional α and β subunits have been recently identified in *C. elegans* which could pair

with βpat-3 and αina-1, respectively (B. D. Williams, personal communication; E. Hedgecock, personal communication). These observations suggest that S and M/L isoforms of UNC-52 could interact with different integrin complexes and function in distinct biological processes. This possibility could be tested using biochemical methods such as affinity chromatography or Far-Western blotting. If this possibility is correct, we would have a definitive explanation for the importance of UNC-52 isoform diversity.

Evidence for a temporal shift between early and late UNC-52 isoforms.

Alternative splicing of exons 16, 17, and 18 gives rise to isoforms that vary in the number of NCAM repeats in domain IV. Mutations in these exons are not lethal, but instead result in a recessive paralyzed phenotype that is manifested late in development. In this study, we characterized the expression of UNC-52 in *unc-52(viable)* mutants throughout their development. In embryos and young larvae, expression and localization of UNC-52 was not noticeably disrupted. However, in older animals, domain IV-containing isoforms were greatly reduced, suggesting that these mutations specifically disrupt accumulation of domain IV-containing isoforms in late larvae and adults. These results imply that there is a transition or "shift" between early and late isoforms of UNC-52. The observation that domain IV-containing isoforms are restricted to body wall muscles in embryos, but become more widely distributed in adults is also indicative of a temporal shift in isoform expression.

The importance of alternative splicing within domain IV is not clear. Several studies have demonstrated that splicing is not essential for viability or normal muscle development. Rogalski et al. (1995) found that *unc-52(viable)* mutations could be suppressed by an "exon-skipping" mechanism. More recently, several deletions in this region were identified in a screen for revertants of the viable allele *st196::Tc1* (Bush, 1997). One of these deletions, *ra515*, removes the entire alternatively spliced region, but

does not noticeably affect muscle development (Bush, 1997). These observations suggest that alternative splicing within this region is associated with fine modulation of function, rather than large-scale changes in biophysical properties. In contrast, alternative splicing events that give rise to the three major groups of isoforms (S, M, and L isoforms) are likely to significantly change the properties of these proteins, including their ability to interact with transmembrane receptors such as integrin or with other basement membrane components.

Summary and concluding remarks.

Using domain-specific antibodies, we characterized the localization of UNC-52/perlecan isoforms in the nematode *Caenorhabditis elegans*. Our results indicate that there are spatial and temporal differences in isoform localization. In embryos, S isoforms of UNC-52 are associated with the pharynx and anal muscles, while domain IV-containing isoforms (M and/or L isoforms) are associated with the body wall muscles. In adult animals, domain IV-containing isoforms become more widely distributed and are detected in basement membranes adjacent to most contractile tissues, including the pharynx and anal muscles. Our studies on mutants indicate that these larger isoforms are essential for myofilament lattice assembly in the body wall muscles and implicate domains IV and/or V in early assembly events.

To date, such complexity has not been reported for mammalian perlecan. Further studies on mammalian perlecan may reveal similar complexity either at the level of splicing or post-translational processing. Alternatively, expression of distinct perlecan isoforms may be limited to simple organisms such as *C. elegans*. This may reflect differences in the biology of perlecan in these organisms. In mammals, perlecan is synthesized by a wide variety of cell types and has been detected in all basement membranes surveyed to date (reviewed in Noonan and Hassell, 1992). Mammalian perlecan has also been implicated in

a wide variety of biological functions, including glomerular filtration, cell adhesion, and growth factor binding. In contrast, nematode perlecan is only associated with contractile tissues and our studies suggest that its primary role is in myofilament lattice assembly.

An intriguing possibility is that the multifunctionality of perlecan in mammals is incompatible with the fine modulation of structure seen in simpler systems. As stated by Duboule and Wilkins (1998) in a recent review:

"Successive recruitment of a gene to produce increasing multifunctionality has a cost: it implies modifications in gene regulation towards a more complex circuitry in order for the gene to enlarge its functional spectrum, its work load. The more complex the combinatorial controls on the expression of a gene, the more difficult it will be to create flexible control of that gene or select for its optimal expression in all cases where it is employed".

Chapter 4. Genetic Interactions.

Background.

In chapter 3, we examined the localization and function of UNC-52 isoforms in *C. elegans*. Our results suggest that alternative splicing of *unc-52* pre-mRNA is associated with temporal and spatial differences in isoform expression. However, our studies raise two important questions: i) how is alternative splicing of *unc-52* pre-mRNA regulated? and ii) how do UNC-52 and other muscle components function in myofilament lattice assembly? In this chapter, we use genetic approaches to address both of these questions.

Genetic analysis has proven to be a powerful tool for dissecting regulatory and developmental pathways. In particular, screens for suppressors or enhancers have been used to identify interacting genes or gene products. In previous studies, mutations in the *sup-38* gene were identified in a screen for suppressors of the *unc-52* paralyzed phenotype (Gilchrist and Moerman, 1992). In this study, we characterize the genetic interactions between *unc-52* and two genes, *mec-8* and *lin-14*, that enhance the *unc-52* paralyzed phenotype (section 4a). Our results suggest that *mec-8* regulates accumulation of certain UNC-52 isoforms through its effects on alternative splicing of *unc-52* pre-mRNA. In

addition, *lin-14* may regulate the developmental profile of UNC-52 expression, possibly through an alternative splicing pathway.

Another form of genetic interaction is called epistasis. A gene is said to be epistatic to another gene if alleles of the first gene mask the phenotype of alleles of the second. The chief usefulness of epistasis is that it enables one to determine the hierarchical relationship between genes in a given pathway. The vulva development pathway in *C. elegans* provides a useful example of epistasis and its implications for developmental processes. In this process, an inductive signal activates a receptor tyrosine kinase encoded by the *let-23* gene (Aroian et al., 1990). This, in turn, activates a *let-60*/Ras signaling cascade that ultimately leads to changes in gene expression and cell fate (reviewed in Greenwald, 1997). Partial loss-of-function (lf) alleles of *let-23* confer a vulvaless (Vul) phenotype (Ferguson and Horvitz, 1985; Ferguson et al., 1987). Gain-of-function (gf) alleles of *let-60* lead to a multivulva (Muv) phenotype (Ferguson and Horvitz, 1985; Ferguson et al., 1987). *let-60* is said to be epistatic to *let-23* because *let-60(gf)* alleles mask the *let-23(lf)* phenotype (Han and Sternberg, 1990). Logically, constitutive activity of a downstream component would be expected to mask the absence of an upstream component.

Epistasis can also be defined from a structural prospective. In myofilament lattice assembly, mutations disrupting early assembly events would be epistatic to mutations affecting later events. However, deducing epistatic relationships between genes with essentially identical mutant phenotypes would uninformative. Instead, antibodies to specific myofilament or adhesion components can be used in combination with muscle-affecting mutants to determine epistatic relationships. If UNC-52 is required for assembly of integrin into adhesion structures, for example, we should find that integrin is disrupted in *unc-52* mutants. Assuming the process is unidirectional, we would expect that UNC-52 is not disrupted in integrin mutants. Using this approach, we examined the epistatic relationship between UNC-52 and other muscle components, including integrin and

vinculin, in myofilament lattice assembly (section 4b). Our results imply that UNC-52 acts upstream of these other components in the assembly process.

Results

A. Regulation of UNC-52 isoform expression.

mec-8 affects accumulation of some UNC-52 isoforms.

mec-8 mutations strongly enhance the phenotype of viable unc-52 mutations, resulting in synthetic lethality. *mec-8; unc-52 (viable)* double mutants are paralyzed and arrest at the two-fold stage of embryonic development, a phenotype shared by *unc-52(null)* mutants (Lundquist and Herman, 1994). We predicted that synthetic lethality of *mec-8; unc-52* double mutants results from the additive effects of these mutations on accumulation of UNC-52 isoforms. To test this prediction, we stained *mec-8(mn463); unc-52(e444)* embryos with antibodies that can distinguish the various isoforms. The mAb MH3 recognizes an epitope encoded by exon 19 which is present in all UNC-52 isoforms with domain IV (Francis and Waterston, 1991; Rogalski et al., 1993, 1995). In wild-type embryos, MH3 stains basement membranes underlying the body wall muscles (Figure 9). The polyclonal serum GM1 recognizes epitopes in domain III of UNC-52 that are present in all UNC-52 isoforms (Moerman et al., 1996). In wild-type embryos, GM1 stains basement membranes associated with the pharynx, body wall muscles, and anal muscles. Staining with these antibodies can be detected in both *mec-8(mn463)* and *unc-52(e444)* mutant embryos.

However, we found that *mec-8(mn463); unc-52(e444)* double mutants fail to stain with MH3, suggesting that UNC-52 isoforms with domain IV are reduced or absent (Figure 20). Pharyngeal and anal muscle staining with GM1 appears to be normal (Figure

Figure 20. *mec-8* affects accumulation of domain IV-containing UNC-52 isoforms.

Embryos in panels A-F were double labeled with GM1 (green, FITC), which recognizes all UNC-52 isoforms, and DM5.6 (red, TRSC), which recognizes myosin heavy chain A (MHC A). Small arrows indicate the pharynx and large arrows indicate a body wall muscle quadrant. Panels A and D show both channels simultaneously, while panels B, C, E, and F show single channel images. Panels A-C show a wild-type embryo, while D-F show an arrested *mec-8(mn463); mnC1 dpy-10 unc-52(e444)* double mutant. Note the reduced staining of the body wall muscles with GM1 and the disorganization of MHC A in the double mutant (panels E and F; compare with B and C). The pharynx and anal muscles (arrowhead in panel E) in the mutant, however, exhibit a wild-type staining pattern (compare panels B and E). Embryos in G-L were double labeled with GM1 (green, FITC), and MH3 (red, TRSC), which recognizes an epitope in domain IV of UNC-52. Panels G-I show a wild-type embryo, J-K a *mec-8(mn463); mnC1 dpy-10 unc-52(e444)* double mutant, and L shows an *unc-52(e444)* single mutant. G and J show both channels simultaneously. Note the absence of MH3 staining in the mutant embryo in panel K. Scale bar indicates 10 microns.

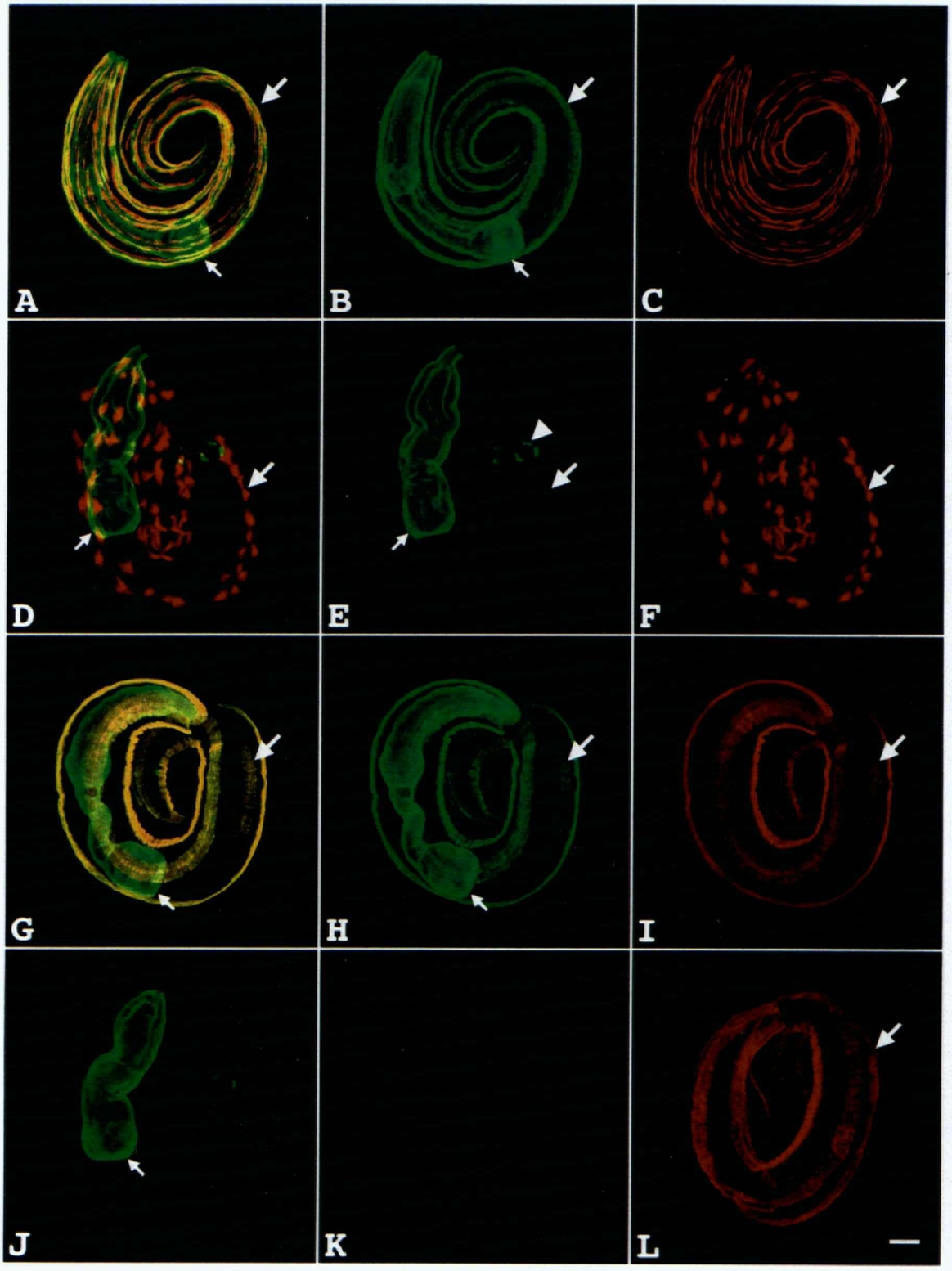
A
B
C
D
E
F
G
H
I
J
K
L

20), however, indicating that not all UNC-52 isoforms are affected. These results suggest that *mec-8; unc-52* synthetic lethality results from absence of UNC-52 isoforms with domain IV, which are required for myofilament lattice assembly in the body wall muscles. The absence of these isoforms is clearly an additive effect because it is not observed in either *mec-8(mn463)* or *unc-52(e444)* animals. These results demonstrate that *mec-8* mutations affect accumulation of a specific subset of UNC-52 isoforms during embryogenesis, presumably through their effects on processing of *unc-52* pre-mRNA.

Allele-specific interactions between *mec-8* and *unc-52*.

To further characterize the interaction between *mec-8* and *unc-52*, we examined the expression of UNC-52 isoforms in other *mec-8; unc-52(viable)* double mutants. Previous work (Lundquist and Herman, 1994; R. K. Herman, personal communication; D. G. Moerman, personal communication) had demonstrated that *mec-8(loss-of-function)* mutations were lethal in combination with any of the viable, paralyzed alleles of *unc-52*, including *e669*, *e998*, and *e1012*. We constructed strains of the genotype *mec-8(u74)/+; unc-52(viable)* and prepared embryos from these strains. These embryos were then double labeled with GM1 and MH3, as described above.

We found that MH3 staining was abnormal in all of these *mec-8; unc-52* double mutants, but the precise effects depended on the *unc-52* allele. Results of these experiments are summarized in Table 6. In *mec-8; unc-52(e444)* and *mec-8; unc-52(e998)* double mutants, for example, no detectable staining with MH3 was observed. Thus, nonsense mutations in exon 18 greatly reduce or eliminate expression of any MH3-reactive isoforms in the absence of *mec-8* function. In *mec-8; unc-52(e669)* and *mec-8; unc-52(e1012)* double mutants, however, some MH3 staining was detected. In these double mutants, we observed strong staining of the anterior-most muscle cells in each of the four body wall muscle quadrants (Figure 21B). The remaining body wall muscle cells,

TABLE 6. MH3 staining in *mec-8* and *mec-8;unc-52* mutant embryos.

Genotype	MH3
mec-8(u74)	+
mec-8(mn463); mnC1 dpy-10 unc-52(e444)	-
mec-8(u74); unc-52(e444)	-
mec-8(u74); unc-52(e998)	-
mec-8(u74); unc-52(e1012)	- (except for head muscles)
mec-8(u74); unc-52(e669)	- (except for head muscles)
mec-8(u74); unc-52(1421)	-
mec-8(u218); unc-52(e669su250) at 15°c.	+
mec-8(u218); unc-52(e669su250) at 25°c.	-
mec-8(u74); unc-52(ra507)	+ (retained within muscle cells)
mec-8(u74); unc-52(ra38)	+ (retained within muscle cells)

however, did not stain. Thus, in the absence of *mec-8* function, nonsense mutations in exon 17 greatly reduce or eliminate most MH3-reactive isoforms, but still allow expression of certain spatially-restricted isoforms.

Recently, the *ra507* allele was also shown to have a synthetic lethal interaction with *mec-8* (Bush, 1997). This allele has a 9-bp insertion in exon 18 that adds three amino acids to IgR10. However, *ra507* homozygotes have no obvious phenotype and appear to have normal muscle structure. We did not expect that *mec-8; unc-52(ra507)* double mutants would be lethal, particularly because the *ra507* allele does not confer an obvious mutant phenotype when homozygous.

This unexpected finding led us to examine the expression of UNC-52 isoforms in *mec-8; unc-52(ra507)* double mutants. We found that *mec-8; unc-52(ra507)* double mutants have unusual defects in the localization of a subset of UNC-52 isoforms. In wild-type embryos at the three-fold stage, MH3 stains basement membranes underlying the body wall muscles. In *mec-8; unc-52(ra507)* embryos, however, MH3 immunoreactivity is predominately found intracellularly and is greatly reduced in the underlying basement membrane (Figure 21E). Staining of the pharynx and the anal muscles with GM1 in this mutant, however, appears to be normal, indicating that expression of other UNC-52 isoforms is not affected (Figure 21C). We conclude that UNC-52 isoforms with domain IV are not secreted, but are instead retained within muscle cells in *mec-8; unc-52(ra507)* double mutants. *mec-8; unc-52(ra38)* double mutants, which also exhibit a synthetic lethal phenotype (R. K. Herman, personal communication), have similar defects in the cellular trafficking of UNC-52 (data not shown).

Figure 21. Expression of UNC-52 isoforms in *mec-8; unc-52* double mutants.

mec-8(u74); unc-52(e1012) (A and B) and *mec-8(u74); unc-52(ra507)* (C and E) double mutants were double labeled with GM1 (A and C) and the mAb MH3 (B and E). Panel A shows GM1 staining of a *mec-8(u74); unc-52(e1012)* double mutant. Note that pharyngeal staining appears to be normal, but body wall muscle staining is greatly reduced, except over the anterior-most muscles. Panel B shows MH3 staining of the same embryo. Note that body wall muscle staining is restricted to the anterior-most muscle cells (indicated with arrows). Panel C shows a *mec-8(u74); unc-52(ra507)* double mutant stained with GM1. Note that pharyngeal staining appears to be normal, but body wall muscle staining is diffuse and disorganized. Panel D and E are magnified views of a section of muscle from a wild-type embryo (D) and a *mec-8(u74); unc-52(ra507)* double mutant (E) stained with MH3. Arrows indicate the position of a muscle cell, while the arrowhead indicates the basement membrane. Note the prominent intracellular staining in the *mec-8(u74); unc-52(ra507)* double mutant as compared with the wild-type embryo. Scale bar indicates 10 microns.

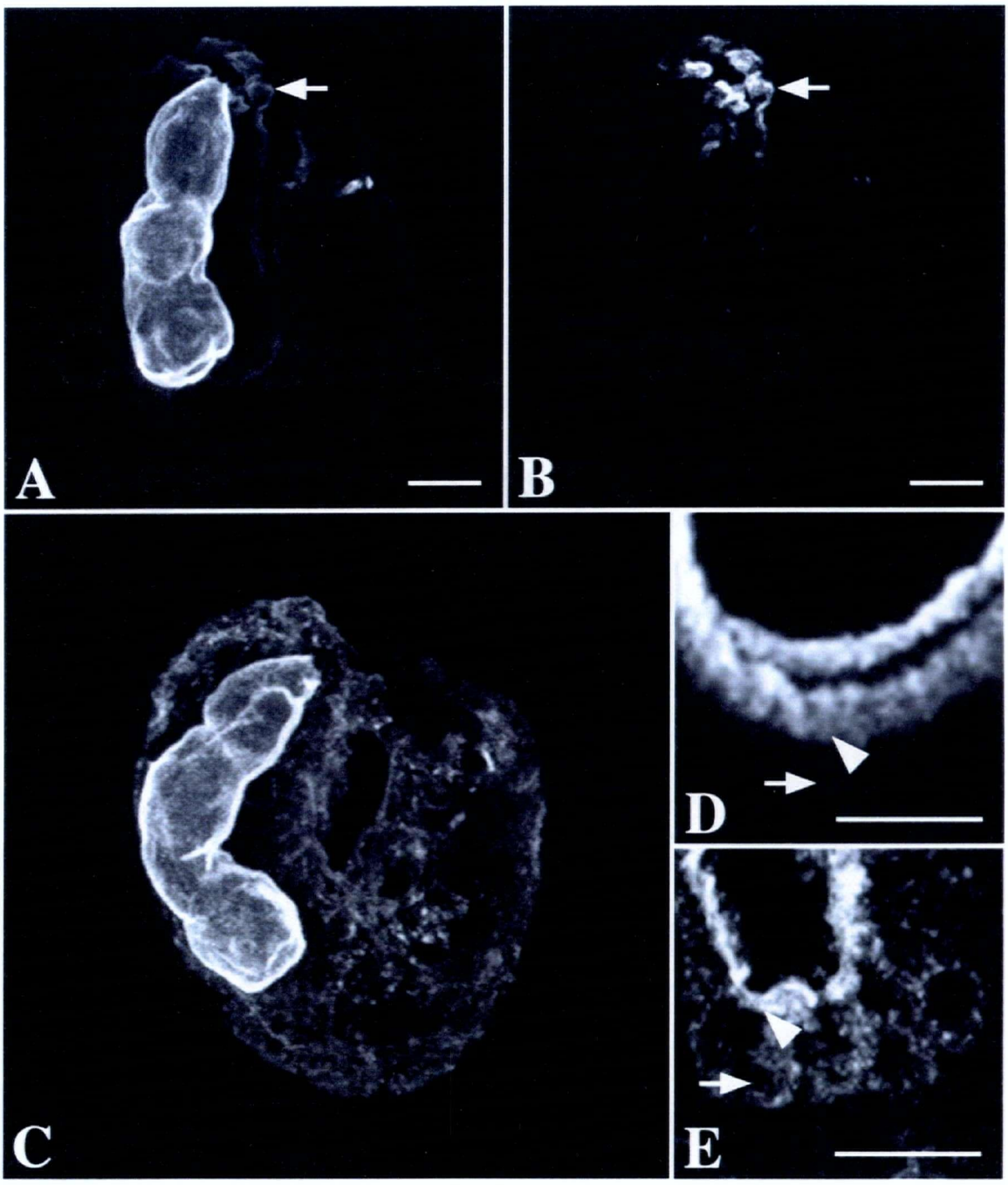
A
B
C
D
E

Genetic interactions between heterochronic genes and viable alleles of *unc-52*.

Viable alleles of *unc-52* have a recessive Unc phenotype that is manifested late in development (Brenner, 1974; Gilchrist and Moerman, 1992). Animals homozygous for viable alleles move normally as young larvae, but become progressively paralyzed as they mature. This progressive paralysis is caused by gradual disruption of myofilaments in body wall muscles posterior to the head (Mackenzie et al., 1978; Waterston et al., 1980). Viable alleles vary in severity; strong alleles such as *e444* cause paralysis early in the fourth larval stage, while milder alleles such as *e1421* cause paralysis during adulthood (Mackenzie et al., 1978; Waterston et al., 1980; Gilchrist and Moerman, 1992). Seven of these mutations have been identified by sequencing PCR-amplified DNA from homozygous mutant animals (Rogalski et al., 1993, 1995). All seven mutations affect alternatively-spliced exons (16, 17, and 18) near the 3' end of the gene and only disrupt a subset of UNC-52 isoforms.

On the basis of several observations, we speculated that viable alleles of *unc-52* affect isoforms that are made late in development and that there is a developmental switch between "early" and "late" isoforms of UNC-52. Firstly, animals homozygous for viable alleles develop normally until relatively late in their lifecycle and then become paralyzed. Because these mutations affect alternatively-spliced exons, the late appearance of the paralyzed phenotype suggests that these exons are spliced out during early development, but not in later development. Secondly, we have stained *unc-52(viable)* mutants with antibodies to UNC-52, and our results suggest that accumulation of UNC-52 is normal during embryogenesis and early larval development (see chapter 3). However, in older animals, staining of body wall muscles is greatly reduced, suggesting that accumulation of UNC-52 is strongly affected later in development. And thirdly, *mec-8* expression, which is required for the 15 - 19 and 16 - 19 splices, is detected in embryos, but not older animals

(A. Davies, C. A. Spike, R. K. Herman, and J. E. Shaw, personal communication), suggesting that *mec-8*-dependent splices are made exclusively during early development.

If alternative-splicing of exons 16, 17, and 18 occurs in a developmentally regulated manner, it is reasonable to assume that it is governed by regulatory genes that control the timing of developmental events. Mutations in the heterochronic genes *lin 4* and *lin-14* have been shown to alter the developmental timing of stage-specific events in *C. elegans* (Ambros et al., 1989). For example, animals homozygous for *lin-14(loss-of-function)* mutations develop precociously, exhibiting adult-specific characteristics after the second larval molt. In contrast, animals homozygous for *lin-14(gain-of-function)* or *lin-4(loss-of-function)* mutations exhibit retarded development, with early characteristics being retained in temporally older animals. To test whether *lin-4* and *lin-14* regulate the developmental timing of UNC-52 isoform expression, we looked for genetic interactions between *unc-52* and these heterochronic genes.

We predicted that *lin-14(loss-of-function)* mutations would cause the paralyzed phenotype of *unc-52(viable)* mutations to be manifested at an earlier developmental stage. We tested this prediction by constructing a *lin-14(n179ts); unc-52(e444)* double mutant. *n179ts* is a temperature-sensitive allele of *lin-14*; at the restrictive temperature (25°), *n179ts* homozygotes exhibit the *lin-14(loss-of-function)* phenotype. *unc-52(e444)* and *lin-14(n179ts); unc-52(e444)* strains were grown at 25° and scored to determine the stage at which paralysis occurred.

Our results demonstrate that *lin-14* mutations alter the stage at which the *unc-52* paralyzed phenotype is manifested. When grown at restrictive temperature (25°), *lin-14(n179ts); unc-52(e444)* double mutants become paralyzed significantly earlier than *unc-52(e444)* single mutants (Figure 22). Under these conditions, *lin-14(n179ts); unc-52(e444)* animals move slowly as second-stage larvae and are paralyzed by the third larval stage, whereas *unc-52(e444)* animals do not become paralyzed until the fourth larval stage. This enhancement of the *unc-52(e444)* phenotype by *lin-14(n179ts)* is strictly temperature-

sensitive; at permissive temperature, *lin-14(n179ts); unc-52(e444)* double mutants become paralyzed at the same stage as *unc-52(e444)* single mutants. Thus, *lin-14(loss-of-function)* mutations enhance the *unc-52(viable)* phenotype and change the developmental stage at which it is manifested. These observations imply that *lin-14* regulates expression of UNC-52 in some manner, perhaps by influencing alternative splicing of *unc-52* pre-mRNA.

Other alleles of *unc-52*, such as *e1012* and *e1421*, gave similar results in combination with *lin-14(n179ts)*. For all combinations tested, the *unc-52* paralyzed phenotype was manifested at an earlier stage in the *lin-14; unc-52* double mutants than in the corresponding *unc-52* single mutants (Figure 22). The precise phenotype of these *lin-14; unc-52* double mutants, however, depended on the severity of the *unc-52* allele. *lin-14(n179ts); unc-52(e444)* double mutants, for example, were completely paralyzed as third-stage larvae when grown at restrictive temperature. In contrast, *lin-14(n179ts); unc-52(e1012)* double mutants were less severely affected and often continued to move, albeit very slowly, at the third larval stage. *lin-14(n179ts); unc-52(e1421)* double mutants were also less severely affected. However, in each of these *lin-14; unc-52* double mutants, *unc-52* mutant phenes were manifested precociously. These results are consistent with our hypothesis that *lin-14* regulates the developmental timing of certain alternative splicing events.

Since *lin-4(loss-of-function)* mutations result in retarded development, we predicted that these mutations should delay the onset of paralysis in *unc-52(viable)* mutants. In effect, *lin-4(loss-of-function)* mutations should suppress *unc-52(viable)* mutations. To test this prediction, we constructed a *lin-4(e912); unc-52(e444)* strain and monitored these animals for the *unc-52* paralyzed phenotype. We found that *lin-4(e912); unc-52(e444)* double mutants became paralyzed at the L4 stage, much like *unc-52(e444)* single mutants. Other *unc-52* alleles, such as *e1012*, gave similar results in combination with *lin-4(e912)*. We conclude that *lin-4(loss-of-function)* mutations do not alter the stage at which the *unc-52(viable)* phenotype is manifested. In addition, *lin-4; unc-52* double mutants displayed

Figure 22. Onset of paralysis in *unc-52* mutants and *lin-14; unc-52* double mutants.

The stage at which the *unc-52* paralyzed phenotype is manifested is shown for three *unc-52* alleles (*e444*, *e1012*, and *e1421*; black columns) and the corresponding *lin-14; unc-52* double mutants (striped columns). In each case, 25 animals (n=25) were scored as described in the methods and materials.

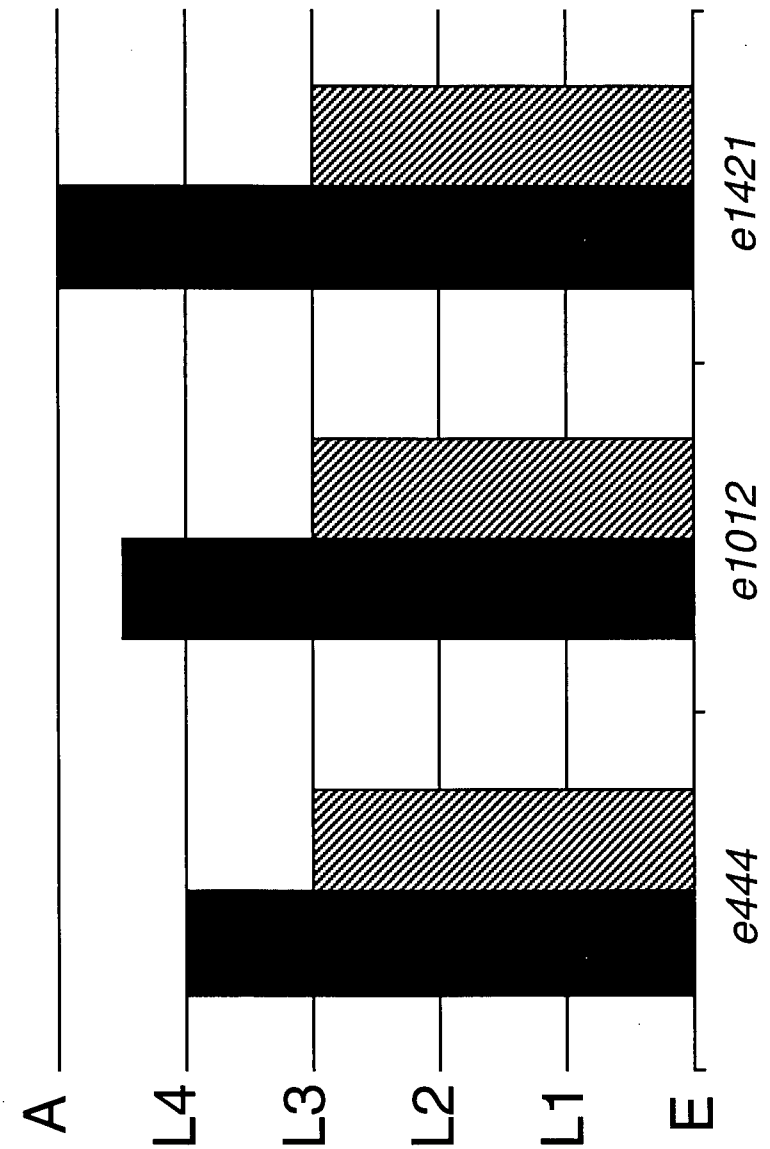
A
L4
L3
L2
L1
E
e1421
e1012
e444

both *lin-4* and *unc-52* phenes without any sign of suppression or enhancement, providing no evidence for genetic interaction between these genes.

B. The role of UNC-52 in muscle sarcomere assembly.

unc-52 acts upstream of other Pat genes in the process of myofilament lattice assembly.

Myofilament lattice assembly is thought to begin at the plasma membrane in regions of contact between adjacent muscle cells (Hresko et al., 1994). UNC-52 and integrin are key early components in the assembly process and are required for organization of cytoskeletal-associated proteins such as vinculin and talin (Hresko et al., 1994; Moulder et al., 1996). However, prior to this study, it was not clear whether integrin and other muscle components affect the localization of UNC-52 in the basement membrane. In this study, we address this question by examining the localization of UNC-52 in eight different muscle-affecting mutants. Our results suggest that UNC-52 acts upstream of these other muscle-affecting genes in the assembly process and lead us to propose an expanded pathway of myofilament lattice assembly.

We stained embryos homozygous for Pat mutations in genes affecting muscle assembly and function with antibodies to UNC-52 (GM1) and MHC A (DM5.6). Included in this study were Pat alleles of *pat-2* (α-integrin; B. D. Williams, personal communication), *pat-3* (β-integrin; Gettner et al., 1995), and *deb-1* (vinculin; Barstead and Waterston, 1989, 1991). Mutant embryos were identified by their characteristic morphology and defects in MHC A organization (Williams and Waterston, 1994). We focused primarily on post-arrest mutant embryos because these animals could be readily distinguished from their phenotypically wild-type siblings. In most cases, we could not reliably distinguish mutant embryos prior to the 1.5-fold stage, but we did examine populations of younger embryos for disorganization of UNC-52. For comparison, we

examined *let-2(mn153)* mutant embryos; mutations in this gene have been shown to disrupt localization of UNC-52 in embryos after the beginning of muscle contraction (Figure 23; K. R. Norman and D. G. Moerman, personal communication). Using this approach, we characterized Pat alleles of nine different muscle-affecting genes, including those encoding known dense body and M-line components (Table 7).

Surprisingly, we found that none of these mutants exhibit defects in the localization of UNC-52. For example, the GM1 staining pattern in *pat-3(st564)* mutant embryos appears to be quite normal, even in arrested embryos (Figure 23). In these mutants, GM1 stains basement membranes associated with the pharynx, body wall, and anal muscles and there is no obvious disruption of the wild-type staining pattern. The morphology of the pharynx and other tissues is abnormal in *pat-3(st564)* mutant embryos, but these defects are observed in all Pat mutants and probably result from the failure of these animals to elongate beyond two-fold. We conclude that βpat-3 integrin is not required for the correct localization of UNC-52.

Similarly, Pat mutations in the *unc-112* gene, which encodes a nematode homolog of MIG-2 (T. M. Rogalski, personal communication), have no affect on localization of UNC-52. We took advantage of a characteristic defect to identify *unc-112* homozygotes prior to the 1.5-fold stage and examine the localization of UNC-52 in these early embryos. When stained with GM1, a small break in each ventral muscle quadrant can be seen in wild-type embryos (also see Hresko et al., 1994). This break may correspond to the position of the amphid commissure (C. R. Norris, I. A. Bazykina, E. M. Hedgecock, and D. H. Hall, personal communication). In *unc-112* mutant embryos, this break is noticeably larger than in wild-type embryos (see Figure 23). This defect is apparent by the early comma stage and can be used to distinguish *unc-112* homozygotes from their phenotypically wild-type siblings. Consequently, we were able to look at early *unc-112* embryos and ensure that there were no defects in the initial localization of UNC-52. We conclude that *unc-112* function is not required for UNC-52 to be localized properly.

Figure 23. Immunolocalization of UNC-52 and myosin in lethal muscle-affecting mutants.

let-2(mn153) (A and B), *pat-3(st564)* (C and D), and *unc-112(st581)* (E and F) mutant embryos were double labeled with GM1 (UNC-52) and DM5.6 (MHC A). Arrows indicate the terminal bulb of the pharynx, while the arrowheads indicate a body wall muscle quadrant. Note the disorganization of UNC-52 in the *let-2* embryo (panel A), and compare with *pat-3* (panel C) and *unc-112* (panel E) embryos. The large arrow in panels E and F indicate gaps in the ventral muscle quadrants which are characteristic of *unc-112* homozygotes. Also note the disorganization of MHC A in all three mutants. Panels A and B were generously provided by K. R. Norman and D. G. Moerman.

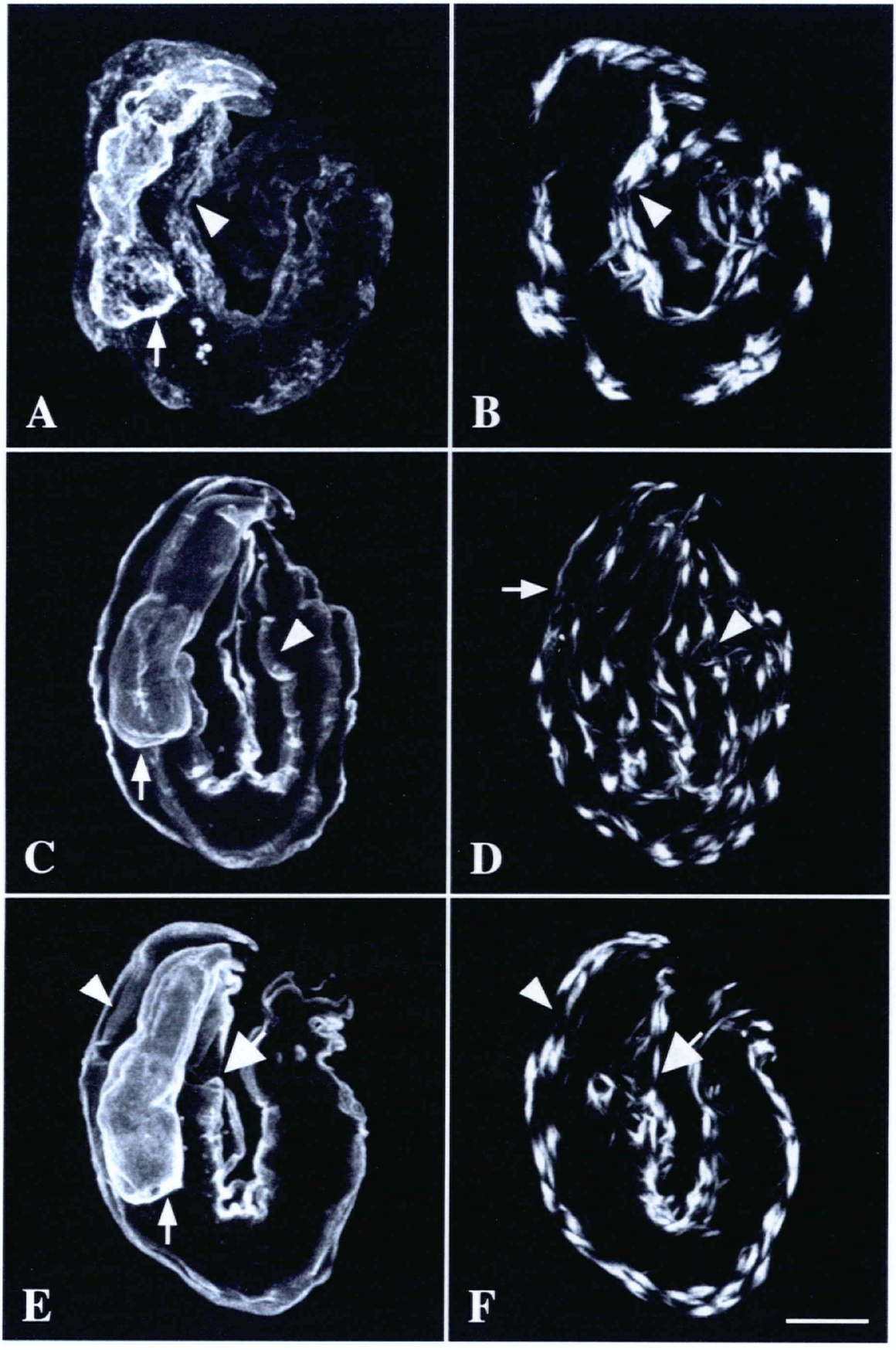
A
B
C
D
E
F

TABLE 7. Distribution of UNC-52 in Pat mutants.

Gene	Gene Product	Allele	Phenotype	GM1 Staining	Reference
*let-2**	α2 (IV) collagen	*mn153*	late paralysis	disorganized	Sibley et al., 1993, 1994.
myo-3	MHC A	*st386*	severe paralysis	normal	Waterston, 1989.
unc-112	MIG-2	*st562, st581*	severe paralysis	normal	Williams and Waterston, 1994.
pat-2	α-integrin	*st538*	severe paralysis	normal	B. D. Williams, pers. comm.
pat-3	β-integrin	*st564*	severe paralysis	normal	Gettner et al., 1995.
pat-4	unknown	*st551*	severe paralysis	normal	Williams and Waterston, 1994.
pat-5	Ca^{++} channel	*st556*	severe paralysis	normal	Lee et al., 1997.
deb-1	vinculin	*st555*	severe paralysis	normal	Barstead and Waterston, 1991.
pat-11	unknown	*st541*	mild paralysis	normal	Williams and Waterston, 1994.
pat-12	unknown	*st430*	mild paralysis	normal	Williams and Waterston, 1994.

*Courtesy of K. R. Norman and D. G. Moerman

Qualitatively similar results were observed with *pat-2*, *pat-4*, and the other muscle-affecting genes (Table 7). We did observe some disorganization of UNC-52 in milder Pat mutants, including *myo-3* and *pat-12*. In these mutants, sections of the dorsal muscle quadrants often pull away from the hypodermis, especially in older embryos (Waterston, 1988; Williams and Waterston, 1994). The basement membrane also pulls away from the hypodermis and remains associated with the detached muscle (data not shown). Disorganization of UNC-52 in these mutants appears to result from detachment of the muscle quadrants and not from a direct effect on UNC-52. We conclude that UNC-52 localization is not directly affected by mutations in any of these muscle-affecting genes, including *pat-2* (α-integrin; B. D. Williams, personal communication), *pat-3* (β-integrin; Gettner et al., 1995), and *deb-1* (vinculin; Barstead and Waterston, 1989, 1991).

Discussion.

A. Regulation of UNC-52 isoform expression.

Alternative splicing of *unc-52* pre-mRNA gives rise to a number of distinct UNC-52/perlecan isoforms. Some of these splicing events result in large-scale differences in domain structure, while others modulate structure within given domains. For example, alternative splicing of exons 16, 17 and 18 gives rise to isoforms that vary in the number of NCAM repeats within domain IV (Rogalski et al., 1993, 1995). These exons each encode a single NCAM repeat and are arranged such that one or more exons can be spliced from the pre-mRNA without disrupting the reading frame. In this study, we examined the role of the *mec-8* gene in regulating some of these alternative splicing events. We also characterized the genetic interactions between *unc-52* and a group of global regulators

called heterochronic genes. We present a possible model for both temporal and qualitative control of isoform expression through *mec-8* and the heterochronic genes.

The *mec-8* gene regulates accumulation of a subset of UNC-52 isoforms.

The *mec-8* gene encodes a putative RNA-binding protein that regulates some of the alternative splices in the domain IV-encoding region of *unc-52* (Lundquist et al., 1996). *mec-8* is required for the exon 15 - 19 and exon 16 - 19 splices, but the other splices are *mec-8*-independent (Lundquist et al., 1996). The *mec-8*-dependent splice products (15 - 19 and 16 - 19) are not absolutely required in *unc-52(+)* animals because myofilament assembly is not disrupted in *mec-8* mutants (Lundquist and Herman, 1994). However, in the absence of *mec-8* function, otherwise viable mutations in alternatively spliced exons of *unc-52* are lethal, presumably because these exons are no longer spliced from *unc-52* pre-mRNA. *mec-8; unc-52(viable)* double mutants exhibit a two-fold arrest phenotype similar to the Pat alleles of *unc-52* (Lundquist and Herman, 1994). We predicted that the synthetic lethal phenotype resulted from the combined effects of *mec-8* and *unc-52* mutations on the accumulation of UNC-52 isoforms.

To test this hypothesis, we examined the expression and localization of UNC-52 isoforms in *mec-8; unc-52* double mutants. In *mec-8(mn463); unc-52(e444)* mutant embryos, UNC-52 isoforms containing domain IV were reduced or absent. However, S isoforms of UNC-52, which are associated with the pharynx and anal muscles in embryos, were expressed at normal levels. Therefore, *mec-8(mn463); unc-52(e444)* double mutants are specifically deficient in domain IV-containing isoforms, much like certain *unc-52(lethal)* mutants. Absence of these isoforms is clearly an additive effect because it is not observed in either *mec-8(mn463)* or *unc-52(e444)* animals. These results demonstrate that *mec-8* mutations disrupt the accumulation of a specific subset of UNC-52 isoforms during embryogenesis by affecting the processing of *unc-52* pre-mRNA.

Spatially-restricted expression of domain IV-containing UNC-52 isoforms in a subset of *mec-8; unc-52* double mutants.

Based on our model of *mec-8*-regulated splicing, we predicted that expression of domain IV-containing UNC-52 isoforms should be detected in some *mec-8; unc-52* double mutants. If the *unc-52* mutation was in exon 17, for example, we would expect the 15 - 18 splice to permit expression of some domain IV-containing products. We confirmed this prediction by constructing *mec-8; unc-52(e669)* and *mec-8; unc-52(e1012)* double mutants and staining these animals with a mAb specific for domain IV of UNC-52. Both *e669* and *e1012* are point mutations that introduce translational stop codons into exon 17 (Rogalski et al., 1995). We detected accumulation of domain IV-containing isoforms in *mec-8; unc-52(e669)* and *mec-8; unc-52(e1012)* double mutants, but these isoforms were restricted to the anterior-most body wall muscle cells in each quadrant. As suggested earlier, domain IV-containing isoforms in these double mutants are probably the result of the 15 - 18 splice. These observations imply that certain *unc-52* alternative splicing events are restricted to a subset of body wall muscle cells.

Recent studies suggest that body wall muscles do not uniformly express the same set of genes. The *unc-129* gene, which encodes a member of the TGF-β family, is expressed in motorneurons and in the dorsal body wall muscles (A. Colavita, S. Krishna, H. Zheng, R. W. Padgett, and J. G. Culotti, personal communication). In addition, the homeotic gene *mab-5* is expressed in a subset of the posterior body wall muscles (D. Cowing and C. Kenyon, personal communication; Wang et al., 1993). These observations suggest that body wall muscle cells in different locations express distinct sets of regulatory and structural genes (also see Moerman and Fire, 1997).

The spatially-restricted expression of certain UNC-52 isoforms implies that they may be specifically required by muscle cells in these locations. Conceivably, anterior

muscles might require a specific UNC-52 isoform either for myofilament lattice assembly or cell adhesion. The distinct arrangement of hypodermal cells in the anterior may necessitate a distinct UNC-52 isoform for either of these processes.

A subset of *mec-8; unc-52* double mutants exhibit defects in the secretion of UNC-52.

We found that *mec-8; unc-52(ra507)* and *mec-8; unc-52(ra38)* double mutants exhibit defects in the cellular trafficking of UNC-52. These *mec-8; unc-52* embryos accumulate high levels of UNC-52 within the body wall muscles and do not secrete significant amounts into the underlying basement membrane. We do not believe that the *ra507* and *ra38* mutations specifically disrupt regions of UNC-52 that are important for cellular trafficking. Rather, we suspect that these mutations disrupt protein folding, resulting in cellular retention by protein chaperones and other components of the cells quality control system. NCAM repeats in UNC-52 contain two conserved cysteine residues that form disulfide bonds that are important for proper tertiary structure. The altered NCAM repeats in these two revertants contain an additional cysteine, which may be incompatible with proper folding and lead to retention by the muscle cells. These observations suggest that *mec-8* may be a useful tool to determine whether mutationally-altered NCAM repeats in UNC-52 are functional at the protein level.

Genetic interactions between *unc-52* and the heterochronic genes.

Developmental age in *C. elegans* is specified by a group of regulators called heterochronic genes (reviewed in Ambros, 1997). After hatching, *C. elegans* goes through four larval stages (L1 - L4) before reaching adulthood. Each of these stages is characterized by specific developmental events such as cell divisions or fusions. The stage-specific patterns

of somatic cell division and fusion are designated S1 - S4 (L1 - L4 stages) and Ad (adult). Through a complex series of interactions, heterochronic genes regulate the timing of these stage-specific events (reviewed in Ambros, 1997). Mutations in heterochronic genes result in precocious or retarded expression of stage-specific events, depending on the gene and the nature of the mutation. For example, *lin-14(loss-of-function)* mutations block expression of the S1 program, resulting in precocious expression of the S2 program (Ambros and Horvitz, 1984). In contrast, *lin-4(loss-of-function)* mutations result in reiteration of the S1 program (Ambros and Horvitz, 1984).

In this study, we show that *lin-14* interacts genetically with *unc-52* and causes precocious expression of the *unc-52(viable)* phenotype. Animals homozygous for *unc-52(viable)* mutations move normally as young larvae, but become paralyzed as they mature. Paralysis is usually manifested at the L4 stage, although there is variation between alleles (Waterston et al., 1980; Gilchrist and Moerman, 1992). *lin-14(n179ts); unc-52(viable)* double mutants, however, manifest the paralyzed phenotype at least one larval stage earlier. These observations imply that *lin-14* regulates expression of UNC-52, either directly or indirectly, during development in *C. elegans*.

The *unc-52(viable)* mutations are clustered in three alternatively-spliced exons in the domain IV-encoding region of *unc-52* (Rogalski et al., 1993, 1995). Because these mutations disrupt alternatively-spliced exons and specifically affect older animals, we suggest that they affect UNC-52 isoforms that are expressed late in development. Our immunological studies on *unc-52(viable)* mutants support the idea of a "switch" between early and late isoforms (see Chapter 3). The genetic interaction between *lin-14* and *unc-52* is also consistent with this idea. Conceivably, *lin-14* could regulate the timing of this developmental switch, perhaps through an alternative splicing pathway.

Expression studies on *mec-8* have provided further evidence for a switch and suggest a possible mechanism for regulating its timing. A *mec-8*::GFP reporter is expressed in body wall muscles and other cell types in embryos, but expression in the

muscles disappears after embryogenesis (A. Davies, C. A. Spike, R. K. Herman, and J. E. Shaw, personal communication). This on/off switch in *mec-8* expression is predicted to shift the mode of splicing from *mec-8*-dependent to *mec-8*-independent. Therefore, *mec-8* not only regulates alternative splicing of *unc-52* transcripts, but also functions as a binary switch between early and late patterns of splicing. At one level, *mec-8* can be regarded as a heterochronic gene because loss of *mec-8* function results in precocious appearance of adult characteristics.

There are several possible explanations for the genetic interaction between *lin-14* and *unc-52*. One possibility is that *lin-14* regulates expression of *mec-8*. However, we feel this is unlikely because *mec-8* expression in body wall muscles is restricted to embryogenesis, and *lin-14* does not regulate the timing of embryonic events (Ambros, 1997). A second possibility is that *lin-14* regulates some aspect of transcript or protein turnover. We suggest that the switch between early and late isoforms is not merely a transition between two splicing pathways, but must logically include a mechanism for turnover of embryonic transcripts or protein. Perhaps degradation of embryonic gene products is linked to developmental age and is regulated in some manner by *lin-14*. However, regardless of the mechanism, the genetic interactions between *lin-14* and *unc-52* suggest that heterochronic genes regulate the developmental profile of UNC-52 expression.

Our observations imply that the *unc-52* paralyzed phenotype is associated with the S4 program. However, we emphasize that the onset of paralysis is a consequence of the dystrophy of the body wall muscles and probably occurs much later in development than the actual switch. In electron microscopy studies, *unc-52(viable)* mutants were found to manifest myofilament lattice defects after the first larval stage (Mackenzie et al., 1979). These observations and *mec-8* expression studies suggest that the "switch" occurs quite early in development, perhaps as early as S1.

However, expression of the *unc-52* paralyzed phenotype was not delayed or suppressed in *lin-4(e912); unc-52(viable)* double mutants, indicating that simple reiteration

of the S1 program is not sufficient to postpone this putative switch. We suggest that heterochronic genes regulate at least one component of a splicing or degradation pathway, which would explain the interaction between *lin-14* and *unc-52*. However, other components in the pathway must be independent of heterochronic genes and these components are limiting in older animals. Perhaps these components decay with chronological time or are regulated by a different molecular "clock".

Recent studies suggest that developmental timing in the soma and gonad is controlled by distinct mechanisms. *lin-14* and other heterochronic genes specify developmental age in the soma, but do not affect the development of the gonad. In contrast, *daf-12* specifies developmental age in both the soma and the gonad (A. Antebi, J. G. Culotti, and E. M. Hedgecock, personal communication). This dual activity implies that *daf-12* is part of two distinct timing mechanisms, one controlling somatic development and the other controlling gonadal development, and may thereby integrate the two programs (A. Antebi, J. G. Culotti, and E. M. Hedgecock, personal communication). Although there are multiple mechanisms for specifying developmental age, clearly these mechanisms must be coordinated during development. A further implication of these studies is that a given tissue or gene could respond to more than one timing mechanism. Because UNC-52 is associated with both somatic and gonadal tissues, regulatory network(s) controlling its expression must be responsive to two distinct timing mechanisms. Consequently, the proposed switch between early and late UNC-52 isoforms could be controlled by both "somatic" and "gonadal" programs.

B. The role of UNC-52 in muscle sarcomere assembly.

UNC-52 acts upstream of integrin and other muscle components in the process of myofilament lattice assembly.

Using antibodies to UNC-52, we examined the localization of UNC-52 in lethal muscle-affecting mutants, including *pat-2* (α-integrin; B. D. Williams, personal communication), *pat-3* (β-integrin; Gettner et al., 1995), and *deb-1* (vinculin; Barstead and Waterston, 1991). We found that none of these mutations disrupt the localization of UNC-52 in basement membranes associated with the body wall muscles or other tissues in *C. elegans*. We conclude that these gene products are not required for proper localization of UNC-52. One interpretation of these results is that UNC-52 acts upstream of these other muscle-affecting genes in the process of myofilament lattice assembly. Our results also imply that basement membrane assembly does not require integrin or any of the other myofilament lattice components surveyed in this study.

In contrast, UNC-52 is clearly required for proper localization of these muscle components. Hresko et al. (1994) found that β-integrin and vinculin were disorganized in *unc-52(null)* mutants. We confirmed these observations and identified a subset of UNC-52 isoforms that are essential for anchoring integrin, either directly or indirectly, to the basement membrane (chapter 3). Domain IV-containing isoforms co-localize with βpat-3 integrin in the body wall muscles and the distribution of βpat-3 is disrupted in *unc-52* mutants lacking these isoforms. We emphasize that UNC-52 has a very direct effect on myofilament lattice assembly and integrin anchorage. In contrast, collagen IV, another basement membrane component, has minimal effect on lattice assembly and is therefore unlikely to interact directly with integrin in this process (Williams and Waterston, 1994; K. R. Norman and D. G. Moerman, personal communication). We suggest that integrin may interact directly with these UNC-52 isoforms and that this interaction is a key early event in myofilament lattice assembly.

Taken together, these results imply that assembly of muscle attachment structures begins at the plasma membrane in regions of contact between adjacent body wall muscle cells (also see Hresko et al., 1994; reviewed in Moerman and Fire, 1997). The binding of integrin to an extracellular ligand, possibly UNC-52, nucleates assembly of dense bodies and M-lines. In turn, accumulation of cytoskeletal proteins such as talin and vinculin at the plasma membrane is contingent on the presence of both UNC-52 and integrin. Finally, assembly of ordered thick and thin filaments is dependent on both membrane-associated and cytoskeletal proteins. This model is summarized in Figure 24.

Molecular interactions in cell adhesion complexes and implications for myofilament lattice assembly.

Genetic and cell biological studies have established a possible hierarchy of events in the assembly of muscle attachment structures in *C. elegans* (also see Hresko et al., 1994). However, the molecular interactions required to assemble these structures are still not known in any detail. Assembly of cell adhesion structures in other systems offers useful insight into the molecular interactions and dynamics involved in assembly of such structures.

Assembly of cell adhesion structures involves a complex series of molecular events including integrin binding and clustering, tyrosine phosphorylation, and accumulation of both structural and signaling components near the plasma membrane (reviewed in Burridge et al., 1997; Yamada and Geiger, 1997). A molecular hierarchy of events has been established beginning with clustering of integrin heterodimers and integrin-ligand binding (Miyamoto et al., 1995). There are distinct cellular consequences for both of these events. For example, clustering of integrins is sufficient to induce a number of proteins, including FAK (focal adhesion kinase) and tensin, to accumulate near the plasma membrane (Miyamoto et al., 1995). However, both clustering and ligand-binding are needed to

Figure 24. A pathway for myofilament lattice assembly in *C. elegans*. (A) A schematic of a dense body indicating the known structural and regulatory components. (B) A possible pathway for assembly based on epistasis experiments described in chapter 4 and observations reported in Rogalski et al. (1993), Hresko et al. (1994), Williams and Waterston (1994), and Moulder et al. (1996).

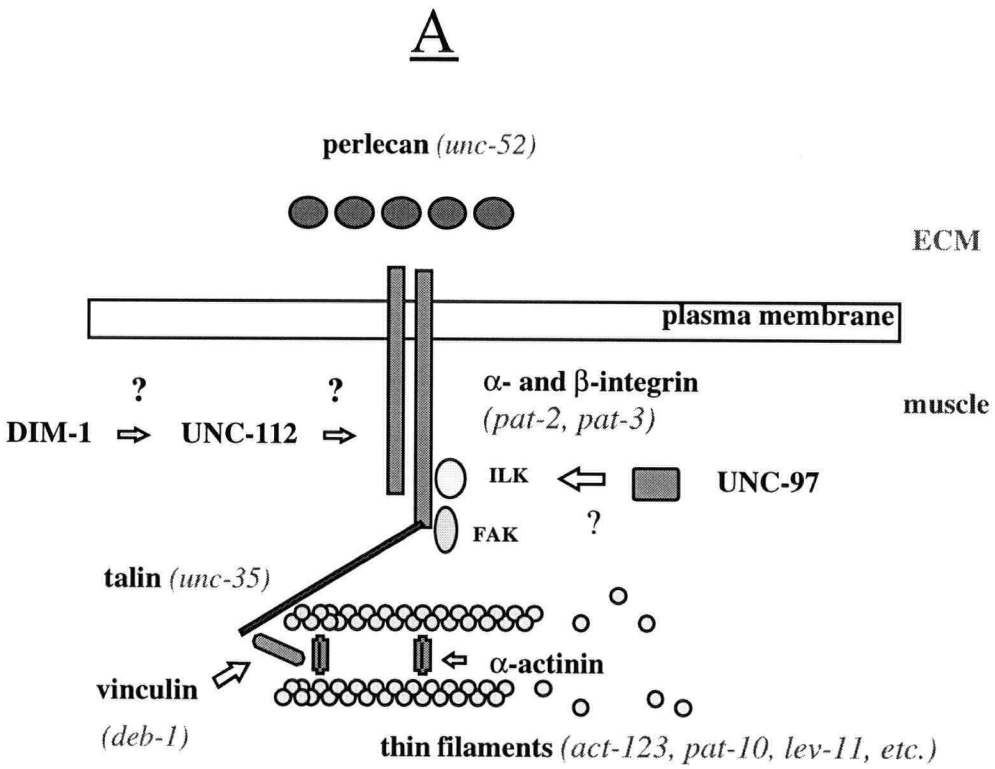
A
perlecan (unc-52)
ECM
plasma membrane
muscle
?
?
DIM-1
UNC-112
α- and β-integrin
(pat-2, pat-3)
ILK
UNC-97
?
FAK
talin (unc-35)
α-actinin
vinculin
(deb-1)
thin filaments (act-123, pat-10, lev-11, etc.)

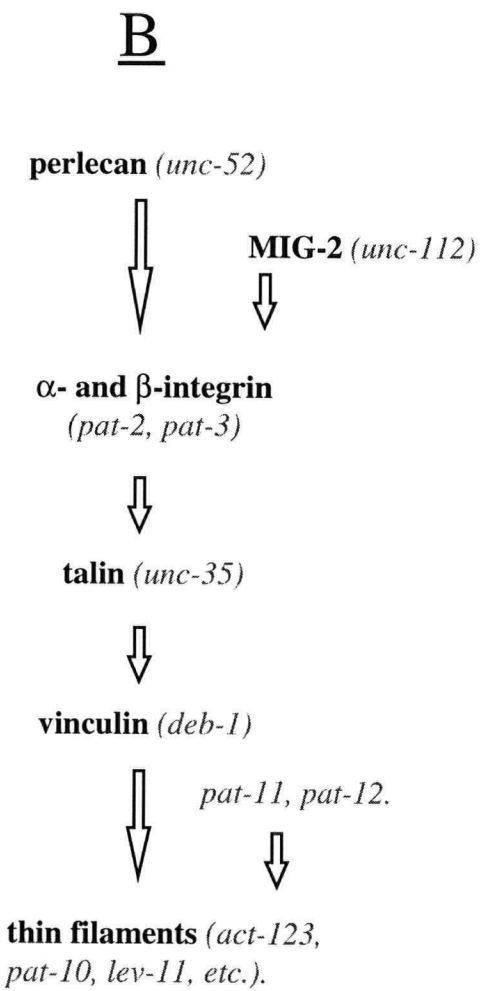
B
perlecan (unc-52)
MIG-2 (unc-112)
α- and β-integrin
(pat-2, pat-3)
talin (unc-35)
vinculin (deb-1)
pat-11, pat-12.
thin filaments (act-123,
pat-10, lev-11, etc.).

induce association with cytoskeletal proteins such as α-actinin, vinculin, and talin. Finally, tyrosine phosphorylation is required for accumulation of actin and paxillin near the plasma membrane (Miyamoto et al., 1995).

Integrin heterodimers appear to be unable to interact with the cytoskeleton before binding their extracellular ligands. Ligand-binding induces a conformational change that allows β-integrin to interact directly with the cytoskeleton (reviewed in Yamada and Miyamoto, 1995). In *unc-52* mutants, cytoskeletal proteins fail to accumulate or polarize beneath the plasma membrane (Rogalski et al., 1993; Hresko et al., 1994; Williams and Waterston, 1994). These observations are consistent with the idea that integrin interacts directly with UNC-52 because the absence of the extracellular ligand would be expected to block integrin association with cytoskeletal proteins.

However, recent studies suggest that integrin clustering requires participation of intracellular proteins (reviewed in Burridge et al., 1997). In particular, the small GTP-binding protein Rho is thought to regulate assembly of cell adhesion structures and promote integrin clustering. Hotchin and Hall (1995) found that integrin clustering in human dermal fibroblasts was dependent on functional Rho activity. Microinjection of C3 transferase, a potent inhibitor of Rho activity, resulted in disassembly of focal adhesions. Hotchin and Hall concluded that extracellular factors are not sufficient to induce adhesion complex assembly and that activity of GTP-binding proteins is also necessary.

Recent studies imply that Rho promotes adhesion complex assembly by regulating actomyosin-based contraction (reviewed in Burridge et al., 1997). Chrzanowska-Wodnicka and Burridge (1996) found that inhibitors of actomyosin contraction block Rho-mediated assembly of adhesion complexes. Rho has been shown to regulate actomyosin-based contraction by activating the Rho-kinase cascade. Rho-kinase can directly phosphorylate the regulatory myosin light chain (MLC) and also inhibits the activity of the myosin phosphatase (Kimura et al., 1996). Increased phosphorylation of the myosin light

chain promotes assembly of myosin II into bipolar filaments and stimulates myosin ATPase activity, leading to increased contractility (Burridge and Chrzanowska-Wodnicka, 1996).

These findings led to a model for adhesion complex assembly in which integrins are clustered in response to tension exerted by the cytoskeleton (Chrzanowska-Wodnicka and Burridge, 1996; reviewed in Burridge et al., 1997). According to this model, integrin-ligand binding promotes association with the cytoskeleton. In response to activation by Rho, actomyosin-based contraction then "pulls" integrins across the surface of the cell. As integrins become clustered in response to this tension, they aggregate and form strong attachments. This model requires that integrin-ligand interactions are sufficiently weak to allow dissociation and reassociation of integrins and their extracellular ligands. We suggest that the substrate must also be sufficiently homogenous to allow multiple interactions while integrins are pulled across the surface of the cell.

This model of integrin clustering has several implications for our study of UNC-52 and its role in muscle assembly. During embryonic development, UNC-52 appears to be homogeneously distributed in basement membranes underlying the body wall muscles. We suggest that this distribution is necessary for clustering of integrin through a mechanism similar to that proposed by Chrzanowska-Wodnicka and Burridge (1996). Integrin clustering would then induce local changes in the basement membrane to reinforce the newly-formed adhesion complex. The accumulation of UNC-52 over dense bodies and M-lines during post-embryonic development may be an example of such changes. This accumulation could result from the availability of multiple binding sites in each adhesion complex. Alternatively, contractile force exerted by the muscle cells may locally deform the basement membrane. Stopak and Harris (1982) demonstrated that mechanical force from fibroblasts locomotion could deform a collagen substrate and align collagen fibers into linear tracts. The force of muscle contraction, which is transmitted to the basement membrane through dense bodies and M-lines, may exert a similar, but more local effect on the basement membrane. In either case, we would predict that accumulation of UNC-52

over dense bodies, M-lines, and muscle cell margins is dependent on these adhesion structures. Although clustering of integrin is clearly dependent on interactions with extracellular proteins, accumulation of extracellular proteins over adhesion complexes may well be dependent on integrin. We suggest that assembly of mature adhesion structures probably involves inductive interactions that remodel and reorganize both the cytoskeleton and associated proteins, and the basement membrane.

Chapter 5. Discussion

Summary and conclusions.

unc-52 encodes the nematode homolog of mammalian perlecan, the major heparan sulfate proteoglycan of the extracellular matrix (Rogalski et al., 1993). This protein has five domains, with similarity to the LDL-receptor (domain II), laminin (domains III and V), and the neural cell adhesion molecule (domain IV). We identified three major classes of protein products that arise through alternative splicing: short (S) (domains I - III), medium (M) (domains I - IV), and long (L) (domains I - V) isoforms. In addition, alternative splicing within the domain IV-encoding region of *unc-52* gives rise to isoforms with variable numbers of NCAM repeats (Rogalski et al., 1993, 1995). In this study, we examined the localization of UNC-52/perlecan isoforms and their role in myofilament lattice assembly and other developmental processes in *C. elegans*.

To study the localization of these UNC-52/perlecan isoforms, we generated domain-specific polyclonal antisera. Immunolocalization studies using an isoform-general antiserum indicate that UNC-52 is localized to basement membranes associated with pharyngeal, body wall, anal, and sex-specific muscles in *C. elegans*. Immunolocalization studies using a domain IV-specific antiserum indicate that there are spatial and temporal differences in isoform localization. In embryos, S isoforms are associated with the

pharynx and anal muscles, while domain IV-containing isoforms (M and/or L isoforms) are associated with the body wall muscles. Domain IV-containing isoforms are more widely distributed in adults and are detected in basement membranes adjacent to most contractile tissues.

To determine the function of these isoforms in myofilament assembly and other developmental processes, we used domain-specific antisera to characterize lethal and viable *unc-52* mutants and established that domain IV-containing isoforms are essential for myofilament assembly in body wall muscles. We speculate that domain IV-containing UNC-52 isoforms interact directly with integrin heterodimers and thereby nucleate formation of dense bodies and M-lines. The role of S isoforms in pharyngeal and anal muscle development, however, remains unclear. Perhaps these isoforms are important for pharyngeal morphogenesis; they may interact with the *ina-1* α-integrin as part of a distinct cytoskeletal network in the pharynx. Therefore, short (domains I - III), medium (domains I - IV), and long (domains I - V) isoforms may have distinct integrin-binding activities. This hypothesis could be tested using biochemical or genetic approaches. We also determined that *unc-52(viable)* mutations disrupt accumulation of domain IV-containing UNC-52 isoforms in late larvae and adults, suggesting that there is a "switch" between "early" and "late" isoforms.

mec-8 encodes a putative RNA-binding protein that regulates a subset of alternative splicing events (Lundquist et al., 1996). We characterized the genetic interactions between *unc-52* and *mec-8*, and presented a model for both temporal and qualitative control of isoform expression through *mec-8* and a group of global regulators called heterochronic genes. Characterization of the genetic interactions between *unc-52* and *mec-8* also revealed the presence of spatially restricted UNC-52 isoforms, and established the usefulness of *mec-8* as a tool for dissecting UNC-52 isoform expression. Finally, we examined the distribution of perlecan in mutants lacking key muscle attachment proteins such as integrin, and our results suggest that perlecan acts upstream of membrane-associated components in

the muscle assembly process. We propose a model for muscle assembly that begins with integrin-basement membrane interactions at the muscle cell surface.

General discussion.

Through genetic and cell biological studies, we now have a detailed picture of the molecular events involved in assembling the ordered array of proteins comprising the myofilament lattice. The assembly of this complex structure is both regulative and spontaneous; the assembly of attachment sites appears to be carefully regulated, while thick filament assembly, at least in its initial stages, is driven by the self-assembly properties of myosin, the chief structural component. Many of the principles underlying myofilament lattice assembly are shared by other developmental processes, including axonal outgrowth and neuromuscular junction (NMJ) formation. In this section, we attempt to identify these principles and discuss their relationship to other developmental and macromolecular assembly processes.

Myofilament lattice assembly begins with the expression of structural and regulatory muscle proteins. There are some differences between organisms in this respect. In vertebrates, expression of muscle structural proteins (with the exception of desmin) is not observed until myoblasts have finished replicating (Devlin and Emerson, 1978; Hill et al., 1986). In *C. elegans*, at least three proteins, myosin, β-integrin, and vinculin, are expressed before the final cell divisions (Hresko et al., 1994). However, there is no strict correlation between the onset of expression of specific muscle proteins and the order of assembly.

The formation of filament attachment sites is nucleated by the interaction of extracellular proteins and their cognate receptors on the muscle cell surface. Genetic studies established the importance of integrin receptors in nucleating assembly of filament

attachment sites in *Drosophila melanogaster* (Volk et al., 1990) and *Caenorhabditis elegans* (Williams and Waterston, 1994; Gettner et al., 1995). In this study, we identified a subset of UNC-52/perlecan isoforms that are essential for myofilament lattice assembly in *C. elegans* body wall muscles. These isoforms may interact directly with integrin heterodimers and nucleate formation of filament attachment sites.

The requirement for cell surface interactions between an extracellular ligand and its receptor is central to a variety of developmental and signaling processes. For example, in NMJ formation, interactions between neural agrin and cell surface receptors such as MASC activate a signaling cascade that results in mobilization of acetylcholine receptors and other molecules to the postsynaptic region of the muscle (Glass et al., 1996; Kleiman and Reichardt, 1996). In a more general sense, the requirement for two or more proteins to form a nucleating complex is seen in such diverse biological processes as transcriptional initiation, gene silencing, and protein translation. This requirement for multiple proteins in nucleation complexes probably prevents the assembly of complexes in the wrong place or at the wrong time, and affords multiple levels of regulation.

Assembly of filament attachment sites also requires clustering of cell surface receptors. This process is clearly dependent on extracellular proteins, but may also involve intracellular proteins such as the GTP-binding protein Rho. Clustering of cell surface receptors is seen in other cytoskeletal associated processes such as focal adhesion assembly, and the parallels between muscle development and focal adhesion assembly were described in detail in Chapter 4. The clustering of cell surface molecules is also seen in NMJ formation. In this process, the signaling cascade initiated by agrin-receptor interactions stimulates clustering of acetylcholine receptors to the postsynaptic region (Glass et al., 1996; Kleiman and Reichardt, 1996). Clustering of acetylcholine receptors is maintained by association with the basement membrane and cytoskeleton (Campanelli et al., 1996; Glass et al., 1996). The difference between muscle assembly and NMJ formation, however, is that receptor clustering in muscle assembly is required for

recruitment of other molecules to the cell surface and initiation of signaling events, rather than being a consequence of these events. However, in both processes, cytoskeletal reorganization is associated with clustering of cell surface molecules. In muscle assembly, receptor binding and clustering have distinct cellular consequences, and both are required for full recruitment of cytoskeletal associated proteins to the nascent attachment structures.

Assembly of filament attachment structures is likely to be regulated by changes in protein conformation and regulatory proteins such as kinases and phosphatases. These regulatory mechanisms play an important role in regulating focal adhesion assembly (see chapter 4). For example, conformational changes in vinculin regulate its ability to interact with actin and integrin linked kinase (ILK) has been identified as a negative regulator of focal adhesion assembly (Hannigan et al., 1996). However, the role of such regulatory mechanisms in myofilament lattice assembly has not been addressed to date. Homologs of ILK and other kinases have been recently identified in *C. elegans*, and the role of these proteins in lattice assembly can now be determined.

The precise relationship between filament attachment sites and myofilaments in lattice assembly is not entirely clear. Myofilament lattice organization is clearly dependent on the presence of filament attachment sites. However, recent studies suggest that myofilament assembly does not actually begin at these sites. Epstein et al. (1993) examined the distribution of thick filament components in the body wall muscles of *C. elegans* embryos. Randomly oriented filaments containing myosin and paramyosin were observed around the periphery of muscle cells prior to formation of distinct myofilaments. These "nascent filaments" are thought to represent intermediates in the assembly process, but do not appear to be associated with the cell membrane or filament attachment sites. The filament attachment structures may not be required for the early stages of filament assembly, but may instead serve as "indicators of spatial patterning" (Hresko et al., 1994). However, how attachment structures themselves are positioned is unclear, and efforts are ongoing to elucidate the patterning mechanism.

Thick filament assembly depends on the intrinsic properties of myosin, the major structural component, and the participation of auxiliary proteins. Huxley (1963) first established that myosin is capable of self-assembly into synthetic thick filaments. Myosin dissociates under conditions of high ionic strength; when ionic strength is lowered, myosin reassembles into thick filaments. These filaments share a number of structural features with native thick filaments, although there is some heterogeneity in filament length. These observations imply that myosin self-assembles into thick filaments *in vivo*. In some models of thick filament assembly, myosin alone regulates such properties as filament length (reviewed in Davis, 1988). However, in most current models of assembly, auxiliary proteins interact with myosin to form mature thick filaments.

The ability of some proteins to self-assemble into large polymers has been observed in the formation of other biological structures. For example, microtubules are cytoskeletal structures that are involved in a variety of processes, including cell movement, vesicle transport, and cell division (reviewed in Downing and Nogales, 1998). Microtubules are polymers of tubulin and self-assemble *in vitro* from purified tubulin subunits (reviewed in Downing and Nogales, 1998). Bacteriophage also take advantage of the self-assembly properties of some proteins. For example, the major head protein of bacteriophage HK97, called gp5, is folded with the assistance of the GroEl chaperonin, and then self-assembles into pentamers and hexamers called capsomers (reviewed in Hendrix and Duda, 1998). These capsomers then initiate assembly of the prohead [an intermediate in head assembly], along with the portal protein, gp3, and the prohead protease, gp4. The prohead dissociates under conditions of high ionic strength; this dissociated mixture of capsomers is capable of reassembly into structures that are indistinguishable from phage proheads. The self-assembly properties of gp5 appear to be important for capsomer formation, prohead assembly, and specification of prohead size.

In contrast, formation of thin filaments is largely dependent on the participation of auxiliary proteins, including actin polymerizing, severing, capping, and cross-linking

proteins. For example, the G-actin binding protein, profilin, is thought to direct filament assembly by promoting polymerization of actin monomers at the barbed ends of the filament (Pollard and Copper, 1986; Pantaloni and Carlier, 1993). Gelsolin and related proteins appear to regulate filament length through their filament capping and severing activities (Weeds and Maciver, 1993; Schafer and Cooper, 1995). Members of the cofilin family also have filament severing and depolymerizing activities (Moon and Drubin, 1995). Trinick (1992) proposed that thin filament length is determined by so-called "molecular rulers". The giant protein nebulin has been proposed as a ruler for determining thin filament length because the size of nebulin from different organisms corresponds closely to the length of their thin filaments (Labeit et al., 1991). Similarly, titan, another giant muscle protein, has been proposed to determine thick filament length (Trinick, 1992). Although this ruler mechanism is attractive, we are not aware of any direct experimental evidence demonstrating that either nebulin or titan determine filament length.

In most multicellular organisms, post-embryonic development is primarily a period of growth and sexual maturation. Muscle cells increase substantially in size during post-embryonic development; within each muscle cell, the myofilament lattice also increases in size. Growth of the myofilament lattice requires that existing filament attachment structures increase in size, thereby increasing the depth of the lattice. The growth of attachment structures probably also increases their mechanical strength, which would accommodate the increased mechanical stress associated with larger body size. Growth also requires that new attachment structures form, increasing the length and width of the myofilament lattice. Consequently, during post-embryonic development, muscle cells must accommodate two seemingly distinct processes: i) growth and fortification of existing structures, and ii) *de novo* assembly of new structures.

In this study, we studied the expression of UNC-52/perlecan isoforms throughout *C. elegans* development and determined the effects of various mutant alleles on accumulation of these isoforms. Through these studies, we established that there are

temporal changes in isoform expression within a given muscle type. For example, a subset of domain IV-containing isoforms are expressed in body wall muscles in embryos. Another subset of domain IV-containing isoforms is expressed in body wall muscles predominately at later developmental stages. On the basis of these observations, we proposed that there is developmental switch between "early" and "late" expressed isoforms of UNC-52/perlecan. There are several possible explanations for this switch in isoform expression. First, the switch to late isoforms could accommodate increased levels of mechanical stress encountered in larger animals. Secondly, the switch could reflect the need to balance *de novo* assembly of new attachment structures with growth of existing structures. Currently, we are not certain which of these models is correct. Further studies on isoform switching in muscle development will hopefully clarify the role of such transitions in myofilament lattice assembly and growth.

A possible mechanism for myofilament lattice growth is suggested by developmental and structural studies in *C. elegans*. During embryonic muscle development, lattice components concentrate beneath the cell membrane in regions of contact between adjacent cells (Hresko et al., 1994; Moerman et al., 1996). These regions of cell-cell contact appear to function as nucleating centers in the assembly of attachment structures. Embryonic attachment structures are distinct from dense bodies in older animals because they lack the protein α-actinin (Hresko et al., 1994). In older animals, specialized attachment structures are found at the ends of muscle cells where they anchor the half I-bands [also regions of cell-cell contact]. These structures are called adhesion plaques and lack α-actinin, like embryonic attachment structures (Francis and Waterston 1985). These observations imply that adhesion plaques are intermediates in dense body assembly and suggest a possible model for myofilament lattice growth. According to this model, assembly of new attachment sites, in the form of adhesion plaques, occurs at the ends of muscle cells. These adhesion plaques are converted to dense bodies by addition of α-actinin, and new adhesion plaques are then assembled. This model is attractive because

assembly processes are restricted to the ends of muscle cells and established structures are not disrupted. Furthermore, there is an implicit patterning mechanism; positional information for the placement of new attachment sites could be conveyed by existing sites at the ends of muscle cells. This model can now be tested using the array of muscle-affecting mutants, GFP fusions, and antibodies available to *C. elegans* researchers. Such studies should provide insight into the mechanisms regulating growth of the myofilament lattice and other highly ordered macromolecular structures.

Summary

Myofilament lattice assembly consists of a series of molecular events beginning at the cell membrane. Because each event is dependent on preceding events, the process can be tightly controlled, temporally and spatially, and inappropriate assembly events are minimized. The general principles governing assembly of the myofilament lattice are shared by other multiprotein assemblages. Although considerable progress has been made in identifying muscle proteins, and elucidating their roles in assembly, the mechanisms governing filament length, positioning of attachment structures, and growth of the lattice are still unknown. In addition, comparative studies on different muscle types are needed to identify both specialized mechanisms and common themes. As our studies on pharyngeal muscle assembly illustrate, there are certainly differences in the roles of specific muscle proteins in different muscle types.

References.

Albertson, D. G., and J. N. Thomson, 1976. The pharynx of *Caenorhabditis elegans*. Philos. Trans. R. Soc. Lond. Biol. Sci. 275: 299-325.

Albertson, D. G., 1984. Localization of the ribosomal genes in *Caenorhabditis elegans* chromosomes by *in situ* hybridization using biotin-labeled probes. EMBO J. 3: 1227-1234.

Ambros, V., and H. R. Horvitz, 1984. Heterochronic mutants of the nematode *Caenorhabditis elegans*. Science 226: 409-416.

Ambros, V., and E. G. Moss, 1994. Heterochronic genes and the temporal control of *C. elegans* development. Trends in Genetics 10.

Ambros, V., 1997. Heterochronic genes., pp. 501-518 in *C. elegans* II, edited by D. L. Riddle, T. Blumenthal, B. J. Meyer and J. Priess. Cold Spring Harbor Laboratory Press, New York.

Avery, L., 1993. The genetics of feeding in *Caenorhabditis elegans*. Genetics 133: 897-917.

Aviezer, D., D. Hecht, M. Safran, M. Elsinger, G. David et al., 1994. Perlecan, basal lamina proteoglycan, promotes basic fibroblast growth factor-receptor binding, mitogenesis and angiogenesis. Cell 79: 1005-1013.

Barstead, R. J., and R. H. Waterston, 1989. The basal component of the nematode dense-body is vinculin. J. Biol. Chem. 264: 10177-10185.

Barstead, R. J., and R. H. Waterston, 1991a. Vinculin is essential for muscle function in the nematode. J. Cell Biol. 114: 715-724.

Barstead, R. J., and R. H. Waterston, 1991b. Cloning, sequencing and mapping of an α-actinin gene from the nematode *Caenorhabditis elegans*. Cell Motil. Cytoskeleton 20: 69-78.

Battaglia, C., U. Mayer, M. Aumailley and R. Timpl, 1992. Basement membrane heparan sulfate proteoglycan binds to laminin by its heparan sulfate chains and to nidogen by sites in the protein core. Eur. J. Biochem. 208: 359-366.

Battaglia, C., A. M., K. Mann, U. Mayer and R. Timpl, 1993. Structural basis of β1 integrin-mediated cell adhesion to a large heparan sulfate proteoglycan from basement membranes. Eur. J. Cell Biol. 61: 92-99.

Baum, P. D., and G. Garriga, 1997. Neuronal migrations and axon fasciculation are disrupted in *ina-1* integrin mutants. Neuron 19: 51-62.

Benian, G. M., T. L. Tinley, X. Tang and M. Borodovsky, 1996. The *Caenorhabditis elegans* gene *unc-89*, required for muscle M-line assembly, encodes a giant modular protein composed of Ig and signal transduction domains. J. Cell Biol. 132: 835-848.

Brenner, S., 1974. The genetics of *Caenorhabditis elegans*. Genetics 77: 71-94.

Burd, C. G., and G. Dreyfuss, 1994. Conserved structures and diversity of functions of RNA-binding proteins. Science 265: 615-621.

Burridge, K., K. Fath, T. Kelly, G. Nuckolls and C. Turner, 1988. Focal adhesions: transmembrane junctions between extracellular matrix and the cytoskeleton. Ann. Rev. Cell Biol. 4: 487-525.

Burridge, K., M. Chrzanowska-Wodnicka and C. Zhong, 1997. Focal adhesion assembly. Trends Cell Biol. 7: 342-347.

Bush, J. A., 1997. "An analysis of UNC-52/perlecan domain IV immunoglobulin repeats in myofilament assembly in *Caenorhabditis elegans*". M.Sc. thesis, University of British Columbia, Canada.

Campanelli, J. T., G. G. Gayer and R. H. Scheller, 1996. Alternative RNA splicing that determines agrin activity regulates binding to heparin and α-dystroglycan. Development 122: 1663-1672.

Chakravarti, S., T. Horchar, B. Jefferson, G. Laurie and J. R. Hassell, 1995. Recombinant domain III of perlecan promotes cell attachment through its RGD sequence. J. Biol. Chem. 270: 404-409.

Chalfie, M., and J. Sulston, 1981. Developmental genetics of the mechanosensory neurons of *Caenorhabditis elegans*. Dev. Biol. 82: 358-370.

Chrzanowska-Wodnicka, M., and K. Burridge, 1996. Rho-stimulated contractility drives the formation of stress fibers and focal adhesions. J. Cell Biol. 133: 1403-1415.

Cohen, I. R., S. Grassel, A. D. Murdoch and R. V. Iozzo, 1993. Structural characterization of the complete human perlecan gene and its promoter. Proc. Nat. Acad. Sci. U.S.A. 90: 10404-10408.

Couchman, J. R., R. Kapoor, M. Sthanam and R. R. Wu, 1996. Perlecan and basement membrane-chondroitin sulfate proteoglycan (bamacan) are two basement membrane chondroitin/dermatan sulfate proteoglycans in the Engelbreth-Holm-Swarm tumor matrix. J. Biol. Chem. 271(16): 9595-9602.

Danielson, K. G., A. Martinez-Hernandez, J. R. Hassell and R. V. Iozzo, 1992. Establishment of a cell line from the EHS tumor: Biosynthesis of basement membrane constituents and characterization of a hybrid proteoglycan containing heparan and chondroitin sulfate side chains. Matrix. 12.

Davis, J. S., 1988. Assembly processes in vertebrate skeletal thick filament formation. Ann. Rev. Biophys. Chem. 17: 217-239.

Devlin, R. B. and C. P. Emerson, Jr., 1978. Coordinate regulation of contractile protein synthesis during myoblast differentiation. Cell 13: 599-611.

Downing, K. H. and E. Nogales, 1998. Tubulin and microtubule structure. Curr. Opin. Cell Biol. 10: 16-22.

Duboule, D. and A. S. Wilkins, 1998. The evolution of "bricolage'. Trends in Genetics. 14: 54-59.

Edelman, G. M., 1986. Cell adhesion molecules in the regulation of animal form and tissue pattern. Ann. Rev. Cell Biol. 2: 81-116.

Epstein, H. F., D. M. Miller, L. A. Gossett and R. M. Hecht, 1982. Immunological studies of myosin isoforms in nematode embryos., pp. 7-14 in Muscle Development: Molecular and Cellular Control., edited by M. L. Pearson, and H. F. Epstein. Cold Spring Harbor Laboratory, New York.

Epstein, H. F., D. M. Miller, I. Ortiz and G. C. Berliner, 1985. Myosin and paramyosin are organized about a newly identified core structure. J. Cell Biol. 100: 905-915.

Epstein H. F., D. L. Casey and I. Ortiz, 1993. Myosin and paramyosin of *Caenorhabditis elegans* embryos assemble into nascent structures distinct from thick filaments and multi-filament assemblages. J. Cell. Biol. 122(4):845-58.

Farquhar, M., 1982. The glomerular basement membrane: A selective macromolecular filter., pp. 335-378 in Cell Biology of Extracellular Matrix, edited by E. D. Hay. Plenum Press, New York.

Ferguson, E. L., and H. R. Horvitz, 1985. Identification and characterization of 22 genes that affect the vulval cell lineages of the nematode *Caenorhabditis elegans*. Genetics 110: 17-72.

Ferguson, E. L., P. W. Sternberg and H. R. Horvitz, 1987. A genetic pathway for the specification of the vulval cell lineages of *Caenorhabditis elegans*. Nature 326: 259-267.

Francis, G. R., and R. H. Waterston, 1985. Muscle organization in *C. elegans*: localization of proteins implicated in thin filament attachment and I-band organization. J. Cell Biol. 101: 1532-49.

Finney, M. and G. B. Ruvkun, 1990. The *unc-86* gene product couples cell lineage and cell identity in *C. elegans*. Cell 63: 895-900.

Francis, R., and R. H. Waterston, 1991. Muscle cell attachment in *Caenorhabditis elegans*. Journal of Cell Biology 114: 465-479.

Fukushige, T., D. F. Schroeder, F. L. Allen, B. Goszczynski, and J. D. McGhee, 1996. Modulation of gene expression in the embryonic digestive tract of *C. elegans*. Dev. Biol. 178: 276-288.

Gettner, S. N., C. Kenyon and L. F. Reichardt, 1995. Characterization of βpat-3 heterodimers, a family of essential integrin receptors in *C. elegans*. J. Cell biol. 129: 1127-1141.

Gilchrist, E. J., and D. G. Moerman, 1992. Mutations in the *sup-38* gene of *Caenorhabditis elegans* suppress muscle-attachment defects in *unc-52* mutants. Genetics 132: 431-442.

Glass, D. J., D. C. Bowen, T. N. Stitt, C. Radziejewski, J. Bruno, T. E. Ryan, D. R. Gies, S. Shah, K. Mattsson, S. J. Burden, P. S. DiStefano, D. M. Valenzuela, T. M. DeChiara and G. D. Yancopoulos, 1996. Agrin acts via a MuSK receptor complex. Cell 85: 513-523.

Goetinck, S., and R. H. Waterston, 1994a. The *Caenorhabditis elegans* UNC-87 protein is essential for the maintenance, but not assembly, of bodywall muscle. J. Cell Biol. 127: 71-78.

Goetinck, S., and R. H. Waterston, 1994b. The *Caenorhabditis elegans* muscle-affecting gene *unc-87* encodes a novel thin filament-associated protein. J. Cell Biol. 127: 79-93.

Goh, P. and T. Bogaert, 1991. Positioning and maintenance of embryonic body wall muscle attachments in *C. elegans* requires the *mup-1* gene. Development. 111:667-681.

Graham, P. L., J. J. Johnson, S. Wang, M. H. Sibley, M. C. Gupta et al., 1997. Type IV collagen is detectable in most, but not all, basement membranes of *Caenorhabditis elegans* and assembles on tissues that do not express it. J. Cell biol. 137: 1171-1183.

Granato, M., H. Schnabel and R. Schnabel, 1994. Genesis of an organ: molecular analysis of the *pha-1* gene. Development 120: 3005-3017.

Guo, X., and J. Kramer, 1989. The two *Caenorhabditis elegans* basement membrane (type IV) collagen genes are located on separate chromosomes. J. Biol. Chem. 264: 17575-17582.

Guo, X., J. Johnson and J. Kramer, 1991. Embryonic lethality caused by mutations in basement membrane collagen of *C. elegans*. Nature 349: 707-709.

Gupta, M. C., P. L. Graham and J. M. Kramer, 1997. Characterization of α1 (IV) collagen mutations in *Caenorhabditis elegans* and the effects of α1 and α2 (IV) mutations on type IV collagen distribution. J. Cell biol. 137: 1185-1196.

Han, M., and P. W. Sternberg, 1990. *let-60*, a gene that specifies cell fates during *C. elegans* vulval induction, encodes a ras protein. Cell 63: 921-931.

Han, M., R. V. Aroian and P. W. Sternberg, 1990. The *let-60* locus controls the switch between vulval and nonvulval cell fates in *Caenorhabditis elegans*. Genetics 126: 899-913.

Hannigan, G. E., C. Leung-Hagesteijn, L. Fitz-Gibbon, M. G. Coppolino, G. Radeva, J. Filmus, J. C. Bell and S. Dedhar, 1996. Regulation of cell adhesion and anchorage-dependent growth by a new β1-integrin-linked protein kinase. Nature 4: 91-96.

Harrington, W. F., 1979. Contractile proteins in muscle., pp. 246-409 in The Proteins, edited by H. Neurath, vol. 3, Academic Press, New York.

Hassell, J. R., P. K. Schrecengost, J. A. Rada, N. SundarRaj, G. Sossi and R. A. Thoft, 1992. Biosynthesis of stromal matrix proteoglycans and basement membrane components by human corneal fibroblasts. Invest. Ophthal. Vis. Sci.

Hayashi, K., J. A. Madri and P. D. Yurchenco, 1992. Endothelial cells interact with the core protein of basement membrane perlecan through β1 and β3 integrins: An adhesion modulated by glycosaminoglycans. J. Cell biol. 119: 945-959.

Hedgecock, E. M., J. G. Culotti, D. H. Hall and B. D. Stern, 1987. Genetics of cell and axon migration in Caenorhabditis elegans. Development. 100: 365-382.

Heikkila, P. and R. Soininen, 1996. The type IV collagen gene family. Contributions to Nephrology 117: 105-129.

Hendrix, R. W. and R. L. Duda, 1998. Bacteriophage HK97 head assembly: a protein ballet. Adv. Virus Res. 50: 235-288.

Heremans, A., B. Vander Schueran, B. Decock, M. Paulsson, J. J. Cassiman, H. V. Den Berghe and G. David, 1989. Matrix-associated heparan sulfate proteoglycan: core protein-specific monoclonal antibodies decorate the pericellular matrix of connective tissue cells and the stromal side of basement membranes. J. Biol. Chem. 109: 3199-3211.

Heremans, A., B. Decock, J. J. Cassiman, H. V. Den Berghe and G. David, 1990. The core proteins of the matrix-associated heparan sulfate proteoglycan binds to fibronectin. J. Biol. Chem. 265: 8716-8724.

Hill, C. S., S. Duran, Z. Lin, K. Weber and H. Holtzer, 1986. Titan and myosin, but not desmin are linked during myofibrillogenesis in postmitotic mononucleated myoblasts. J. Cell Biol. 103: 2185-2196.

Hirsh, D., D. Oppenheim and M. Klass, 1976. Development of the reproductive system of *Caenorhabditis elegans*. Dev. Biol. 49: 220-235.

Hotchin, N. A., and A. Hall, 1995. The assembly of integrin adhesion complexes requires both extracellular matrix and intracellular rho/rac GTPases. J. Cell biol. 131: 1857-1865.

Hresko, M. C., B. D. Williams and R. H. Waterston, 1994. Assembly of body wall muscle and muscle cell attachment structures in *Caenorhabditis elegans*. J. Cell Biol. 124: 491-506.

Hudson, B. G., S. T. Reeders and K. Tryggvason, 1993. Type IV collagen: structure, gene organization, and role in human diseases. Molecular basis of Goodpasture and Alport syndromes and diffuse leiomyomatosis. J. Biol. Chem. 268: 26033-26036.

Hutter, H., and R. Schnabel, 1994. *glp-1* and inductions establishing embryonic axes in *C. elegans*. Development 120: 2051-2064.

Huxley, H. E., 1963. J. Mol. Biol. 7: 281.

Hynes, R. O., 1992. Integrins: versatility, modulation and signaling in cell adhesion. Cell. 69: 11-25.

Inoue, K., K. Hoshijima, J. Sakamoto and Y. Shimura, 1990. Binding of the Drosophila *Sex-lethal* gene product to the alternative splice site of *transformer* primary transcript. Nature 344: 461-463.

Inoue, K., K. Hoshijima, I. Higuchi, H. Sakamoto and Y. Shimura, 1992. Binding of the Drosophila *transformer* and *transformer-2* proteins to the regulatory elements of *doublesex* primary transcripts for sex-specific RNA processing. Proc. Natl. Acad. Sci. USA 89: 8092-8096.

Iozzo, R. V., I. R. Cohen, S. Grassel and A. D. Murdoch, 1994. The biology of perlecan: the multifaceted heparan sulfate proteoglycan of basement membranes and pericellular matrices. Biochem. J. 302: 625-639.

Kagawa, H., K. Sugimoto, H. Matsumoto, T. Inoue, H. Imadzu et al., 1995. Genome structure, mapping and expression of the tropomyosin gene *tmy-1* of *Caenorhabditis elegans*. J. Mol. Biol. 251: 603-613.

Kallunki, P., and K. Tryggvason, 1992. Human basement membrane heparan sulfate proteoglycan core protein: A 467-kD protein containing multiple domains resembling elements of the low density lipoprotein receptor, laminin, neural cell adhesion molecules and epidermal growth factor. J. Cell Biol. 116: 559-571.

Kimble, J. and D. Hirsh, 1979. The postembryonic cell lineages of the hermaphrodite and male gonads in *Caenorhabditis elegans*. Dev. Biol. 87: 396-417.

Kimura, K., M. Ito, M. Amano, K. Chihara, Y. Fukata, M. Nakafuku, B. Yamamori, J. Feng, T. Nakano, K. Okawa, A. Iwamatsu and K. Kaibuchi, 1996. Regulation of myosin phosphatase by Rho and Rho-associated kinase (Rho-kinase). Science 273: 245-248.

Kleinman, H. K. and B. S. Weeks, 1989. Laminin: structure, functions and receptors. Cur. Opin. Cell Biol. 1:964-967.

Kleiman, R. J. and L. F. Reichardt, 1996. Testing the Agrin Hypothesis. Cell 85: 461-464.

Kramer, J. M., 1994. Genetic analysis of extracellular matrix in *C. elegans*. Annual Review of Genetics 28: 95-116.

Kramer, J., 1997. Extracellular Matrix, pp. 471-500 in *C. elegans* II, edited by D. L. Riddle, T. Blumenthal, B. J. Meyer and J. Priess. Cold Spring Harbor Laboratory Press, New York.

Kuhn, K., 1994. Basement membrane (type IV) collagen. Matrix Biol. 14: 439-445.

Labeit, S., T. Gibson, A. Lakey, K. Leonard, M. Zeviani, P. Knight, J. Wardale and J. Trinick, 1991. Evidence that nebulin is a protein ruler in muscle thin filaments. FEBS Lett. 282: 313-316.

Larrain, J., J. Alvarez, J. R. Hassell and E. Brandan, 1997. Expression of perlecan, a proteoglycan that binds myogenesis inhibitory basic fibroblast growth factor, is down regulated during skeletal muscle differentiation. Experimental Cell Research 234: 405-412.

Laurie, G. W., J. T. Bing, H. K. Kleinman, J. R. Hassell, M. Aumailley et al., 1986. Localization of binding sites for laminin, heparan sulfate proteoglycan and fibronectin on basement membrane (type IV) collagen. J. Mol. Biol. 189: 205-216.

Laurie, G. W., S. Inoue, J. T. Bing and J. R. Hassell, 1987. Visualization of the large heparan sulfate proteoglycan from basement membrane. Amer. J. Anat. 181: 320-326.

Lee, R., L. Lobel, M. Hengartner, H. R. Horvitz and L. Avery. Mutations in the $\alpha 1$ subunit of an L-type voltage-activated Ca++ channel cause myotonia in *Caenorhabditis elegans*. EMBO 16: 6066-6076.

Lundquist, E. A., and R. K. Herman, 1994. The *mec-8* gene of *Caenorhabditis elegans* affects muscle and sensory neuron function and interacts with three other genes: *unc-52*, *smu-1* and *smu-2*. Genetics 138: 83-101.

Lundquist, E. A., R. K. Herman, T. M. Rogalski, G. P. Mullen, D. G. Moerman et al., 1996. The *mec-8* gene of *C. elegans* encodes a protein with two RNA recognition motifs and regulates alternative splicing of *unc-52* transcripts. Development 122: 1601-1610.

MacKenzie, J. M., R. L. Garcea, J. M. Zengel and H. F. Epstein, 1978. Muscle development in *Caenorhabditis elegans*: Mutants exhibiting retarded sarcomere development. Cell 15: 751-762.

MacKrell, A. J., B. Blumberg, S. R. Haynes and J. H. Fessler, 1988. The *lethal myospheroid* gene of *Drosophila* encodes a membrane protein homologous to vertebrate integrin β subunits. Proc. Natl. Acad. Sci. U.S.A. 85: 2633-2637.

Mango, S., E. J. Lambie and J. E. Kimble, 1994a. The *pha-4* gene is required to generate the pharyngeal primordium of *Caenorhabditis elegans*. Development 120: 3019-3031.

Martin, G. R. and R. Timpl, 1987. Laminin and other basement membrane components. Ann. Rev. Cell Biol. 3: 57-85.

Mello, C., J. M. Kramer, D. Stinchcomb and V. Ambros, 1991. Efficient gene transfer in *C. elegans*: extrachromosomal maintenance and integration of transforming sequences. EMBO 10: 3959-3970.

Miller, D. M., I. Ortiz, G. C. Berliner and H. F. Epstein, 1983. Differential localization of two myosins within nematode thick filaments. Cell 34: 477-490.

Miller, D. M., F. E. Stockdale and J. Karn, 1986. Immunological identification of the genes encoding the four myosin heavy chain isoforms of *Caenorhabditis elegans*. Proc. Natl. Acad. Sci. U.S.A. 83: 2305-2309.

Miyamoto S., H. Teramoto, O. A. Coso, J. S. Gutkind, P. D. Burbelo, S. K. Akiyama and K. M. Yamada, 1995. Integrin function: molecular hierarchies of cytoskeletal and signaling molecules. J. Cell. Biol. 131: 791-805.

Moerman, D. G., H. Hutter, G. P. Mullen and R. Schnabel, 1996. Cell autonomous expression of perlecan and plasticity of cell shape in embryonic muscle of *Caenorhabditis elegans*. Dev. Biol. 173: 228-242.

Moerman, D. G., and A. Fire, 1997. Muscle: Structure, function and development., pp. 417-470 in *C. elegans* II, edited by D. L. Riddle, T. Blumenthal, B. J. Meyer and J. Priess. Cold Spring Harbor Laboratory Press, New York.

Moon, A. and D. G. Drubin, 1995. The ADF/cofilin proteins: stimulus-responsive modulators of actin dynamics. Mol. Biol. Cell 6: 1423-1431.

Morris J. E., G. Gaza and S. W. Potter, 1994. Specific stimulation of basal lamina heparan sulfate proteoglycan in mouse uterine epithelium by Matrigel and by transforming growth factor β1. In Vitro Cell Dev. Biol. Anim. 30:120-128.

Moulder, G. L., M. M. Huang, R. H. Waterston and R. J. Barstead, 1996. Talin requires β-integrin, but not vinculin, for its assembly into focal adhesion-like structures in the nematode *Caenorhabditis elegans*. Mol. Biol. Cell. 7: 1181-1193.

Murdock, A. D., G. R. Dodge, I. Cohen, R. S. Tuan and R. V. Iozzo, 1992. Primary structure of the human heparan sulfate proteoglycan from basement membrane (HSPG2/perlecan). J. Biol. Chem. 267: 8544-8557.

Noonan, D. M., A. Fulle, P. Valente, S. Cai, E. Horigan et al., 1991. The complete sequence of perlecan, a basement membrane heparan sulfate proteoglycan, reveals extensive similarity with laminin A chain, low density lipoprotein-receptor, and the neural cell adhesion molecule. J. Biol. Chem. 266: 22939-22947.

Noonan, D. M., and J. R. Hassell, 1993. Perlecan, the large low density proteoglycan of basement membranes: Structure and variant forms. Kidney Int. 43: 53-60.

Ohji, M., N. SundarRaj, J. R. Hassell and R. A. Thoft, 1994. Basement membrane synthesis by human corneal epithelial cells in vitro. Invest. Ophthalmol. Vis. Sci. 35: 479-485.

Pantaloni, D. and M. F. Carlier, 1993. How profilin promotes actin filament assembly in the presence of thymosin B-4. Cell 75: 1007-1014.

Patthy, L. and K. Nikolics, 1994. Agrin-like proteins of the neuromuscular junction. Neurochem. Int. 24: 301-316

Paulsson, M., P. D. Yurchenco, G. C. Ruben, J. Engel and R. Timpl, 1987. Structure of low density heparan sulfate proteoglycan isolated from a mouse tumor basement membrane. J. Mol. Biol. 197: 297-313.

Perkins L. A., E. M. Hedgecock, J. N. Thomson and J. G. Culotti, 1986. Mutant sensory cilia in the nematode *Caenorhabditis elegans*. Dev. Biol. 117: 456-487.

Pollard, T. D. and J. A. Cooper, 1986. Actin and actin-binding proteins. A critical evaluation of mechanisms and functions. Ann. Rev. Biochem. 55: 987-1035.

Priess, J. R., and D. I. Hirsh, 1986. *Caenorhabditis elegans* morphogenesis: the role of the cytoskeleton in elongation of the embryo. Dev. Biol. 117: 156-173.

Priess, J. R., and J. N. Thomson, 1987. Cellular interactions in early *C. elegans* embryos. Cell 48: 241-250.

Rogalski, T. M., B. D. Williams, G. P. Mullen and D. G. Moerman, 1993. Products of the *unc-52* gene in *Caenorhabditis elegans* are homologous to the core protein of the mammalian basement membrane heparan sulfate proteoglycan. Genes Dev. 7: 1471-1484.

Rogalski, T. M., E. J. Gilchrist, G. M. Mullen and D. G. Moerman, 1995. Mutations in the *unc-52* gene responsible for body wall muscle defects in adult *Caenorhabditis elegans* are located in alternatively spliced exons. Genetics 139: 159-169.

Rosenbluth, J., 1965. Structural organization of obliquely striated muscle fibers in *Ascaris lumbridoides*. J. Cell Biol. 25: 495-515.

Ruoslahti E., 1988. Structure and biology of proteoglycans. Ann. Rev. Cell Biol. 4: 229-255.

Ruoslahti E., 1996. RGD and other recognition sequences for integrins. Ann. Rev. Cell Dev. Biol. 12:697-715.

Russell, D., M. Brown and J. Goldstein, 1989. Different combinations of cysteine-rich repeats mediate binding of low-density lipoprotein receptor to two different proteins. J. Biol. Chem. 264: 21682-21688.

Ryner, L. C., and B. S. Baker, 1991. Regulation of *doublesex* pre-mRNA processing occurs by 3'-splice site activation. Genes Dev. 5: 2071-2085.

Schafer, D. A. and J. A. Cooper, 1995. Control of actin assembly at filament ends. Ann. Rev. Cell Dev. Biol. 11: 497-518.

Schnabel, H., and R. Schnabel, 1990. An organ-specific differentiation gene, *pha-1*, from *Caenorhabditis elegans*. Science 250: 686-688.

Schulze, B., T. Sasaki, M. Costell, K. Mann and R. Timpl, 1996. Structural and cell-adhesive properties of three recombinant fragments derived from perlecan domain III. Matrix Biology. 15: 349-357.

Sibley, M. H., J. J. Johnson, C. C. Mello and J. M. Kramer, 1993. Genetic identification, sequence, and alternative splicing of the *Caenorhabditis elegans* α2 (IV) collagen gene. J. Cell biol. 123: 255-264.

Sibley, M. H., P. L. Graham, N. von Mende and J. M. Kramer, 1994. Mutations in the α2 (IV) basement membrane collagen gene of *Caenorhabditis elegans* produce phenotypes of differing severities. EMBO Journal 13: 3278-3285.

Skubitz, A. P. N., P. C. Letourneau, E. Wayner and L. T. Furcht, 1991. Synthetic peptides from the carboxyl-terminal globular domain of the A chain of laminin: their ability to promote cell adhesion and neurite outgrowth, and interact with heparin and α1 integrin subunit. J. Cell Biol.115: 1137-1148.

Smith, D. B., and K. S. Johnson, 1988. Single-step purification of polypeptides expressed in *Escherichia coli* as fusions with glutathione S-transferase. Gene 67: 31-40.

Sonnenberg, A., C. J. T., Linders, P. W. Modderman, C. H. Damsky, M. Aumailley and R. Timpl, 1990. Integrin recognition of different cell-binding fragments of laminin (P1, E3, E8) and evidence that the α6 β1, but not α6 β4, functions as a major receptor for fragment E8. J. Cell Biol. 110: 2145-2155.

Sosnowski, B. A., J. M. Belote and M. McKeown, 1989. Sex-specific alternative splicing of RNA from the *transformer* gene results from sequence-dependent splice site blockage. Cell 58: 449-459.

Stopak, D. and A. K. Harris, 1982. Connective tissue morphogenesis by fibroblast traction. Dev. Biol. 90: 383-398.

Sulston, J. E., E. Schierenberg, J. G. White and J. N. Thomson, 1983. The embryonic cell lineage of the nematode *Caenorhabditis elegans*. Dev. Biol. 100: 64-119.

Suter, D. M. and P. Forscher, 1998. An emerging link between cytoskeletal dynamics and cell adhesion molecules in growth cone guidance. Curr. Opin. Neurobiol. 8:106-116.

Timpl, R., 1993. Proteoglycans of basement membranes. Experientia 49: 417-428.

Timpl, R. and J. C. Brown, 1996. Supramolecular assembly of basement membranes. BioEssays 18: 123-132.

Trinick, J., 1992. Molecular rulers in muscle? Curr. Biol. 2: 75-77.

van Det, N. F., J. van den Born, J. T. Tamsma, N. A. Verhagen, L. P. van den Heuvel, J. H. Berden, J. A. Bruijn, M. R. Daha and F. J. van der Woude, 1995. Proteoglycan production by human glomerular visceral epithelial cells and mesangial cells *in vitro*. Biochem. J. 307: 759-768.

Venolia, L., and R. H. Waterston, 1990. The *unc-45* gene of *Caenorhabditis elegans* is an essential muscle-affecting gene with maternal expression. Genetics 126: 345-353.

Volk, T., L. I. Fessler and J. H. Fessler, 1990. A role for integrin in the formation of sarcomeric cytoarchitecture. Cell 63: 525-536.

Waterston, R. H., H. F. Epstein and S. Brenner, 1974. Paramyosin in *Caenorhabditis elegans*. J. Mol. Biol. 90: 285-290.

Waterston, R. H., J. N. Thomson and S. Brenner, 1980. Mutants with altered muscle structure in *Caenorhabditis elegans*. Dev. Biol. 77: 271-302.

Waterston, R. H., 1988. Muscle, pp. 281-335 in The nematode *Caenorhabditis elegans*., edited by W.B. Wood. Cold Spring Harbor Press, New York.

Waterston, R. H., 1989. The minor myosin heavy chain, MHC A, of *Caenorhabditis elegans* is necessary for the initiation of thick filament assembly. EMBO J. 8: 3429-36.

Waterston, R. H., J. E. Sulston and A. R. Coulson, 1997. The Genome, pp. 23-45 in *C. elegans* II, edited by D. L. Riddle, T. Blumenthal, B. J. Meyer and J. Priess. Cold Spring Harbor Laboratory Press, New York.

White, J., 1988. The Anatomy, pp. 81-122 in The Nematode *Caenorhabditis elegans*., edited by W. B. Wood. Cold Spring Harbor Laboratory Press, New York.

Williams, B. D., and R. H. Waterston, 1994. Genes critical for muscle development and function in *Caenorhabditis elegans* identified through lethal mutations. J. Cell Biol. 124: 475-490.

Weeds, A. and S. Maciver, 1993. F-actin capping proteins. Curr. Opin. Cell Biol. 5 :63-69.

Wood, W. B., 1988. Embryology, pp. 215-241 in The Nematode *Caenorhabditis elegans*., edited by W. B. Wood. Cold Spring Harbor Laboratory Press, New York.

Yamada, K. M. and S. Miyamoto, 1995. Integrin transmembrane signaling and cytoskeletal control. Curr. Opin. Cell Biol. 7: 681-689.

Yamada, K., and B. Geiger, 1997. Molecular interactions in cell adhesion complexes. Curr. Opin. Cell Biol. 9: 76-85.

Yoshioka, K., A. F. Michael, J. Velosa and A. J. Fish, 1994. Detection of hidden nephritogenic antigen determinants in human renal and non-renal basement membranes. Am. J. Pathol. 121: 156-165.

Yurchenco, P., Y. S. Cheng and G. C. Ruben, 1987. Self-assembly of high molecular weight basement membrane heparan sulfate proteoglycan into dimers and oligomers. J. Biol. Chem. 262: 17668-17676.

Yurchenco, P. D., and J. C. Schittny, 1990. Molecular architecture of basement membranes. FASEB J. 4: 1577-90.

Yurchenco, P. D., and J. J. O'Rear, 1994. Basal lamina assembly. Curr. Opin. Cell Biol. 6: 674-681.

Appendix A. Muscle-affecting genes in *C. elegans*.

Gene	Phenotype	Gene Product
deb-1	severe Pat	vinculin
let-802	Pat	myotactin
lev-11	mild Twitcher	tropomyosin
mua-1	progressive paralysis	TF, Sp1 family
mua-2	progressive muscle detachment	
mua-3	progressive muscle detachment	unknown ORF
mua-4	progressive muscle detachment	
mua-5	progressive muscle detachment	
mua-6	progressive paralysis	
mua-7	defective muscle attachment	
mup-1	embryonic arrest and detached muscle	
mup-2	larval lethal and muscle deformation	troponin T
pat-2	severe Pat	α-integrin
pat-3	severe Pat	β-integrin
pat-4	severe Pat	
pat-6		
pat-8	severe Pat	
pat-9	severe Pat	
pat-10	severe Pat	troponin C
pat-11	mild Pat	
pat-12	mild Pat	
act-123	(gf) slow to paralyzed, some lethal	actin
myo-1		pharyngeal myosin
myo-2		pharyngeal myosin
myo-3	severe Pat	myosin heavy chain
ace-1	Unc as double ace, Let as triple ace	acetylcholinesterase
ace-2	Unc as double ace, Let as triple ace	
ace-3	Unc as double ace, Let as triple ace	
unc-15	limp, paralyzed	paramyosin
unc-22	Twitcher	twitchin
unc-23	"benthead", muscle detachment	
unc-27	sluggish	troponin
unc-35	loopy, irregular movement	talin

unc-45	limp, paralyzed, also Pat alleles	unknown ORF
unc-52	limp, paralyzed, also Pat alleles	perlecan
unc-54	limp, paralyzed	myosin heavy chain
unc-60	limp, slow	cofilin family
unc-68	weak kinker	ryanodine receptor
unc-78	slow	
unc-82	slow	
unc-87	limp, sluggish	calponin family
unc-89	moves well	twitchin family
unc-90	small, rigid paralysis	
unc-93	"rubberband", wild-type null	unknown ORF
unc-94	slow	
unc-95	slow to paralyzed	
unc-96	slightly slow	
unc-97	limp, paralyzed	5-LIM protein
unc-98	slow	
unc-105	small, hypercontracted	degenerin family
unc-109	paralyzed, recessive lethal	
unc-111	moves well	
unc-112	limp, paralyzed, also Pat alleles	MIG-2 homolog
unc-113	slightly slow	
unc-114	paralyzed	
unc-120	sluggish, paralyzed	

Appendix B. Antibodies used in this study.

Antibody	Specificity	Reference
MH2/3	UNC-52 (domain IV)	Francis and Waterston, 1991
MH25	βpat-3 integrin	Gettner et al., 1995
DM5.6	myosin heavy chain A	Miller et al., 1983
NW68	α2 (IV) collagen	Graham et al., 1997
GM1/2	UNC-52 (domain III)	This study
GM3/4	UNC-52 (domain IV)	This study
GM9/10	UNC-52 (domain V)	This study